IMPACT OF CLIMATE CHANGE ON A SOUTHERN TRIBUTARY OF BRAHMAPUTRA BASIN

a study report

by

VINNARASI R
Post Graduate Research Scholar

PROF. ARUP KUMAR SARMA
B.P.Chaliha Chair Professor for Water Resources

DEPARTMENT OF CIVIL ENGINEERING
INDIAN INSTITUTE OF TECHNOLOGY GUWAHATI

DECEMBER 2011

DOCUMENT CONTROL AND DATA

Report Title	:	Impact of Climate Change on A Southern Tributary of Brahmaputra Basin
Publication Date	:	Dec, 2011
Type of Report	:	Technical Report
Pages and Figures	:	71 Pages, 61 Figures and 19 Tables
Authors	:	Vinnarasi R Post Graduate Student, IIT Guwahati E mail: vinnarasi@iitg.ac.in Arup Kumar Sarma *B.P. Chaliha Chair Professor for Water Resources*, IIT Guwahati Email: aks@iitg.ac.in
Originating Unit	:	Indian Institute of Technology Guwahati, Guwahati, Assam, India
Security Classification	:	Restricted
Distribution Statement	:	Among concerned only

ABSTRACT

In India, climate condition differs from place to place. Especially the North-East region receives heavy rainfall than other parts of India. Short duration of high intensity rainfall and longer dry spell are the major problem in impact of climate change. It also affects river morphology due to flood or drought. Therefore the strategic planning of water resources management is essential for efficient utilization of water in future. Reliable forecasting of future precipitation influenced by the climate change scenario is an important field of research.

The present study has been taken up to quantify the impact of climate change on the precipitation characteristics of Dhansiri River, a southern tributary of Brahmaputra basin. Considering the variation of precipitation in the entire basin, five stations have been chosen based on their contrasting features and also on the availability of data.

In this study the Global Climate model has been selected by two different approaches. First approach is comparison of three different Global Climate Models without using National Centre for Environmental Prediction (NCEP) reanalysis data. In the next approach, the model has been selected by using NCEP reanalysis data. Downscaling has been done by statistical downscaling using regression analysis and using Artificial Neural Network. The downscaling model uses CGCM3, HadCM3, and MRCGCM2 monthly weather data under A2 Scenario to determine the precipitation variations and variation in number of dry days in a month at a specific site. The downscaling result has been used to predict the future rainfall intensity.

The result shows 20% increase in the average annual precipitation by 2100. Also, there is an indication that the rainfall in the future during early months of present monsoon season would substantially decrease, whereas the rainfall is likely to be increased in later part of the year. In future, average rainfall intensity will increase by 10% in 2100.

Contents of the Report

List of figures

List of tables

Symbols and Abbreviations

Symbols Abbreviation	Expansion
BMPs	Best Management Practices
IPCC	Intergovernmental Panel on Climate Change
GCM	Global Climate Model
SWAT	Soil and Water Assessment Tool
GHG	Green House Gas
WEPP	Water Erosion Prediction Project
NCEP	National Centre for Environmental Prediction
SVM	Support Vector Machine
RVM	Relevance Vector Machine
RCM	Regional Climate Model
AGCM	Atmospheric Global Climate Model
OGCM	Oceanic Global Climate Model
GLM	Generalized Linear Model
GAM	Generalized Additive Model
ANN	Artificial Neural Network
ABT	Aggregated Boosted Trees
B-circ	Vorticity Binning method
C-circ	Continuous Velocity method
WGEN	Weather GENerator
HadCM3	Hadley centre Coupled Model version 3
CGCM1	First generation of Coupled Global Climate Model
CGCM3	Third generation of Coupled Global Climate Model
SRES	Special Report of Emission Scenerio
CCSR	Center for Climate System Reseach

CHAPTER

1

INTRODUCTION

In recent days the word climate change is gaining importance in different fields because of it expected impacts. This Chapter emphasises causes of Climate Change and its effect with special emphasis on impact of climate change on Water Resources. Based on the status analysis the scope and objective of the study is presented in this chapter.

1.1 CLIMATE CHANGE

Climate change is defined as "Change in weather over a long span of time as a result of human or natural influences". The Intergovernmental Panel on Climate Change (IPCC) report in 2007 strongly conformed that climate change due to human activities and that consequences are likely to be serious. The IPCC has identified five key areas that will be affected by climate change

1) Water
2) Agriculture
3) Ecosystem
4) Health
5) Coastlines

In last 100 years the temperature has increased by 0.8^{o}C especially two third of this amount increased in last three decades alone. The IPCC assessed that in the 21st century, the global temperature is likely to rise a further 1.5 to 1.9^{o}c for lowest emission scenario and 3.4 to 6.1^{o}c for their highest emission scenario. The risk of climate change is now far more than in 2005 because the impact of climate is very faster than expected. The main cause of climate change is Global Warming.

1.2 GLOBAL WARMING

Greenhouse gases, as defined by the IPCC, are "The Gaseous constituents of the atmosphere, both natural and anthropogenic, that absorb and emit radiation at specific wavelengths within the spectrum of thermal infrared radiation emitted by the earth's surface, the atmosphere itself and by clouds". Greenhouse gases increase due to human activities such as deforestation and burning fossil fuel.

Greenhouse gases include carbon dioxide, methane and nitrous oxide. IPCC suggested that in order to avoid dangerous climate change, the greenhouse gas concentrations should keep below 450 ppm carbon dioxide equivalent. Already the concentrations of carbon dioxide reached 380 ppm in 2008 and also its rising rate is 2 ppm each year.

1.3 IMPACTS OF CLIMATE CHANGE

Global warming and sea-level rise are the main impacts of climate change. Arctic sea ice is melting more rapidly than expected amount in the IPCC report. The impacts of climate change are

1) Sea-level rise due to the high rate of melting in glaciers
2) Forest are burning more frequently
3) Droughts and floods are occurring in other side
4) In hot region the crop yield decreases but in cold regions its increases
5) Increasing health problems like vector-borne diseases, water borne diseases etc..,
6) Weather pattern is changing

Therefore the study of climate change is necessary. This problem can been solved in three ways

1) Reducing greenhouse gases
2) Adaptation
3) Mitigation

1.3.1 IMPACTS OF CLIMATE CHANGE ON WATER RESOURCES

As per IPCC, water is one of the areas affected by climate change. Climate change will shrink the resource of fresh water. Water scarcity has been expected in future at various seasons. Uneven distribution of precipitation in space and time and variation in the rate of evaporation, depending on temperature and relative humidity, which impacts the amount of water available to replenish groundwater supplies (more runoff and minimum infiltration), is likely to occur.

1.3.1.1 Hydrological cycle

Hydrological cycle begins with evaporation and ends with precipitation. Due to increasing concentration of greenhouse gases, the changes in hydrological cycle includes

1) Changes in the seasonal distribution and amount of precipitation
2) An increase in precipitation intensity under most situations
3) Increased evapotranspiration and a reduction in soil moisture
4) Changes in the balance between snow and rain
5) Changes in vegetation cove resulting from changes in temperature and precipitation
6) Consequent changes in management of land resources
7) Accelerated melting glacial ice
8) Increase in fire risk in many areas
9) Increased coastal inundation and wetland loss from sea-level rise
10) Effects of carbon dioxide on plant physiology, leading to reduced transpiration and increase water use efficiency

1.3.1.2 Changes in precipitation and drought patterns

IPCC-AR4 found that due to climate change, annual precipitation increases in tropics and at high latitudes and decrease in sub-tropics. More precipitation will increase a region's susceptibility to hazards, depending on variety of factors including,

- Flooding
- Rate of soil erosion
- Mass movement of land
- Soil moisture availability

Historical discharge records indicate that in each 1^{o}C rise of temperature, global runoff will increase by 4%. Applying this projection of changes in evapotranspiration and precipitation, leads to the conclusion that global runoff is likely to increase 7.8% globally by the end of the century.

1.3.1.3 MELTING GLACIER ICE

Warmer winter temperature can also affect water supplies, which causes a decrease in the volume of snow pack. Rise in sea-level will also increase salinity in groundwater and estuaries and decrease fresh water availability in coastal areas.

1.4 DEVELOPMENT OF RESEARCH IN THE AREA OF IMPACT OF CLIMATE CHANGE IN WATER RESOURCES ENGINEERING.

- Divya et al. (1995) studied the climate change and hydrology with emphasis of Indian subcontinent.
- Hauke Heyen et al. (1995) suggested the statistical downscaling of Atlantic air pressure to sea-level anamolies in the Baltic sea.
- Robert L. Wilby et al. (1997) described the hydro-meteorological variables using GCM output.
- X-C Zhang (2005) developed a simple for statistical downscaling to predict soil erosion and crop production.
- A.K.Gosain et al. (2006) has developed a hydrologic modelling for various river basins in India consider climate change effect.
- Hongwen Kang et al. (2007) have used multi-model output in statistical downscaling for precipitation in Philippines and Thailand.
- Subimal Ghosh et al.(2007) developed a new methodology of statistical downscaling based on SVM and RVM for modelling stream flow of Mahanadi river in monsoon period.
- Masum Ur Rahman et al. (2010) studied the morphological behaviour of the major river system in Bangladesh considering the effect of climate change.
- Clement Tisseiul et al. (2010) has predicted stream flow behaviour by comparison of four statistical downscaling model.

1.5 SCOPE OF THE STUDY

The north east region of India is well rich in rainfall as well as rivers. The river Brahmaputra is one of the largest perennial rivers in the world. The source of this river is from the Kailash range of Himalayas. Total length of this river is 2880km and width as high as 18 km. The river starts from Tibet, covering a length of 1600km in Tibet, over 160 km in Arunachal Pradesh, 720km in Assam and rest in Bangladesh. It has so many tributaries; Dhansiri River is one of the tributary of Brahmaputra in south bank. In Dhansiri River, catchment areas are receiving less rainfall when compared to other areas in Assam. Especially there is no snow melt contribution in this river. This River Basin has been selected as the study area.

In this study, statistical downscaling using regression analysis and Artificial Neural Network has been done for precipitation and number of dry days in the catchment of Dhansiri River. Using the precipitation depth and number of dry days, the average intensity has been computed.

1.5.1 OBJECTIVE

- To predict precipitation, number of dry days and stream flow using statistical downscaling with GCM model output.
- To predict average rainfall intensity using downscaling result.
- Comparison of rainfall runoff modelling and direct downscaling of stream flow.
- To obtain the morphological behaviour in future.

1.6 ORGANISATION OF THE REPORT

Chapter 1 Begins with the introduction of the impact of climate change in water resources

Chapter 2 Looks up onto past studies done on climate change in water resources and the downscaling techniques

Chapter 3 Explains GCM and their usage and also tells about the need of downscaling

Chapter 4 Defines the study area and collection of data

Chapter 5 Explains the statistical downscaling based on regression analysis and their results

Chapter 6 Tells about the downscaling tool Using ANN and their results

Chapter 7 Explains the variation of average rainfall intensity in future

Chapter 8 Brings general discussion, future work and conclusion

CHAPTER 2

LITERATURE REVIEW

This literature review focuses on the climate change effect in water resources. In this report downscaling techniques, forecasting precipitation and stream flow, bank erosion has been discussed.

2.1 CLIMATE CHANGE EFFECT IN INDIA

Since the 19^{th} century, the average global near surface air temperature has increased by 0.5°C. The contribution of greenhouse gas from India is about 4% due to agricultural practices, biomass burning, power generation from coal-based thermal plants, transportation and deforestation. In India, the hydrology, water resources and agriculture are the major areas affected of climate change (Divya et al., 1995).

Raj Hari Sharma et al. (2005)have analysed the hydrological changes in Bagmati watershed which has hydroelectric plant in upper region of river and agricultural fertile land in lower region. Due to the climate change, precipitation during monsoon decreased and pre and post monsoon precipitation increased, but mean yearly flow in river decreased. Due to this, magnitude of flood decreased but frequency and duration of flood increased. Hydropower generation decreased and concentration of pollution increased because of less water availability. Due to the increasing demand and reduced supply, water conflicts between India and Nepal are likely to increase in future. It has been suggested that a proper modality of water sharing should be designed in advance.

P.P.Mujumdar (2008)have presented an overview of the current scenario and recent work in India to assess the Climate change impact on water resources. Due to climate change, severe water scarcity in one region and flood hazards in other regions occur. It also affects water quality, agriculture etc… Research studies integrating the atmospheric and hydrological models to understand the climatic influence on hydrologic extremes are needed in the country.

2.2 CLIMATE CHANGE AND WATER RESOURCES

Hauke Heyen et al. (1995) have identified a statistical relation between the anomalies of large-scale Sea-level air pressure and the locally influenced sea level in winter and this model has been applied into Baltic sea gauges, the results from validation part is better. They also suggested that increase of air pressure leads to decrease in the mean sea level. Results show decreasing trend of sea level in future.

Robert L. Wilby et al. (1997) have investigated the empirical relation between climatic variables and local variables. They found that NCEP reanalysis data was not similar to the GCM dataset, so they made a relation between the two dataset and the hydro-meteorological data has been forecasted. But the percentage of error is two high because of high resolution climatic variables.

Yonas B. Dibike et al. (2005) have predicted future variation in river flow and reservoir inflow using downscaled data from SDSM (regression based approach) and LARS-WG(weather generator). The downscaled data from two models are not identical even though both are showing increasing trend in daily temperature and variations in daily precipitation. The study has been done in Chute-de Diable sub-basin of Saguenay watershed. The results show increase in future river flow and reservoir inflow.

X-C Zhang (2005) have developed a simple method for statistical downscaling of GCM monthly output and for further using that output to predicted soil erosion and crop production by WEPP model. The results show that the soil loss will increase by 44% and wheat productivity will increase by 14% due to the increasing trend of surface runoff.

A.K.Gosain et al. (2006) have used HadRM2 daily weather data to determine the spatial-temporal water availability in the river system. The SWAT model has been used to carry out hydrologic modelling of various river basins in the country. They report that the GHG scenario may deteriorate the conditions in terms of severity and droughts and intensity of floods in many parts of the country. Detail study has been done about two rivers, one facing drought (Krishna) and other river facing flood (Mahanadi).

Alex Serrat Capdecila et al. (2007) have presented a methodology to quantify climate change impacts on the hydrologic system of a semi-arid basin in the San Pedro basin in Arizona and Sonara using GCM projections, statistical downscaling process and hydrologic models. Climate change projections from a group of 17 climate models run under 4 different global climate IPCC scenarios has been used in this study. In this river basin, winter rains contribute upto 80% of total recharge while summer monsoon storm although providing most of the yearly rainfall, adds up to the other 20% only.

Hongwen Kang et al. (2007) have predicted the station scale precipitation in the Philippines and Thailand using multi-model output statistical downscaling. Correlation and singular value decomposition analysis has been used for predictor selection. Current GCM has been slightly modified and a movable window has been used to adjust the bias. They found that in some location, the statistical downscaling is not suitable because precipitation is governed mainly by local complicated terrain other than large-scale process.

Masum Ur Rahman et al. (2010) have studied the effect of climate change on morphological behaviour of the major river systems in Bangladesh (i.e., Ganga, Yamuna& Padma). Mathematical modelling has been done using MIKE 11 & MIKE 21.Since Bangladesh is situated with Himalayan ranges on upstream side and Bay of Bengal on the downstream side, rise in sea level results in change of base level of the river. They predicted the rise in precipitation, temperature & sea level. Comparison of existing condition & climate condition has been given, which can be more helpful for further studies.

Subimal Ghosh et al. (2010) assessed climate change impact in Mahanadi river basin using probabilistic approach. In this study, uncertainty model has been developed by statistical downscaling with bias correction. Downscaling involves conversion of large scale GCM outputs of climate variables to local scale hydrologic variables. In this study, they have chosen three GCMs and two Scenarios.

Mohammed Karamouz et al. (2011) have developed an algorithm for selecting the BMPs to improve the urban drainage system performance that considers the anthropogenic and climate change effect. The algorithm has been applied in Tehran metropolitan area and it includes downscaling, rainfall-runoff model, optimization model and uncertainty analysis. Downscaling and rainfall-runoff model has been modelled using SDSM and stormNET, the amount of rainfall increases in dry season, it leads more flash floods. By this approach the flooded area and flood volume will decrease and the future urban drainage system will also improve.

Subimal Ghosh et al. (2007) have described a methodology of statistical downscaling based on SVM and RVM. In this study, 2m air temperature, MSLP, 500hpa geo-potential height, specific humidity has been considered as the predictors for modelling stream flow of Mahanadi River in monsoon period. NCEP/NCAR reanalysis data was used to train the model. Finally, they have concluded that, due to increase in temperature, the stream flow is decreasing. Limitation of this study is that they have assumed that the land use pattern is same in future as in the present. They used only CCSR/NIES (GCM model) with B2 Scenario for downscaling.

2.3 REVIEW OF DOWNSCALING APPROACHES

Downscaling is a technique for bringing down the large scale global variable to local hydrological variables for impact studies. Downscaling approach is classified into two categories: 1) Dynamic Downscaling and 2) Statistical Downscaling. Dynamic downscaling represents the use of high-resolution regional climate models (RCMs), which are nested with GCMs. It is a step by step process. The main drawback of RCMs is large demand on computer resources and the complexity of their operation. Statistical downscaling is a statistical model to make a relation between large-scale phenomenon and local quantities. This relation is applied to GCM outputs to obtain local and regional climate change signals.

Eduardo Zorita et al. (1998) suggested an analog method for statistical downscaling, which is simplest among other statistical methods like linear method, classification method and neural network. For monthly data, analog method and linear method are giving similar results.

R.L.Wilbey et al. (1998) have done a comparative study of five different statistical downscaling models. They are B.circ, C.circ, WGEN, SPELL and ANN. Among these models B.circ and C.circ is giving better results than the others.

Vasubanhu Mishra et al. (2001) have done dynamic downscaling in Amazon river basin by using multiple atmospheric global circulation model(AGCM) integrations at T42 spectral resolution and the prescribed sea surface temperature has been used to drive regional spectral model(RSM) simulations at 80-km resolution for the summer season (January-February – March). The solutions from two models were compared and RSM has been found to be better than SACZ.

Jinwon Kim et al. (2000) presented the prediction precipitation and stream flow in northern California coastal basin using dynamic downscaling. Regional climate system model (RCSM) has been used to simulate the precipitation and stream flow. The correlation coefficient between observed and simulated stream flow is 0.88 in their study.

Masoud Hassemi et al. (2007) have done downscaling for precipitation and temperature in 10 meteorological stations using ASD and SDSM. The predictor selection in ASD model was based on backward stepwise regression. HadCM3 and CGCM1 model have been used for future prediction and NCEP reanalysis data has been used for calibration. The comparison of both results indicates ASD is better than SDSM for temperature, but for precipitation neither of them gives good result. Selection of predictor and model selection is changing from station to station, so downscaling model has been taken as different for different station.

Clement Tisseiul et al. (2010) compared four statistical downscaling models (GLM, GAM, ANN, ABT) for predicting stream flow, among these models ABT gives better result. This study has been done in 51 hydrological gauging stations located in southwest France. It considers two types of regimes i.e., pluvial & nival. Based on GCM cnrm-cm3 and scenarios A2 and A1B, the future has been predicted. In both regimes stream flow rate is decreases.

2.4 BANK EROSION

Zhengyi Yao et al. (2010) studied bank erosion and accretion in Ningxia –Inner Mongolia reaches of China’s yellow river. In this study, the changes in the river shape and positions from 1958 to 2008 have been studied using maps produced by field surveys, aerial photographs and satellite images. The changes in the channel cause various problems like loss of riparian land, flood hazards, alteration of aquatic and riparian ecosystem etc…Since the error terms were of magnitude smaller than the actual shifts in the bank positions, the approach provides a useful tool for monitoring the river changes.

DongdongJia et al. (2010) presented a 3d model for turbulent flow, sediment transport, bank erosion and channel formation. This model has been applied to simulate morphological changes in the Shishou bend of the middle Yangtze River in China. They considered the double layer sediment structure in riverbanks with a cohesive upper layer and a non-cohesive lower layer of sand and gravels.

Carol R.W.H et al. (2004) have modelled bank erosion and overbank deposition during extreme flood on the Carson River. It contains 7000 tons of residual mercury. It is now distributed throughout the river's bank sediments and floodplain deposits. To simulate this extreme situation, an US EPA hydrodynamic model (RIVMOD) has been modified to include the divide channel approach to estimate floodplain depths and velocities. Nearly 87% of bank mass eroded in a 6-year time span occurred during the single 1997 flood event. The overall deposition has been modelled using separate function for CSS and wash load.

Chu-Agor M.L et al. (2009) have developed an empirical sediment transport function for predicting sediment mobilization (i.e., seepage erosion and undercutting) over time for soils with cohesive properties. The empirical relationship was derived and evaluated based on three dimensional soil block experiments.

Ronald C. De Rose et al. (2010) published a methodology for measuring the meander migration rates and amount of sediment produced by river bank. Cliff erosion has been derived from comparison of LIDAR-derived DEMs and those derived from photogrammetric analysis of historical aerial photography for 50 year time scale. The study has been conducted in Waipaoa River. The confined nature of the river bank is more resistant, therefore the meander migrations of the reach is low but in other hand, high sediment loads and net aggradation of the active channel over the survey period and more extensive riparian vegetation and stop bank construction along the lower of the two reaches occur. So, future investigation about the global bank erosion rate is an important task. The results from this study gives that the average meander migration rate is 0.22 and 0.12 m/a, bank and cliff erosion is 74.3 and 23.3kt/a respectively and suspended sediment load is <2%. Here cliff erosion is the dominant process with 69 t0 88% of sediment delivered from channel side processes.

Jennifer G. Duan (2005) stated a probabilistic approach to calculate rate of bank erosion. Bank erosion occurs due to two process i.e., basal erosion due to fluvial hydraulic force and bank failure under the influence of gravity. The frequency of bank failure is correlated to the frequency of flooding, therefore bank failure frequently occur in recessing limb of a storm hydrograph. This approach is applicable for cohesive bank material of planar bank failure. Limitation of this study is lack of field data, so further research need to done considering the impact of flood hydrographs, evolution of tension crack with basal erosion, bank material saturation prior to bank erosion and time period to wash away failed bank material. This paper indicates that the rate of bank erosion is a function of the hydraulic forces, bank geometry, bank material cohesion & frequency of failure.

2.5 SECONDARY CURRENT

Ichiro Kimura et al. (2010) have discussed about the suspended sediment transport in a shallow side cavity. They have chosen 4 types of depth-averaged plane 2d models with/without effects of secondary currents. Those models have been applied to two kinds of shallow flow fields: a simple circular channel with rigid rotating flow and an open channel flow with a rectangular side cavity.

Athanasios N. Papanicolaou et al. (2007) developed a methodology for investigating the adequacy of representation of the distribution of the near bank shear stress τ_s, when secondary currents are present and estimation of the critical erosional strength τ_{cr} and other sediment erodible parameters for fluvial erosion in a stream with pronounced cross-sectional irregularities located within the loess region of the Palouse basin of Washington state, United States.

Nikolas E. Kotsovinos et al. (1987) explained the flow pattern of secondary currents in wide channel. In this analysis they found the width of secondary flow is equal to the depth of the flow through the macroscopic evidence and the experimental data.

2.6 SUMMARY

From the above literature review, it has been established that the climate change impact on water resources is a major problem throughout the world. Especially, the North East Region of India is facing lot of challenges because the irregular precipitation pattern. Even in 10 to 20km distance, the amount of precipitation is varying. It leads to changes in the river flow, therefore river morphology is affected due to increase or decrease in discharge, bank erosion, sediment transport etc…

CHAPTER

3

GCM AND THEIR DOWNSCALING

GCM stands for Global Climate Model. These are used to describe climate behaviours like weather forecasting, understanding climate & projecting climate change. Downscaling is a technique that is used to scale down the Global Climate Model to local Hydrological Model. This chapter discusses the need of downscaling, their types, generation of GCMs, their scope and their reliability.

3.1 GLOBAL CLIMATE MODEL

GCM is a mathematical representation of the general circulation of the planetary atmosphere or ocean and also simulates the time series of climate variables globally, accounting for effects of greenhouse gases. It is based on the Navier-Stoke's equation on a rotating sphere with thermodynamic terms for various energy sources. GCMs are available for grid points, obtained by dividing the earth surface into the series of rectangles.

The key components of GCMs are Atmospheric and Oceanic GCMs along with sea ice and land surface components. The Atmospheric Global Climate Models (AGCMs) and Oceanic Global Climate Models (OGCMs) are combined to formed atmosphere-ocean Coupled Global Climate Models (CGCMs). GCMs are also known as Global Circulation Model. GCM datasets are available for use from Intergovernmental panel on climate change (IPCC 2007) and Canadian Centre for Climate Modelling and Analysis (CCCma).

3.1.1 EMISSION SCENARIOS

Emission Scenarios have been used to make projections of possible future climate change, it incorporates future human activity. Different types of Scenarios have been formulated, each one having different assumptions for future greenhouse gas pollution, land-use and others driving forces. In SRES, (Special Report of Emission Scenario) four types of Scenarios have been suggested. They are A1(economic focus for homogenous world), A2 (economic focus for heterogeneous world, B1 (environmental focus for homogenous world) and B2 (environmental focus for heterogeneous world).

3.1.2 TYPES OF GCM

The Fourth Assessment Report (AR4) of IPCC has suggested 22 different types of GCM models with respect to different emission Scenarios. Their details are tabulated below.

S. No.	Centre	Model	Emission Scenarios
1.	Beijing climate centre	BCCM1	1PT02X, 1PT04X
2.	Bjerknes Centre for climate	BCM2.0	SR-A2, SR-B1
3.	Canadian Centre for Climate Modelling and Analysis (CCCma)	CGCM3 – T47 (T47 Resolution)	1PT02X, 1PT04X, SR-A1B, SR-A2, SR-B1
4.	Canadian Centre for Climate Modelling and Analysis (CCCma)	CGCM3 – T63 (T63 Resolution)	SR-A1B, SR-B1
5.	Centre National de Recherches Meterorologiques	CNRMCM3	1PT02X,1PT04X,COMMIT, SR-A1B, SR-A2, SR-B1
6.	Australia's Commonwealth Scientific and Industrial Research Organisation (CSIRO)	CSIROMK3	1PT02X , SR-A2, SR-B1
7.	Max Planck Institute fur Meteorologie	ECHAM5OM	1PT02X, 1PT04X, SR-A1B, SR-A2, SR-B1
8.	Meteorological Research University of Bonn Meteorological Research Institute of KMA Model and Data Group at MPI-M	ECHO-G	1PT02X
9.	Geophysical Fluid Dynamics Laboratory (GFDL), USA	GFDLCM2.0	COMMIT, SR-A1B, SR-A2, SR-B1
10.	Geophysical Fluid Dynamics Laboratory	GFDLCM2.1	COMMIT, SR-A1B, SR-A2, SR-B1

	(GFL), USA		
11.	GISS	GISSE- H	1PT02X, SR-A1B
12.	GISS	GISSE-R	1PTO2X,1PTO4X,SR-A1B,SR-A2, SR-B1
13.	UK Met. Office	HADCM3	SR-A1B,SR-A2,SR-B1
14.	UK Met. Office	HADGEM1	SR-A1B,SR-A2,SR-B1
15.	INGV, National Institute of Geophysics and Volcanology, Italy (2)	INMCM3.0	IPTO2X,IPTO4X,2XCO2,AMIP,COMIT,SLAB,SR-A1B,SR-A2,SR-B1
16.	Institute for Numerical Mathematics	INMCM3.0	1PTO2X,1PTO4X,2XCO2,AMIP,COMMIT,SLAB,S-A1B,SR-A2,SR-B1
17	Institute Pierre Simon Laplace	IPSLCM4	1PTO2X,1PTO4X,COMMIT,PDCTL,SR-A1B,SR-A2,SR-B1
18.	National Institute for Environmental Studies	MIROC3.2 hires	SR-A1B, SR-B1,Extremes (AMIP,SR-A1B,SR-B1)
19.	Meteorological Research Institute, Japan Meteorological Agency, Japan	MRI-CGCM2.3.2	SR-A2,SR-A1B,SR-B1
20.	National Institute for Environmental Studies	MIROC3.2 medres	SR-A1B,SR-A2,SR-B1,Extremes (AMIP, COMMIT, SR-A1B, SR-A2, SR-B1)
21.	National Centre for Atmospheric Research (NCAR), USA	NCARPCM	COMMIT,SR-A1B,SR-A2,SR-B1
22.	National Centre for Atmospheric Research (NCAR), USA	NCARCCSM3	SR-A1B,SR-A2,SR-B1

Table 3.1 Types of GCM models

3.1.3 TYPES OF GCMS USED

In this study, three different resolution GCM models with A2 simulation run have been used. A2 scenario considers the forcing effect of greenhouse gases and sulphate aerosol direct effect, which are based on IPCC SRES-A2 (Special Report of Emission Scenario A2). The three models are CGCM3, HadCM3, MRCGCM2.3.2; each model has been briefly discussed below.

CGCM3 stands for the third generation of Coupled Global Climate Model. Atmospheric Global Climate Model (AGCM3) and Oceanic Global Climate Model are the two main component of this model. AGCM3 comprises of 47 wave triangularly truncated spherical harmonic expansion represented as T47. In this model, spatial resolution for AGCM3 is roughly 3.75 degrees lat/lon and 31 levels in the vertical. In OGCM3 each atmospheric grid is divided into four with spatial resolution approximately equal to 1.85 degrees and vertical levels equal to 29. AGCM3 considers domains which extend upto 50km above the surface, into the Stratopause region. The third assessment includes three layers of soil, one layer of snow and one layer of vegetative canopy.

HadCM3 stands for Hadley centre Coupled Model version 3. This model does not require flux adjustment. In this model, spatial resolution for AGCM3 is roughly 2.5 degrees of latitude and 3.75 degrees of longitude forming the global grid of 96×73 grid cells with 19 levels. In the oceans, this model has a resolution of 1.25 degrees of latitude and longitude with 20 levels. This model has been used in lot of projects involving climate change and its prediction and has been used in IPCC third assessment report. This model has higher resolution compared to other models.

Meteorological Research Institute has developed the model MRI-CGCM2.3.2. It is a coupled model; the components of the model are atmosphere, ocean, sea ice, land surface and vegetation. Atmospheric and oceanic coupled global climate model have been chosen for this study. The spatial resolution for atmospheric model is approximately 2.8 degrees of latitude and longitude with 30 layers (16 layers above 200hpa and 5 layers below 850hpa). In the oceans, it has the resolution of 2.5 degrees of latitude and 2 degrees for longitude. The numerical scheme used in the atmospheric model is spectral transform method and in the ocean it is Arakawa B-grid.

3.2 DOWNSCALING

GCMs have low resolution; therefore the GCM output cannot be used directly in the local impact studies due to cloud cover and other effects. Downscaling technique is used to bring the GCM output of global climate variables to local scale hydrologic variables. Downscaling techniques can be classified into two types, they are discussed below.

3.2.1 DYNAMIC DOWNSCALING

Dynamic Downscaling represents the use of high-resolution Regional Climate Models (RCMs) which are nested with GCMs. The RCMs are similar to GCMs, but

RCM generally improves with the higher-order statistics of the meteorological variables. Dynamic Downscaling is a step by step process. A drawback of RCM is large demand of computer resources and the complexity of their operation, which requires a trained person.

3.2.2 STATISTICAL DOWNSCALING

Statistical Downscaling has been used to observe the statistical relationship between the large scale climate variables to local hydrologic variables. This relation can be applied to future GCM outputs to obtain local and regional climate change factors. Statistical Downscaling is time conserving technique. This technique is broadly divided into three categories, namely

(1) Weather typing

(2) Weather generators

(3) Regression-based downscaling.

In this study regression-based downscaling has been used.

CHAPTER

4

CASE STUDY

4.1 STUDY AREA

The aim of this study is to predict the future stream flow variation in the southern region of Dhansiri River. Dhansiri is one of the tributary of Brahmaputra where the snow melt is absent. It originates from Laisang Peak of Nagaland and flows from south to north over a distance of 352km. The total catchment area is 1220km^2. Before joining the south bank of Brahmaputra, the river passes through the Dimapur district of Nagaland and Golaghat district of Assam. The bank of Dhansiri River is rich in wild life with Itanki National Park on one side and Dhansiri Reserved Forest on the other side.

In this study, Dhansiri River (southern region) has been selected. For performing rainfall-runoff modelling, some of the stations in the catchment of Dhansiri River have been selected based on their contrasting features and also on the availability of data. The selected stations are Furkatting, Lengree, Rungagora, Sockieting, and Bokakhat. Lengree is in the upper reach of the river and Bokakhat in the lower reach. The stations are marked in Fig. 4.2.

4.2 DATA COLLECTION

Three types of data have been used in this study, namely

1) Observed Precipitation Data
2) NCEP reanalysis data
3) GCM data for three models as mentioned in section 3.1.3.

4.2.1 OBSERVED RAINFALL DATA

Observed monthly rainfall data has been collected for different places nearby Dhansiri River. The period of data collection has been tabulated below

S. No.	Station	Time Period
1.	Furkatting	1992-2010
2.	Lengree	1978-2010
3.	Rungagora	1997-2010
4.	Sockieting	1993-2010
5.	Bokakhat	1927-2010

Table 4.1 Time period for individual station

4.2.2 NCEP/NCAR REANALYSIS DATA

NCEP reanalysis data are basically, the observed predictors. NCEP data are used to choose the best GCM model. The spatial resolution of reanalysis data is 2.5 degrees of latitude and longitude. Based on the respective station latitude and longitude, the NCEP data has been downscaled for two grids. The time period of this data is 1965-2010.

4.2.3 GCM DATA

The GCM data are downloaded from Intergovernmental Panel on Climate Change in two different assessments: fourth Assessment Report (AR4) and Third Assessment Report (AR3). The three model data has been downloaded from AR4.Due to less availability of past data, HadCM3 model also downloaded from AR3. The time period of fourth Assessment is from 2001 to 2100 and the third assessment is 1890-2099.

4.3 OVERLAYING TOPOSHEET INTO GOOGLE MAP

Some of the places' latitude and longitude were not available, therefore the Toposheet has been overlaid into the Google earth for finding the latitude, longitude and altitude for each station. The latitude and longitude is very important for downscaling. The values are tabulated below

S. No.	Station	Latitude	Longitude
1.	Furkatting	26.46°N	94.00°E
2.	Lengree	26.02°N	93.75°E
3.	Rungagora	26.73°N	93.76°E
4.	Sockieting	26.61°N	94.08°E
5.	Bokakhat	26.62°N	93.60°E

Table 4.2Latitude and Longitude

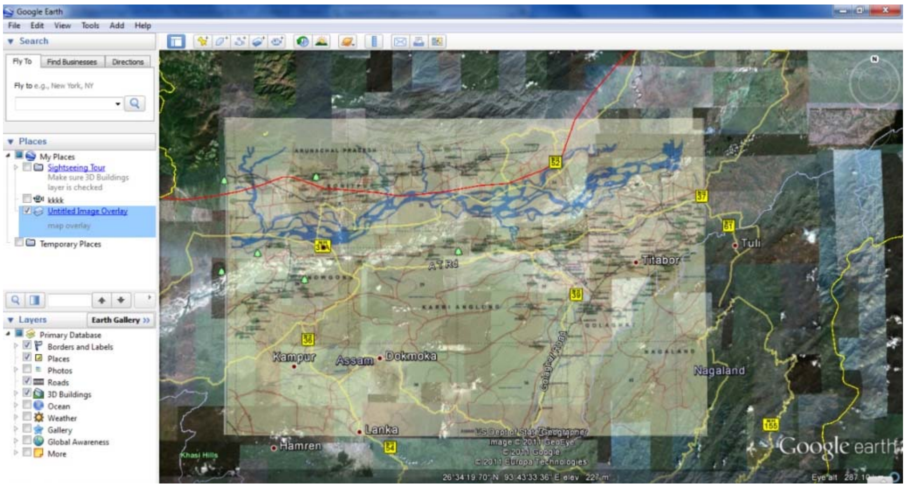

Fig. 4.1 Map overlaid on Google Earth

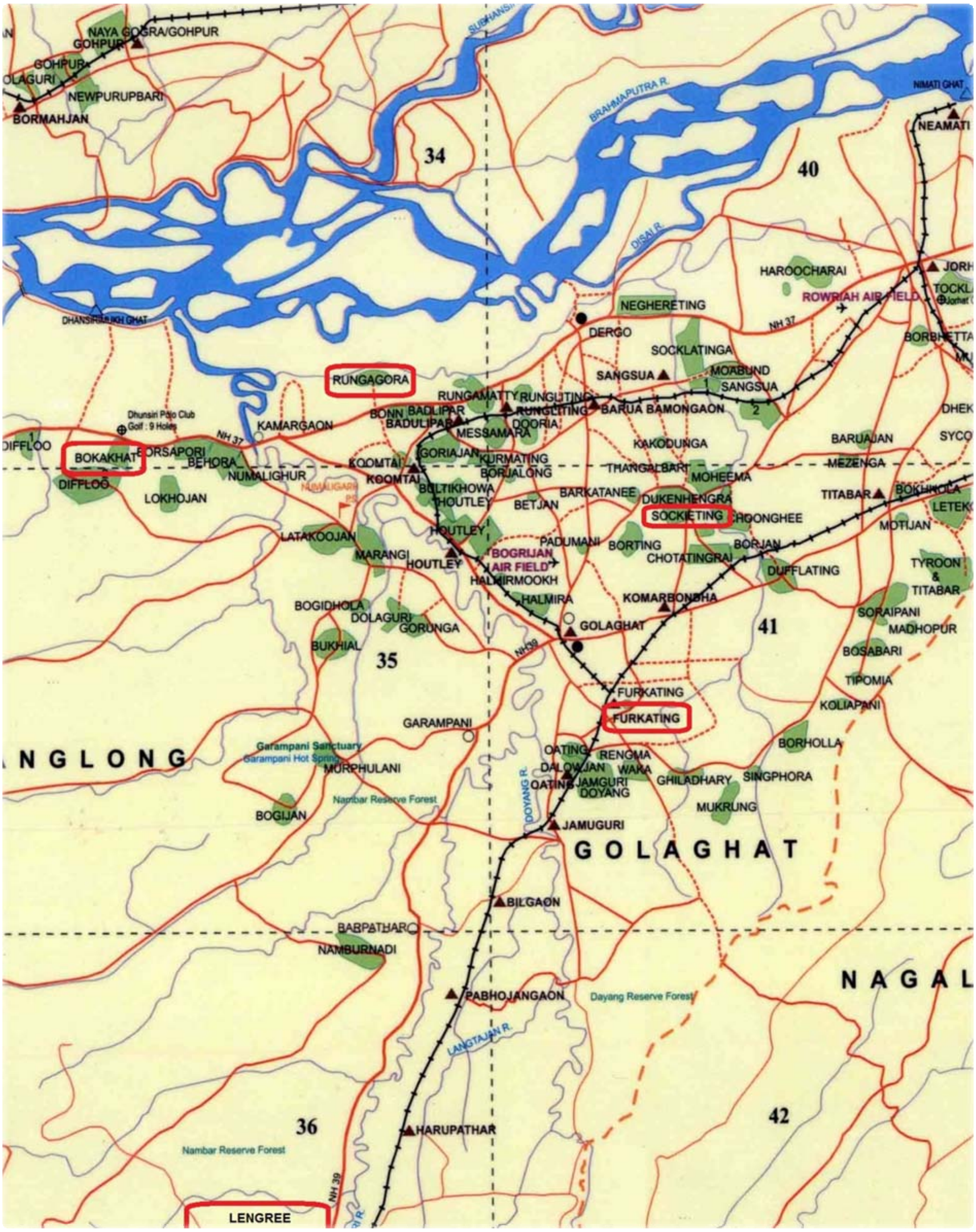

Fig. 4.2 Stations selected for study

CHAPTER

5

STATISTICAL DOWNSCALING

In this chapter, statistical downscaling techniques and forecasting of precipitation has been discussed. The statistical downscaling has been done by Multiple Linear Regression. Predictor selection has been based on the correlation and Stepwise Regression. These methods and results are briefly presented below.

5.1 MULTIPLE LINEAR REGRESSIONS

Regression analysis is very helpful for forecasting, it is divided into two categories namely simple regression and multiple regression. In this study, the independent variables are more than one so multiple linear regression has been used. In the multiple linear regressions, the basic model has been designed by using least square method.

5.1.2 ASSUMPTIONS

Following five fundamental assumptions are required for the least square procedure to work as the Gauss-Markov theorem expects

- The relationship between Y and X_1, X_2.... is linear
- The residuals are normally distributed with zero mean.
- The residuals have a constant variance σ^2.
- The successive residuals are not correlated. i.e., there is no autocorrelation.
- The X variables are fixed and are not correlated with the u_t values

5.1.3 PROCEDURE

In Multiple Linear Regression Analysis the basic steps have four categories, namely

- Specification: Here selection of predictor and model has been done.
- Calibration: This is used to form a relation between the output and input.

- Validation: This is used to find the accuracy of model.
- Forecasts: This uses the model from validation to predict the future variations

5.2 DATA PROCESSING

The large scale climate variables has to be pre-processed before using it for calibration

5.2.1 INTERPOLATION

The geographic location of study area (latitude and longitude), NCEP grid points and GCM grid points vary; therefore interpolation is needed for processing of the data. Here two dimension linear interpolations by MATLAB programming have been used. The NCEP grid points and GCM grid points are interpolated to match the location of study area.

5.2.2 STANDARDIZATION

Basically, the difference between observed and climate variables occur due to parameterization. The difference between observed and climatic variables is called bias. Standardization is used to reduce the biases in the mean and variance of GCM predictors relative to those of the observed or NCEP data. In this study AR4 and AR3 data has been used. The baseline period for AR4 is from 2001 to 2010, which is a very short time. The baseline period for AR3 is from 1965 to 2010. In this process of standardization, the mean is subtracted from the baseline period and divided by standard deviation for both NCEP and GCM outputs are performed as follows, given by Subimal Ghosh et al (2007)

$$v_{s\tan,t}(k) = \frac{v_t(k) - \mu_v(k)}{\sigma_v(k)}$$

Where, $V_t(k)$ =Original value of the k^{th} predictor variable at time t,

$\mu_t(k)$ = The mean value of the k^{th} predictor variable and

$\sigma_v(k)$ =Standard deviation of the k^{th} predictor variable

5.3 SELECTION OF PREDICTORS

The predictors are selected by Stepwise Regression method. Stepwise regression consists of two main approaches namely forward selection and backward elimination. Here combination of two approaches is used. The predictor selection carried out by automatic procedure includes simple correlation and partial correlation. The process will continue until it reaches the best f-test, t-test, adjusted R^2 (co-efficient of determination), Akaike information criterion, Bayesian information criterion and Mallows'Cp. The equation for the data is given by

$$y_i = \beta_o + \beta_1 x_{i1} + \beta_2 x_{i2} + ...\beta_p x_{ip}$$

Where, y_i is the predict ant, x_i is the predictor and β is the constant Simple Correlation. It is the correlation between two variables without the influence of other variables. When the correlation co-efficient between y and x is computed by first eliminating the effect of all other variables, it is called partial correlation.

5.3.1 CORRELATION

Correlation is a statistical relationship between two variables. It will show whether the two variables are strongly correlated, weakly correlated or independent of each other. How precipitation is correlated with other variables is discussed below:

5.3.1.1 Physical correlation

Precipitation is mainly affected by sea level pressure, humidity,temperature and wind speed. In atmospheric circulation pattern, the first process is evaporation and precipitation forms through condensation. Due to increase in temperature, the evaporation will take place and due to low pressure, the warm air containing water vapour will lift up, which increases moisture content in the air i.e., humidity. So it clearly indicates that temperature, humidity and wind speed are directly proportional to precipitation. And sea level pressure is inversely proportional to precipitation.

5.3.1.2 Pearson correlation

It is statistical technique to calculate the correlation coefficient for two variables. Precipitation data have been taken from recorded data at Furkatting, Lengree, Rungagora, Sockieting, and Bokakhat. Predictors have been collected from IPCC and NCEP reanalysis data. Correlation between precipitation and predictors with respect to different models are tabulated below.

Predictors	**Correlation Coefficient**			
	NCEP	**HadCM3**	**CGCM3**	**MRCGCM2**
ta	0.572	0.505	0.504	0.503
pressure	-0.569	-	-	-
rhum	0.476	-	-	-
slp	-0.593	-0.498	-0.520	-0.494
u-wind	0.443	0.253	0.332	0.420
v-wind	0.619	0.261	0.524	0.347
ta850	0.588	0.506	-	-
ta500	0.552	0.468	-0.309	-
ta200	0.583	-	0.423	-
Zg850	-0.566	-0.428	-	-
Zg500	0.493	0.474	-	-

Zg200	0.558	0.449	-	-
ua850	0.472	-0.100	-	-
ua500	-0.590	-0.481	-	-
ua200	-0.596	-0.496	-	-
va850	0.674	0.099	-	-
va500	0.299	0.169	-	-
va200	-0.401	-0.271	-	-
hur850	0.495	0.372	-	-
hur500	0.566	0.466	-	0.451

Table 5.1 Correlation coefficient for NCEP data compared with GCM data at Furkatting

It clearly indicates that slp, ta, v-wind have stronger correlation than the other predictors. CGCM3 and HadCM3 models have been chosen based on the correlation coefficient. Without comparing NCEP data, the correlation coefficients for different models are computed, as shown below.

Predictors	**Correlation coefficient**	
	Precipitation	**Dry Days**
Specific Humidity	0.507	-0.755
Total Precipitation	0.541	-0.561
Sea level Pressure	-0.525	0.877
Surface Down welling Shortwave Radiation	-0.055	-0.272
Zonal Surface Wind Speed	0.332	-0.547
Meridional Surface Wind Speed	0.524	-0.780
Surface Air Temperature	0.504	-0.821
Convective Precipitation	0.212	-0.448
Air Temperature @ 500hpa	-0.309	-0.029
Air Temperature @ 500hpa	0.422	-0.133

Table 5.2 Correlation coefficient for Furkatting using CGCM3 model

Predictors	**Correlation coefficient**	
	Precipitation	**Dry Days**
Total Soil Moisture Content (mrso)	0.362	-0.458
Total Precipitation	0.351	-0.701
Convective Precipitation	0.386	-0.757
Sea Level Pressure	-0.498	0.858
Surface Downscaling Shortwave Radiation	0.143	-0.421
Snow Melt	-0.293	0.445
Surface Air Temperature	0.505	-0.866
Surface Temperature	0.506	-0.865
Zonal Surface Wind Speed	0.253	-0.605
Meridional Surface Wind Speed	0.261	-0.622
Zonal Wind Speed@200hpa	-0.496	0.724
Zonal Wind Speed @500hpa	-0.481	0.725
Zonal Wind Speed @850hpa	-0.101	-0.069
Meridional Wind Speed@200hpa	-0.271	0.466
Meridional Wind Speed@500hpa	0.169	-0.086

Meridional Wind Speed@ 850hpa	0.099	-0.456
Relative Humidity @ 200hpa	0.469	-0.683
Relative Humidity @ 500 hpa	0.466	-0.711
Relative Humidity @ 850hpa	0.372	-0.529
Temperature @ 500hpa	0.468	-0.868
Temperature @ 850hpa	0.506	-0.689
GeopotentialHeight @ 500hpa	0.474	-0.665
GeopotentialHeight @ 850hpa	-0.428	-0.781

Table 5.3 Correlation coefficient for Furkatting using HadCM3 model

Predictors	**Correlation coefficient**	
	Precipitation	**Dry Days**
Total Precipitation	0.397	-0.698
Sea level Pressure	**-0.494**	0.839
Specific Humidity	**0.507**	-0.815
Surface Downscaling Shortwave Radiation	0.297	-0.624
Zonal Surface Wind Speed	0.420	-0.807
Meridional Surface Wind Speed	0.347	-0.781
Surface Air Temperature	**0.503**	-0.839
Convective Precipitation	0.435	-0.742
Relative Humidity @ 200hpa	0.429	-0.582
Relative Humidity @ 500hpa	**0.451**	-0.697

Table 5.4 Correlation coefficient for Furkatting using MRI_CGCM2 model

Predictors	**Correlation coefficient**	
	Precipitation	**Dry Days**
Specific Humidity	0.749	-0.799
Total Precipitation	0.624	-0.603
Sea level Pressure	-0.718	0.856
Surface Down welling Shortwave Radiation	0.084	-0.306
Zonal Surface Wind Speed	0.713	-0.844
Meridional Surface Wind Speed	0.579	-0.619
Surface Air Temperature	0.631	-0.748
Air Temperature @ 200hpa	0.157	-0.200
Air Temperature @ 500hpa	0.047	-0.103
Convective Precipitation	0.136	-0.265

Table 5.5 Correlation coefficient for Lengree using CGCM3

Predictors	**Correlation coefficient**	
	Precipitation	**Dry Days**
Total Soil Moisture Content (mrso)	0.547	-0.481
Total Precipitation	0.601	-0.707

Convective Precipitation	0.650	-0.760
Sea Level Pressure	-0.731	0.828
Surface Downscaling Shortwave Radiation	0.173	-0.315
Snow Melt	-0.287	0.382
Surface Air Temperature	0.742	-0.850
Surface Temperature	0.743	-0.849
Zonal Surface Wind Speed	0.496	-0.644
Relative Humidity @ 200hpa	0.676	-0.693
Relative Humidity @500hpa	0.680	-0.710
Relative Humidity @ 850hpa	0.601	-0.615
Temperature @ 500hpa	0.703	-0.708
Temperature @ 850hpa	0.734	-0.849
GeopotentialHeight @ 500hpa	0.706	-0.704
GeopotentialHeight @ 850hpa	-0.630	0.722
Zonal Wind Speed @ 200hpa	-0.705	0.693
Zonal Wind Speed @ 500 hpa	-0.710	0.712
Zonal Wind Speed @ 850hpa	-0.189	0.043
Meridional Wind Speed@200hpa	-0.431	0.506
Meridional Wind Speed@500hpa	0.276	-0.150
Meridional Wind Speed@ 850hpa	0.571	-0.692
Meridional Surface Wind Speed	0.457	-0.620

Table 5.6 Correlation coefficient for Lengree using HadCM3

Predictors	**Correlation coefficient**	
	Precipitation	**Dry Days**
Specific Humidity	0.685	-0.707
Total Precipitation	0.502	-0.577
Sea level Pressure	-0.680	0.776
Surface Downwelling Shortwave Radiation	0.132	-0.243
Zonal Surface Wind Speed	0.692	-0.750
Meridional Surface Wind Speed	0.534	-0.519
Surface Air Temperature	0.590	-0.677
Air Temperature @ 200hpa	0.152	-0.181
Air Temperature @ 500hpa	0.043	-0.081
Convective Precipitation	0.196	-0.327

Table 5.7 Correlation coefficient for Rungagora using CGCM3 model

Predictors	**Correlation coefficient**	
	Precipitation	**Dry Days**
Total Soil Moisture Content (mrso)	0.521	-0.489
Total Precipitation	0.545	-0.627
Convective Precipitation	0.576	-0.667
Sea Level Pressure	-0.653	0.751
Surface Downscaling Shortwave Radiation	0.173	-0.284
Snow Melt	-0.347	0.395

Surface Air Temperature	0.674	-0.751
Surface Temperature	0.675	-0.750
Zonal Surface Wind Speed	0.451	-0.559
Relative Humidity @ 200hpa	0.371	-0.582
Relative Humidity @500hpa	0.540	-0.606
Relative Humidity @ 850hpa	0.544	-0.515
Temperature @ 500hpa	0.509	-0.652
Temperature @ 850hpa	0.638	-0.755
GeopotentialHeight @ 500hpa	0.678	-0.648
GeopotentialHeight @ 850hpa	0.640	-0.613
Zonal Wind Speed @ 200hpa	0.630	0.677
Zonal Wind Speed @ 500 hpa	-0.545	0.658
Zonal Wind Speed @ 850hpa	-0.627	0.631
Meridional Wind Speed@200hpa	-0.608	0.095
Meridional Wind Speed@500hpa	-0.206	0.367
Meridional Wind Speed@ 850hpa	-0.270	-0.109
Meridional Surface Wind Speed	0.134	-0.323

Table 5.8 Correlation coefficient for Rungagora using HadCM3 model

Predictors	**Correlation coefficient**	
	Precipitation	**Dry Days**
Specific Humidity	0.761	-0.871
Total Precipitation	0.657	-0.652
Sea level Pressure	-0.810	0.759
Surface Downwelling Shortwave Radiation	0.159	-0.012
Zonal Surface Wind Speed	0.759	-0.837
Meridional Surface Wind Speed	0.559	-0.760
Surface Air Temperature	0.729	-0.661
Air Temperature @ 200hpa	0.173	-0.244
Air Temperature @ 500hpa	0.051	-0.078
Convective Precipitation	0.251	-0.125

Table 5.9 Correlation coefficient for Sockietting using CGCM3 model

Predictors	**Correlation coefficient**	
	Precipitation	**Dry Days**
Total Soil Moisture Content (mrso)	0.594	-0.721
Total Precipitation	0.632	-0.610
Convective Precipitation	0.683	-0.648
Sea Level Pressure	-0.784	0.777
Surface Downscaling Shortwave Radiation	0.222	0.002
Snow Melt	-0.431	0.499
Surface Air Temperature	0.779	-0.834
Surface Temperature	0.780	-0.837
Zonal Surface Wind Speed	0.374	-0.345

Relative Humidity @ 200hpa	0.415	-0.752
Relative Humidity @500hpa	0.718	-0.776
Relative Humidity @ 850hpa	0.720	-0.757
Temperature @ 500hpa	0.561	-0.828
Temperature @ 850hpa	0.704	-0.807
GeopotentialHeight @ 500hpa	0.776	-0.839
GeopotentialHeight @ 850hpa	0.699	-0.823
Zonal Wind Speed @ 200hpa	0.659	0.613
Zonal Wind Speed @ 500 hpa	-0.700	0.844
Zonal Wind Speed @ 850hpa	-0.741	0.837
Meridional Wind Speed@200hpa	-0.731	0.297
Meridional Wind Speed@500hpa	-0.080	0.496
Meridional Wind Speed@ 850hpa	-0.391	-0.307
Meridional Surface Wind Speed	0.195	-0.095

Table 5.10 Correlation coefficient for Sockietting using HadCM3 model

The above correlation coefficients have been computed using IPCC AR4 dataset. In this study two types of approaches have been used,

1) Initially,three GCM models have been compared for Furkatting station using IPCC AR4, without using NCEP data. But, later MRI-CGCM2 model has been eliminated for other stations due to the weak correlation and also dataset is not available for future,
2) NCEP reanalysis data have been used for calibration and validation, and this model has been used to project the future precipitation using HadCM3 model in IPCC AR3. This approach has been used in Bokakhat. This approach has been applied for precipitation model only.

Predictors	**Correlation coefficient**	
	NCEP	**HadCM3(IPCC-AR3)**
Surface Air Temperature	0.769	-0.779
Pressure	-0.774	-
Relative Humidity	0.552	0.797
Sea level Pressure	-0.808	-0.692
Zonal Surface Wind Speed	0.541	-0.813
Meridional Surface Wind Speed	0.755	-
Air Temperature @ 850hpa	0.789	-0.753
Air Temperature @ 500hpa	0.754	-0.621
Air Temperature @ 200hpa	0.758	-0.525
Geo-potential height @ 850hpa	-0.760	-
Geo-potential height @ 500hpa	0.644	-
Geo-potential height @ 200hpa	0.746	-
Zonal Wind Speed @ 850hpa	0.577	-

Zonal Wind Speed @ 500hpa	-0.729	-
Zonal Wind Speed @ 200hpa	-0.760	-
Meridional Wind Speed @850hpa	0.817	-
Meridional Wind Speed @500hpa	0.288	-
Meridional Wind Speed @200hpa	-0.488	-
Relative Humidity @ 850hpa	0.598	-
Relative Humidity @ 500hpa	0.689	-

Table 5.11 Correlation coefficient for Bokakhat using Third assessment data

A few numbers of predictors for each station has been chosen based on the above test of correlation and stepwise regression. The chosen predictors are tabulated below.

Station	**Predictands**	**Predictors**	
		CGCM3	**HadCM3**
Furkatting	Precipitation	Specific Humidity Total Precipitation Sea Level Pressure Meriodional surface win d speed Surface air temperature	Sea level Pressure Surface air temperature Air temperature @ 850hpa Geo-potential height @500hpa Zonal wind speed @ 200hpa
	No. of Dry Days	Sea level pressure Total precipitation	Sea level pressure
Lengree	Precipitation	Specific Humidity Sea level pressure Air temperature	Sea level pressure Surface air temperature Air temperature @ 850hpa
	No. of Dry Days	Sea level pressure	Sea level pressure
Rungagora	Precipitation	Specific Humidity	Air temperature @ 500hpa
	No. of Dry Days	Sea level pressure	Sea level pressure
Sockieting	Precipitation	Sea level pressure	Zonal wind speed @ 500hpa
	No. of Dry Days	Specific Humidity Total precipitation	Zonal wind speed @ 500hpa

Table 5.12 Predictor selection using forth assessment data

Station	**Predictands**	**Predictors**	
		NCEP	**HadCM3**
Bokakhat	Precipitation	Sea level Pressure Air temperature @ 500hpa	Sea level Pressure Air temperature @ 500hpa

Table 5.13 Predictor selection using third assessment data

5.4 MODEL CALIBRATION AND VALIDATION

The Calibration of the models has been done by three approaches with the following relations.

1) Multiple Linear Regressions without additive residual

$$y_i = \beta_1 x_{i1} + \beta_2 x_{i2} + ...\beta_p x_{ip}$$

2) Multiple Linear Regressions with residuals

$$y_i = \beta_1 x_{i1} + \beta_2 x_{i2} + ...\beta_p x_{ip} + r_i$$

3) Multiple Linear Regressions with a multiplying factor.

$$y_i = (\beta_1 x_{i1} + \beta_2 x_{i2} + ...\beta_p x_{ip})m$$

Where, y_i=precipitation, x_i=predictors, β =coefficient, r_i = residual, m=multiplying factor. The calibration and validation for each station has been explained below with the graphical plots.

5.4.1 PRECIPITATION MODEL

Above mentioned (5.3.1.2) approaches have been applied for the precipitation model. The model has been developed for first four stations (Furkatting, Lengree, Rungagora, and Sockieting) by IPCC-AR4 data, which is available only for a short time period (2001-2010) therefore, alternative years has been chosen for calibration and remaining years for validation. The AR3 data have been used for Bokakhat station. This station has data for long time period and therefore the model developed by using NCEP data is more reliable.

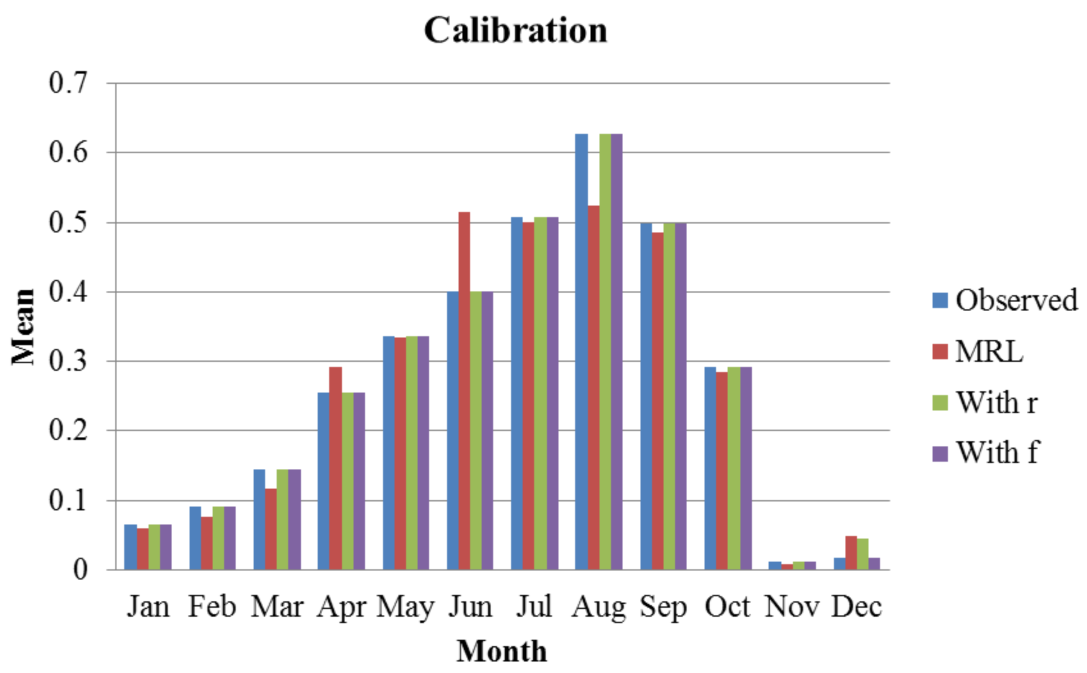

Fig 5.1 Calibration for Furkatting using CGCM3 model

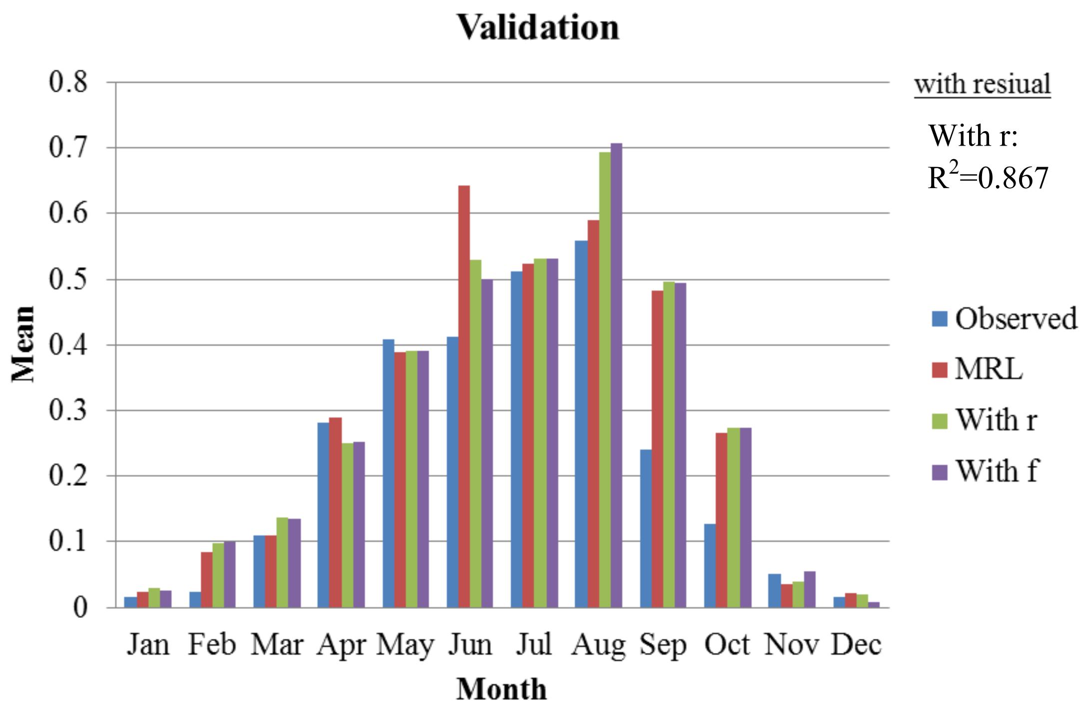

Fig. 5.2 Validation for Furkatting using CGCM3 model

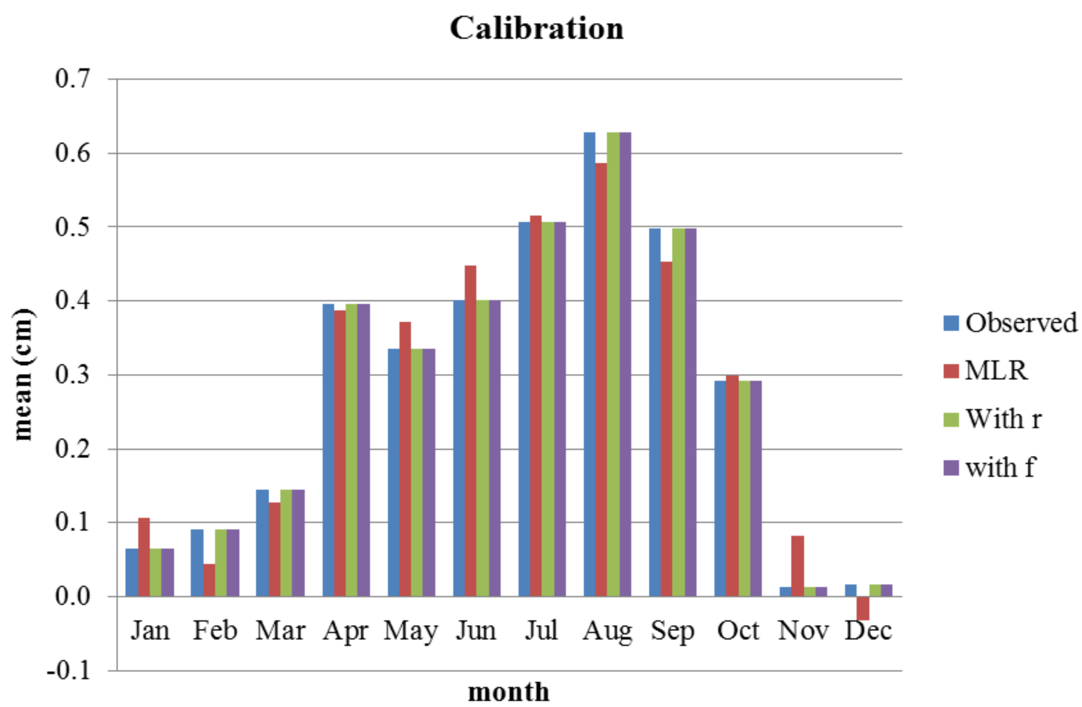

Fig 5.3 Calibration for Furkatting using HadCM3

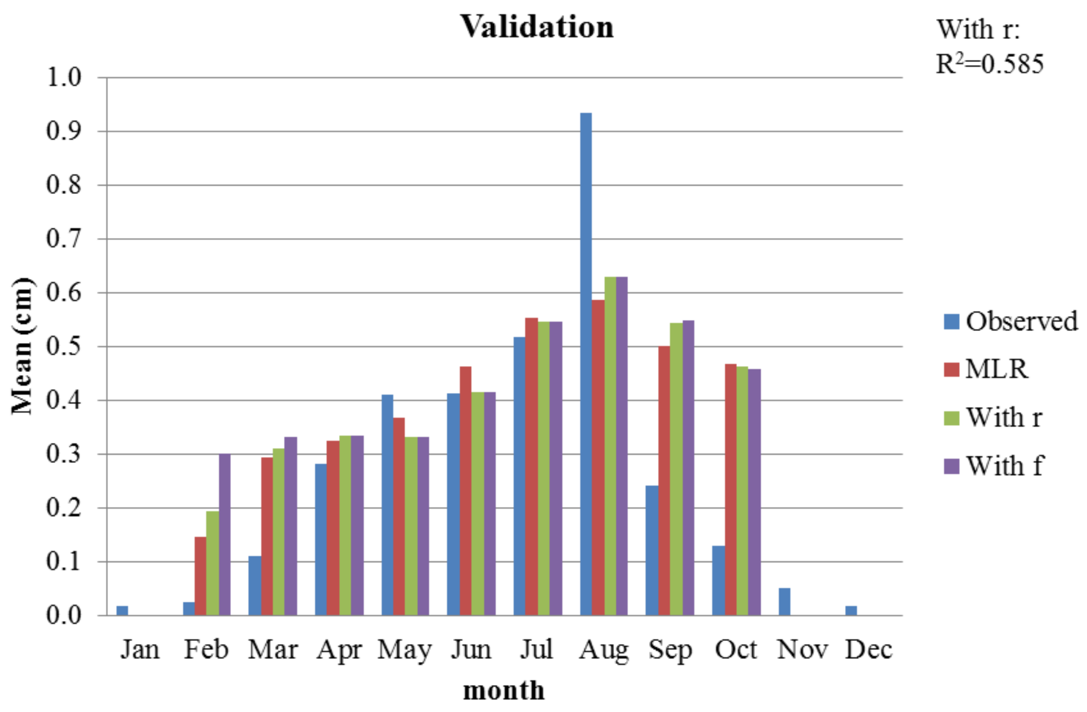

Fig 5.4 Validation for Furkatting using HadCM3

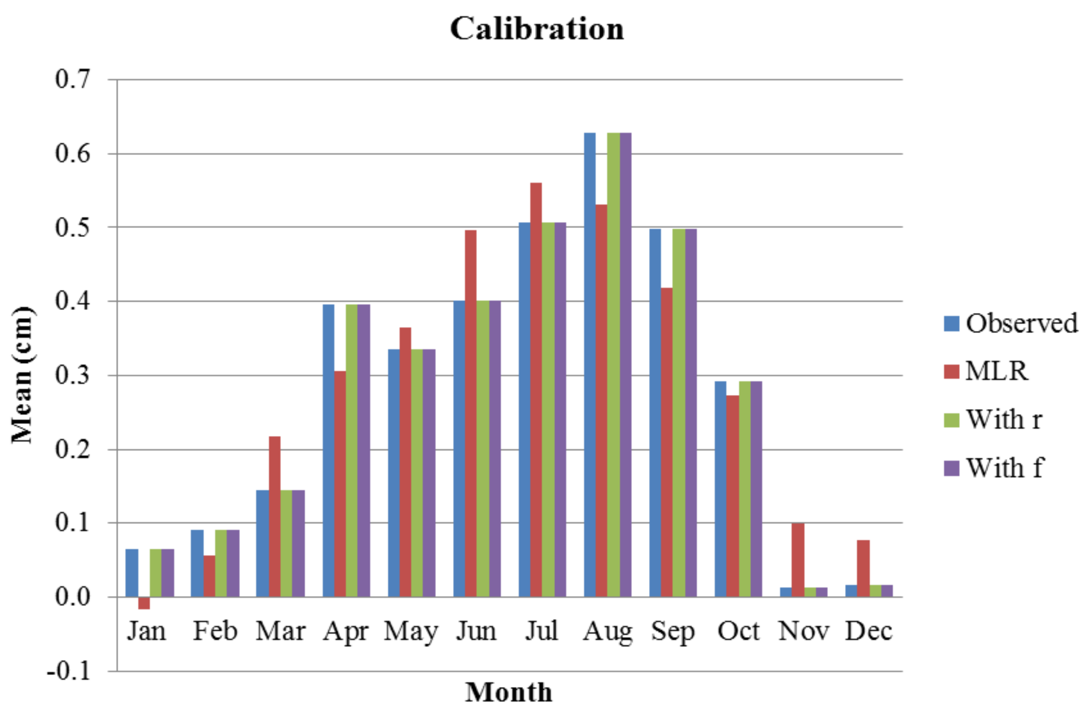

Fig 5.5 Calibration for Furkatting using MRI-CGCM2

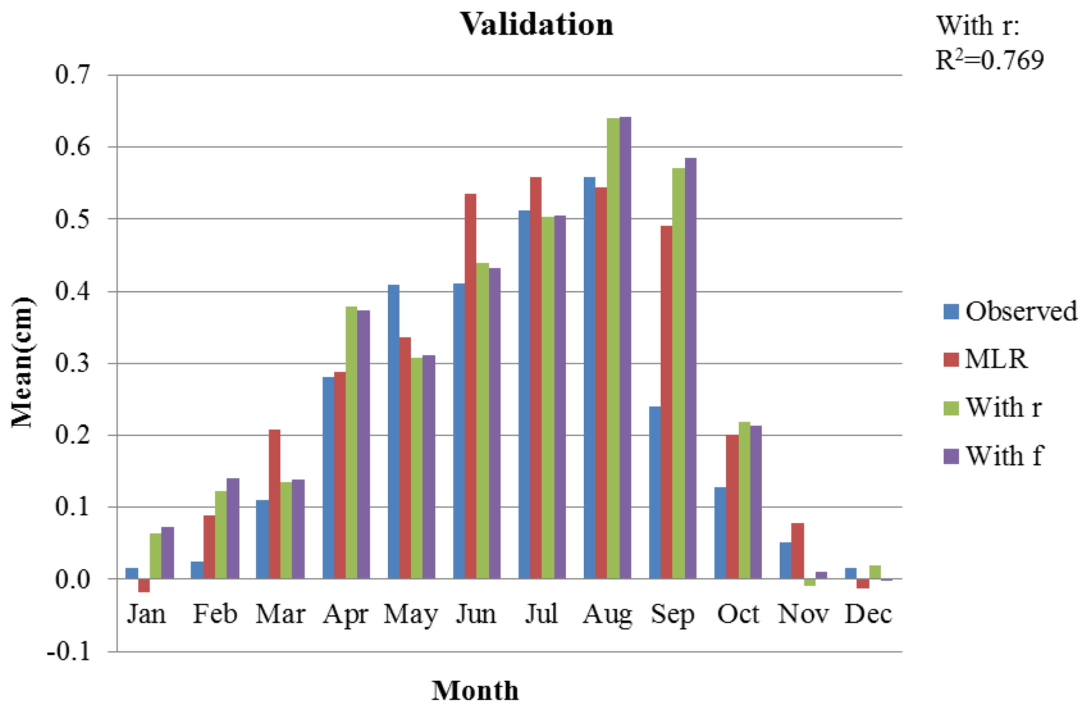

Fig 5.6 Validation for Furkatting using MRI-CGCM2

The above graph clearly shows that Multiple Linear Regression with residuals gives good calibration and validation. MRI-CGCM3 model has been eliminated for further station due to weak correlation and also unavailability of future data.

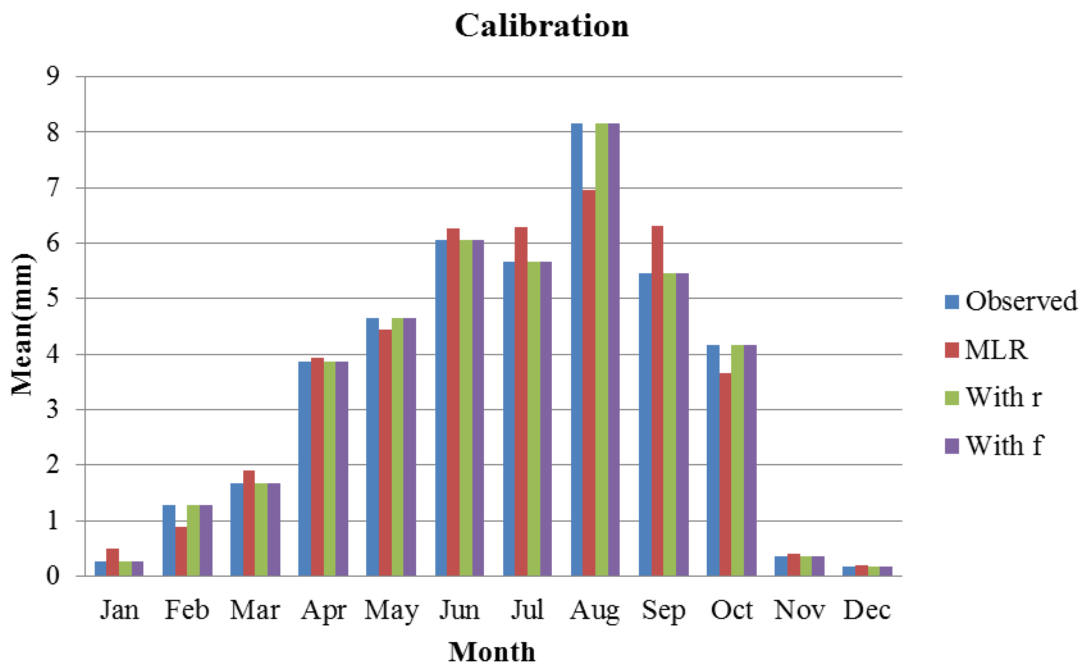

Fig 5.7 Calibration for Lengree using CGCM3

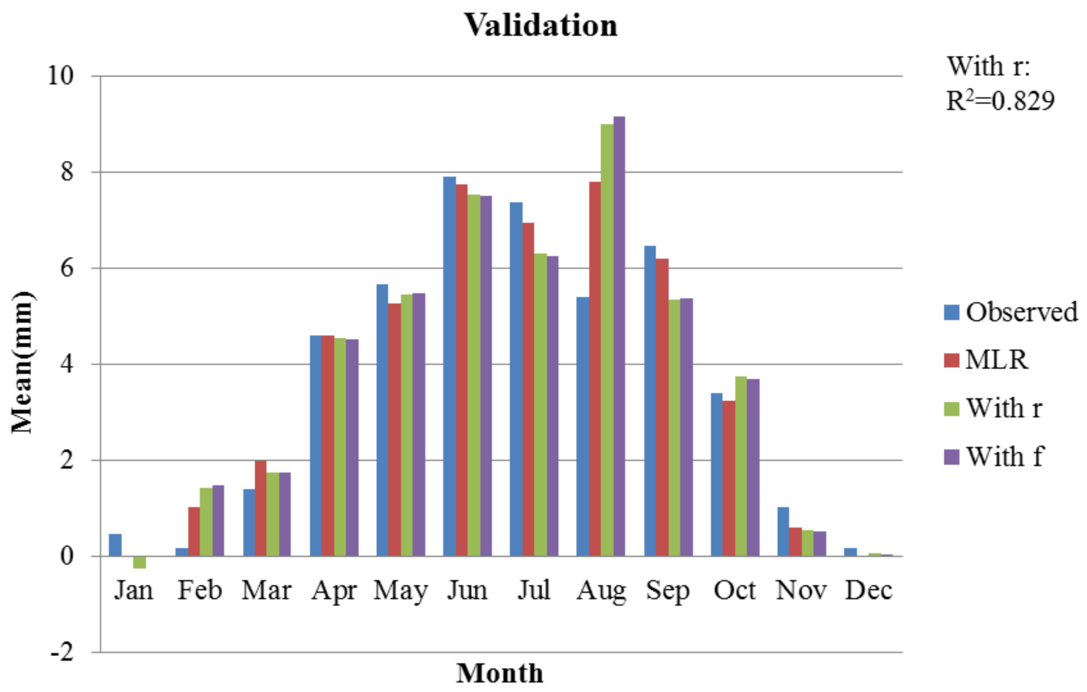

Fig 5.8 Validation for Lengree using CGCM3

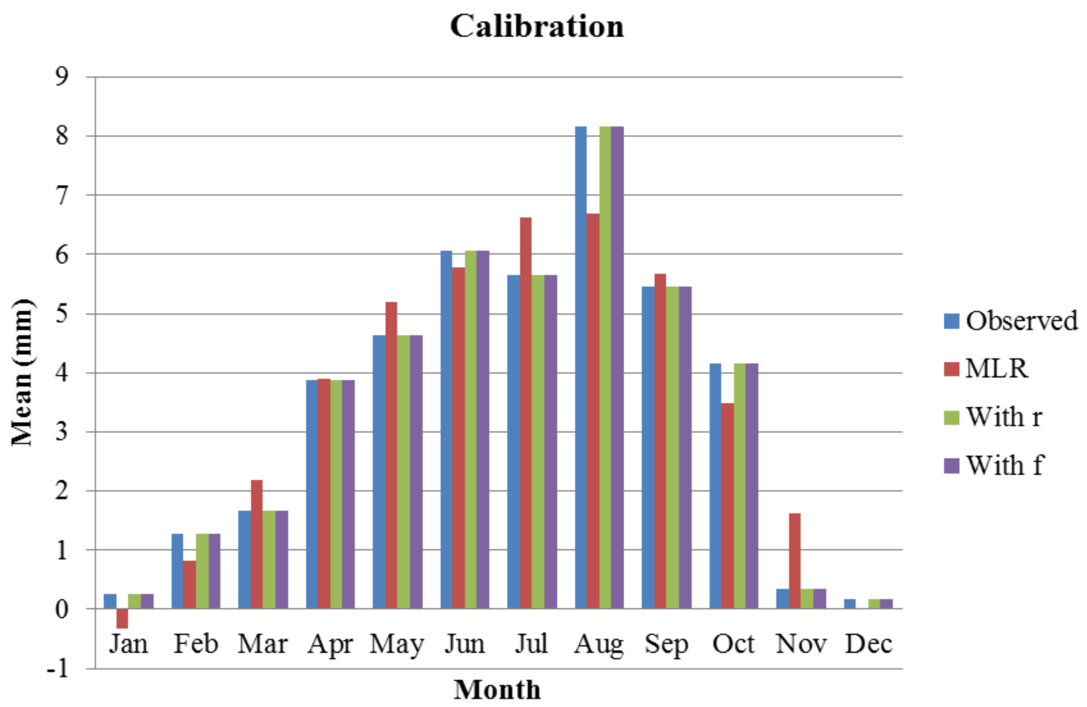

Fig 5.9 Calibration for Lengree using HadCM3

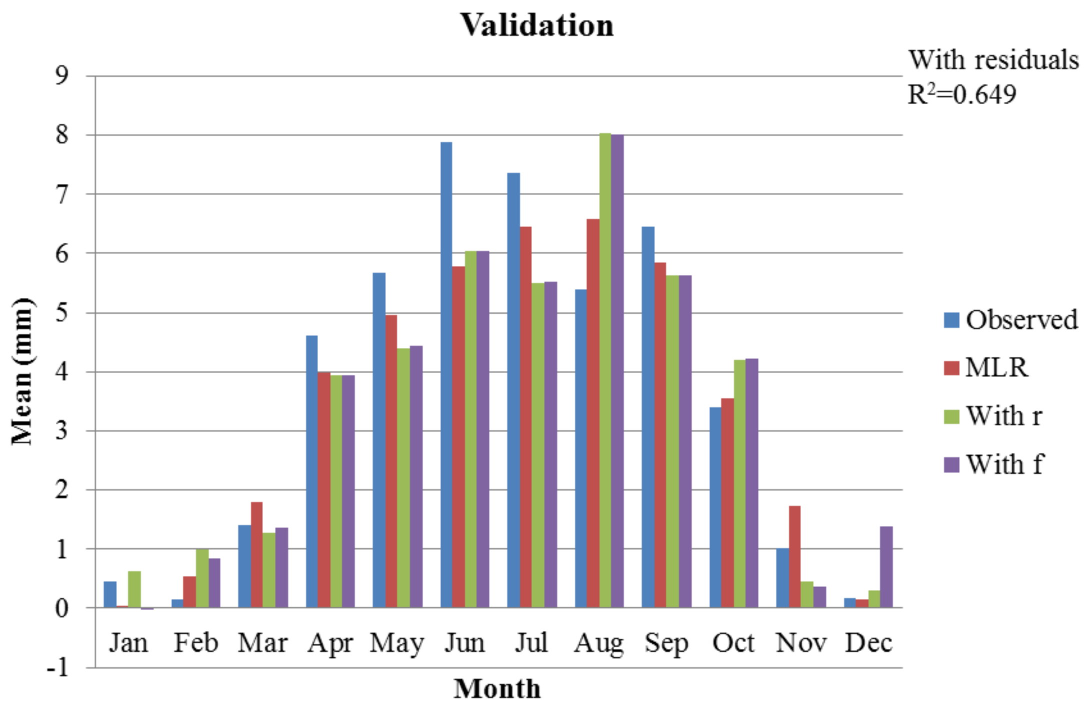

Fig 5.10 Validation for Lengree using HadCM3

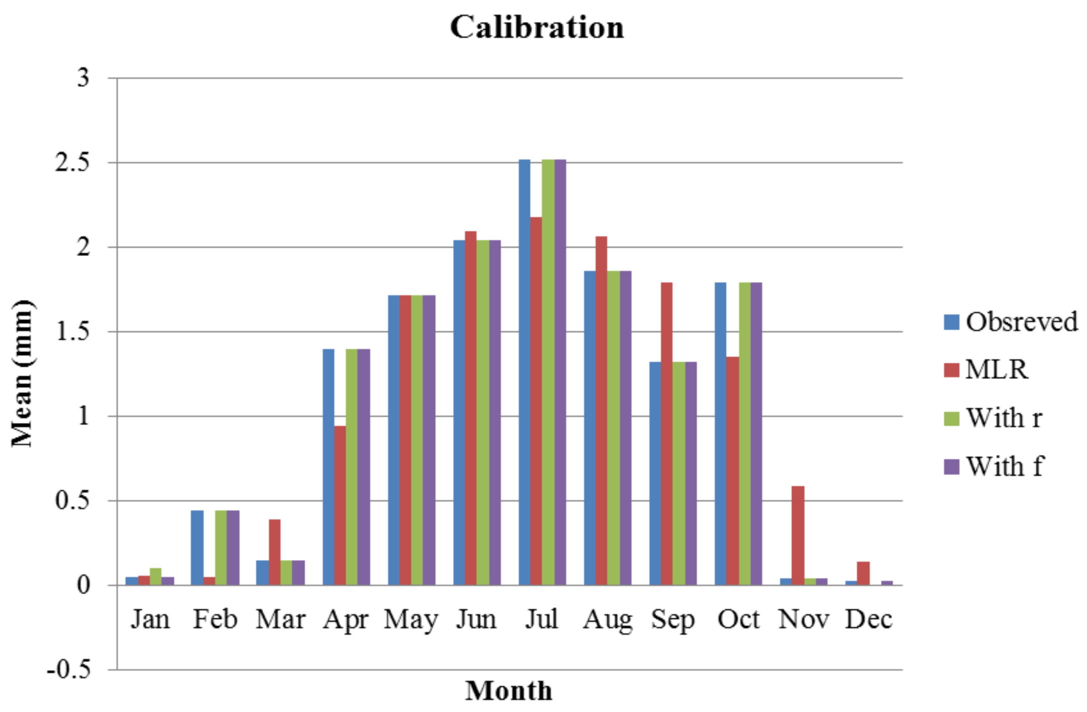

Fig 5.11 Calibration for Rungagora using CGCM3

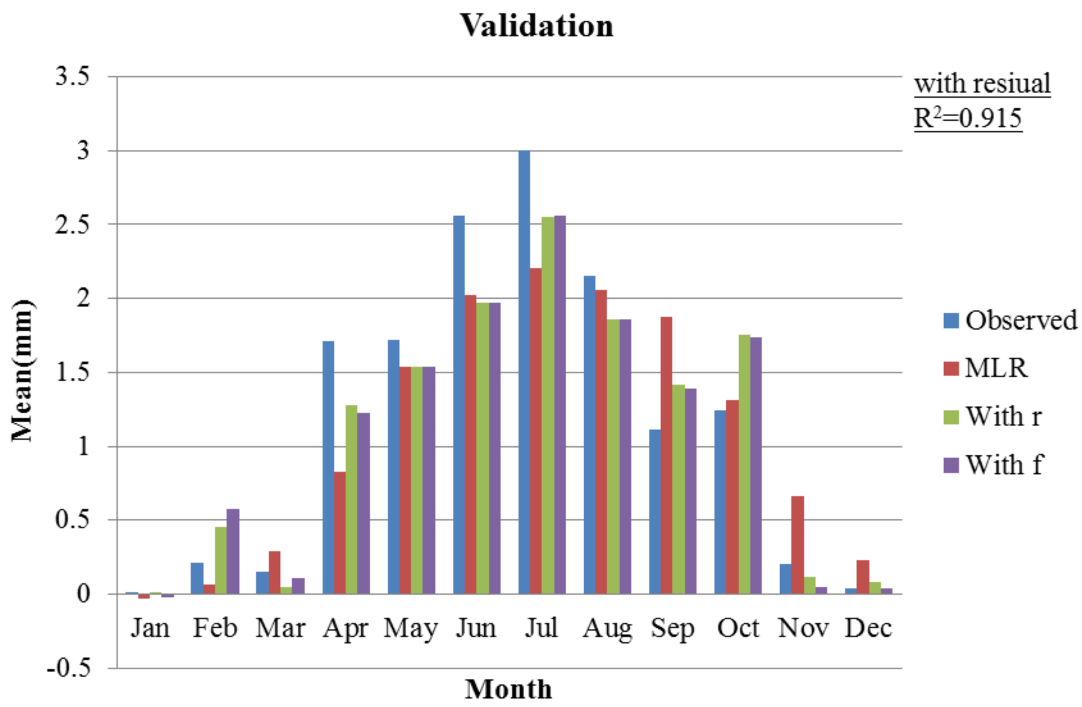

Fig 5.12 Validation for Rungagora using CGCM3

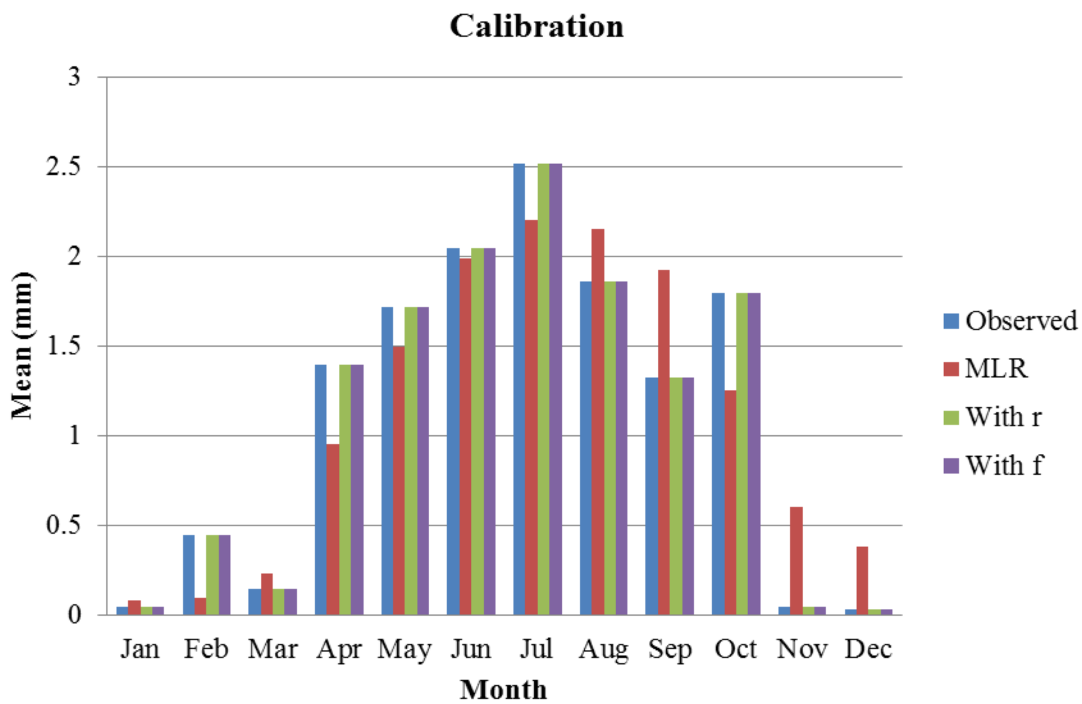

Fig 5.13 Calibration for Rungagora using HadCM3

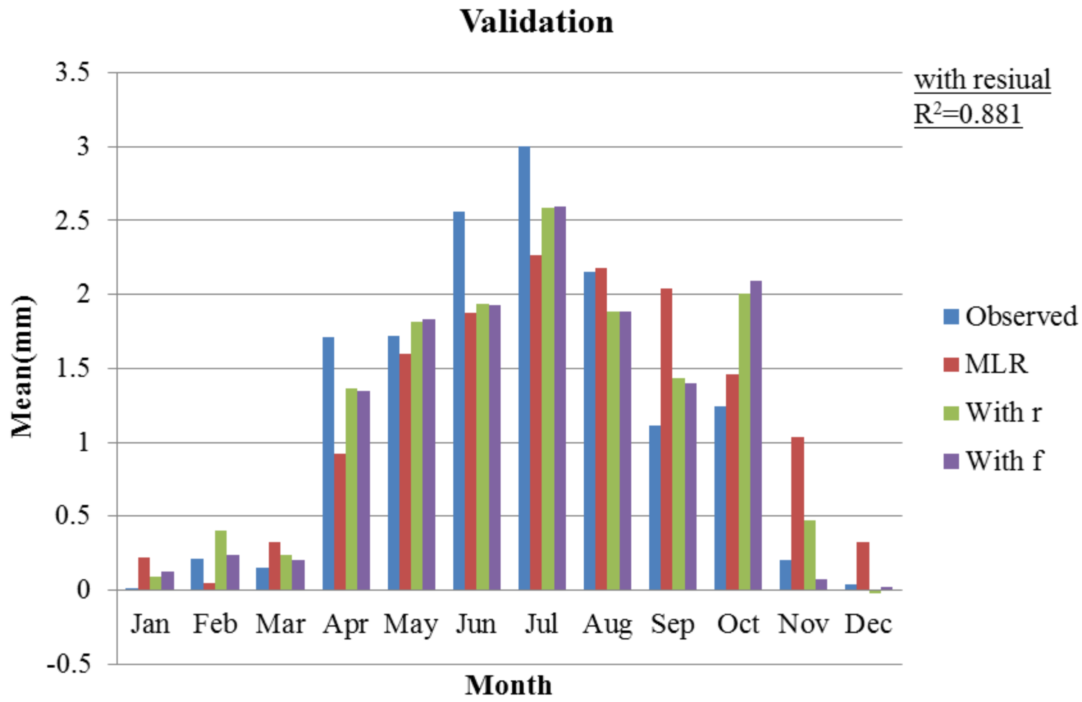

Fig 5.14 Validation for Rungagora using HadCM3

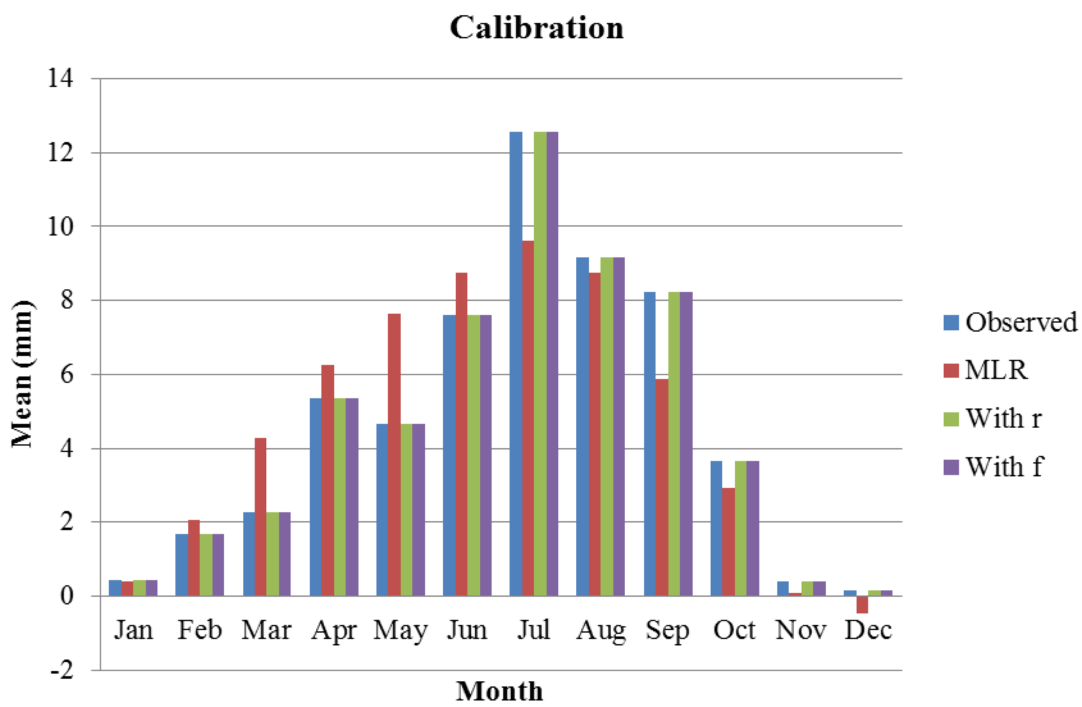

Fig 5.15 Calibration for Sockieting using CGCM3

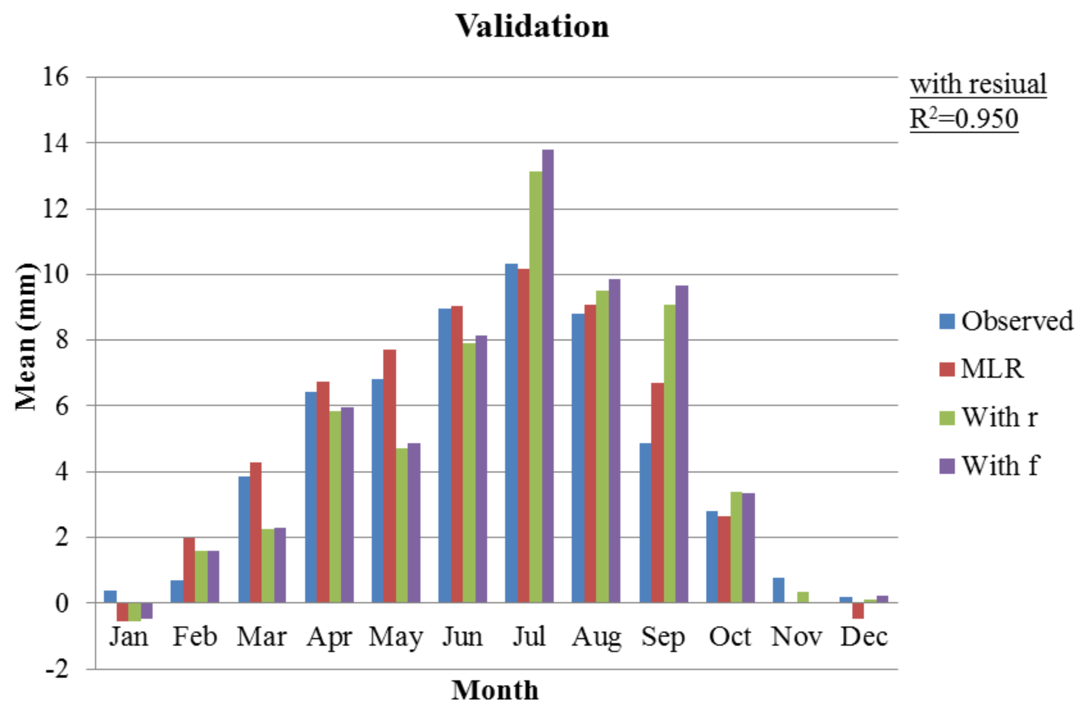

Fig 5.16 Validation for Sockieting using CGCM3

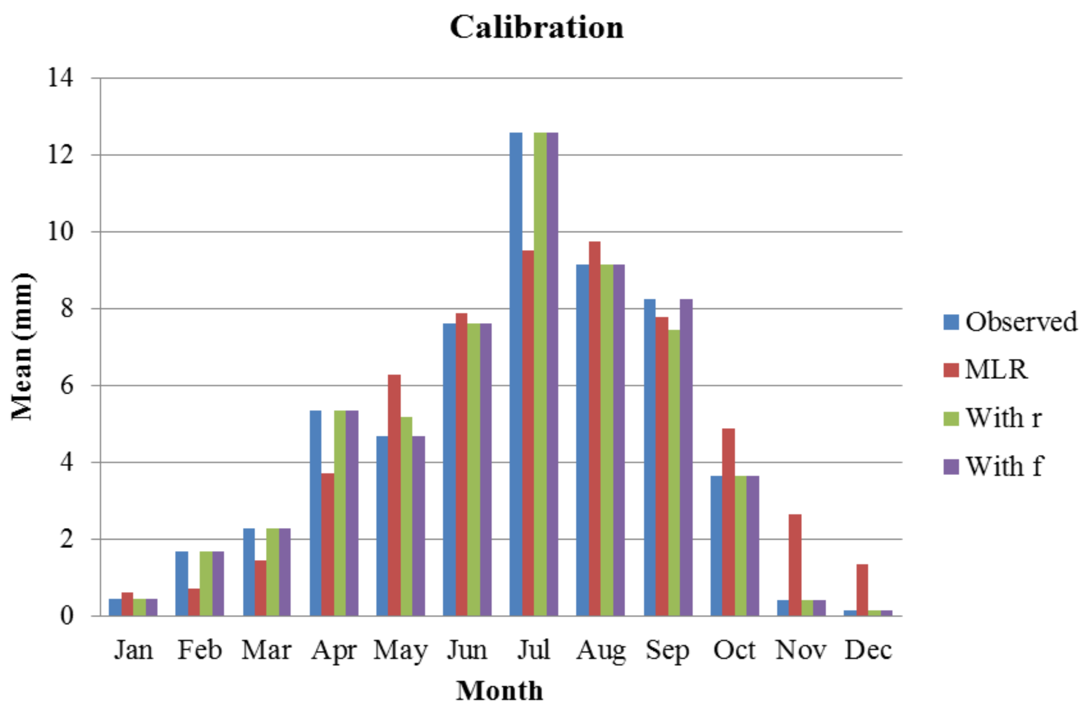

Fig 5.17 Calibration for Sockieting using HadCM3

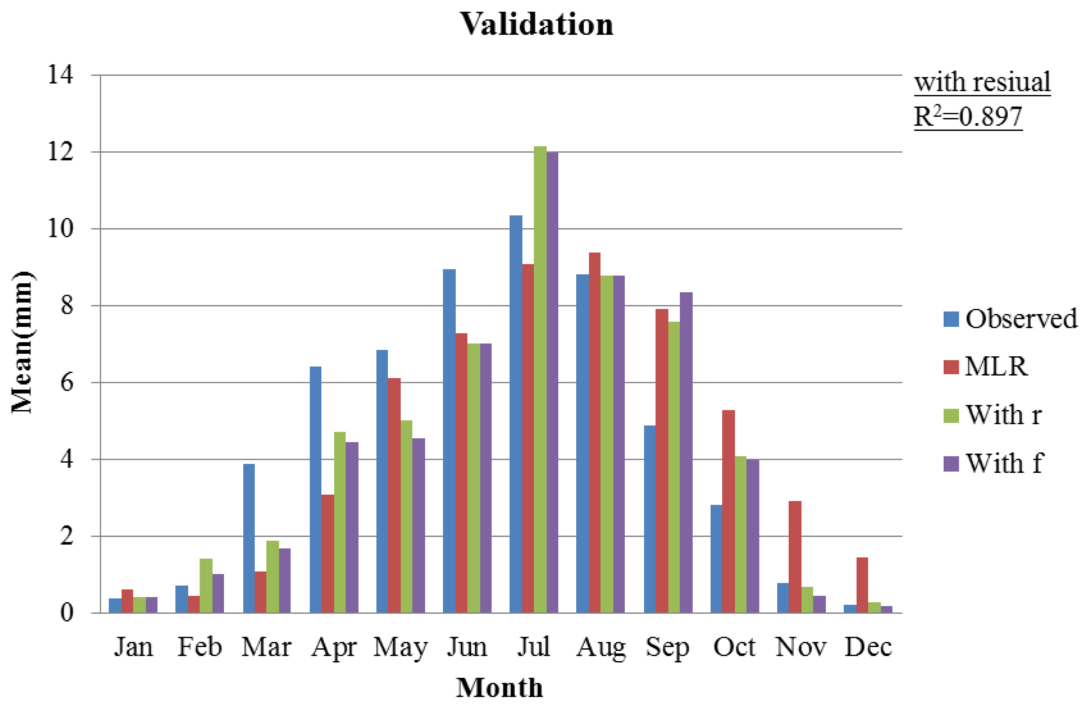

Fig 5.18 Validation for Sockieting using HadCM3

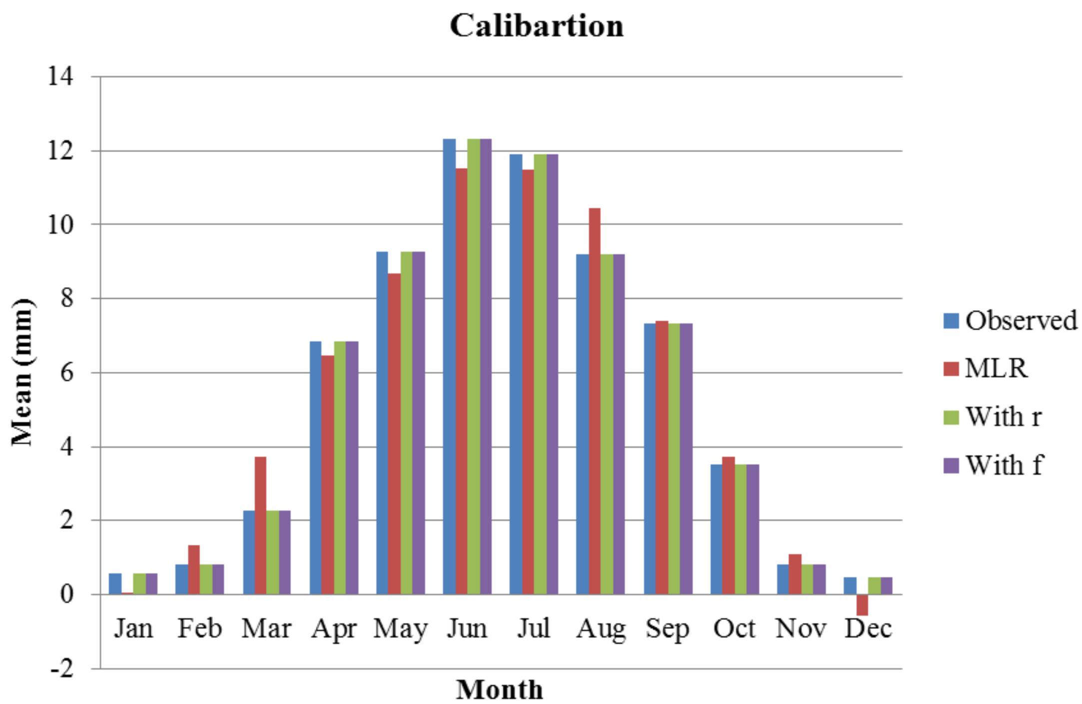

Fig 5.19 Calibration for Bokakhat using NCEP

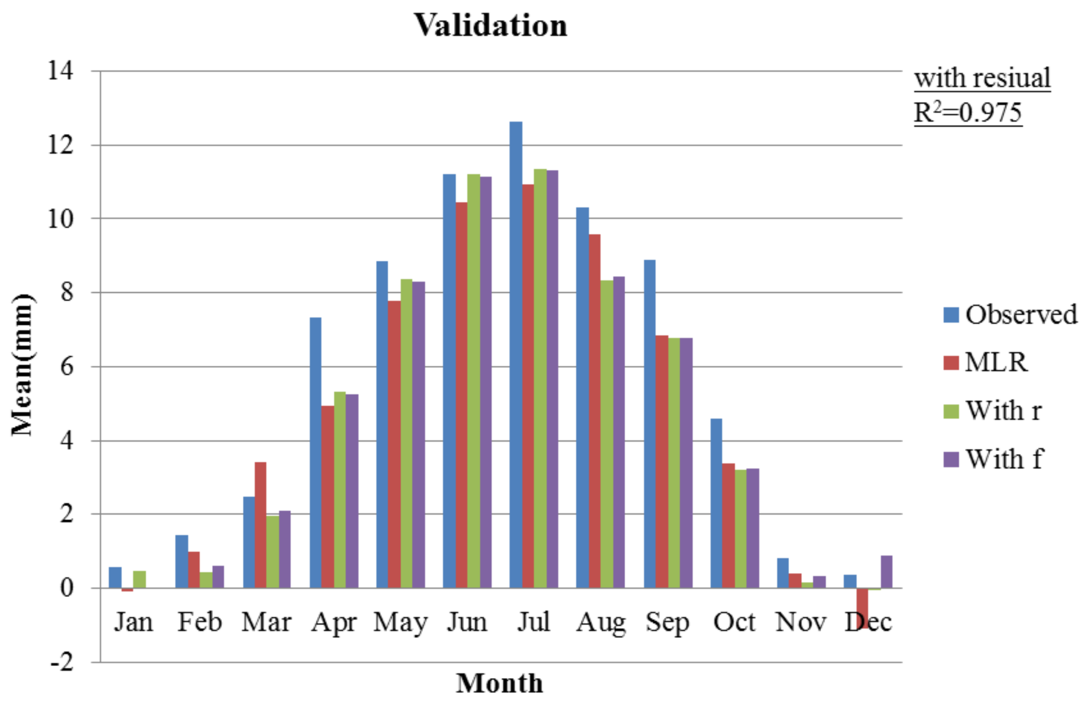

Fig 5.20 Validation for Bokakhat using NCEP

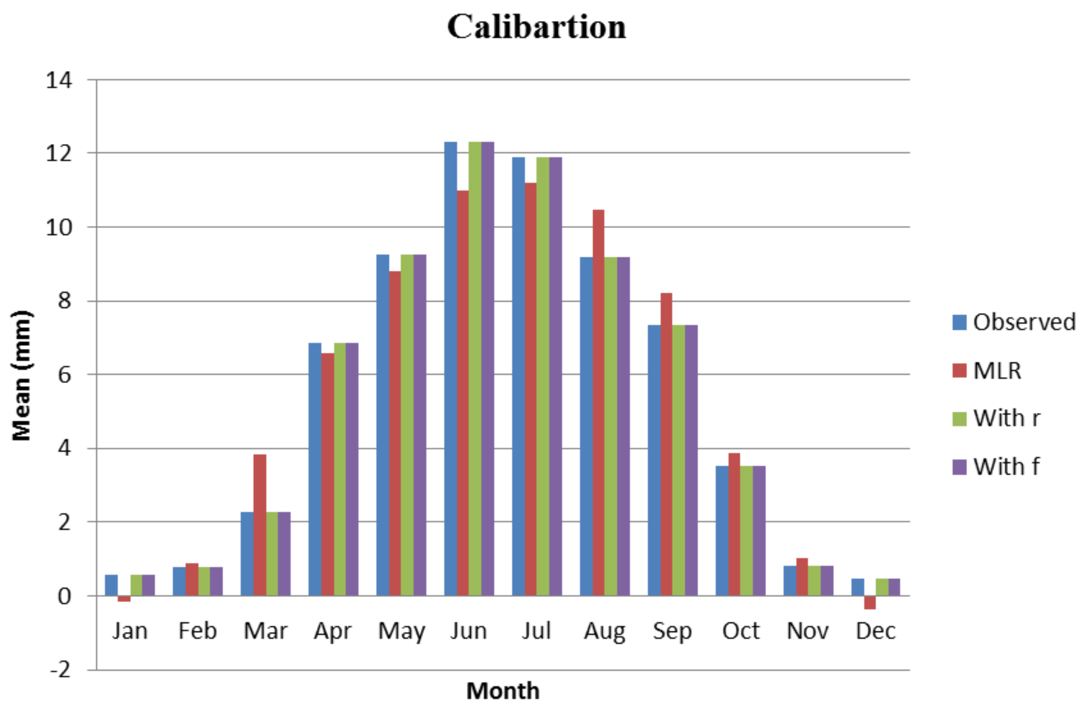

Fig 5.21 Calibration for Bokakhat using HadCM3

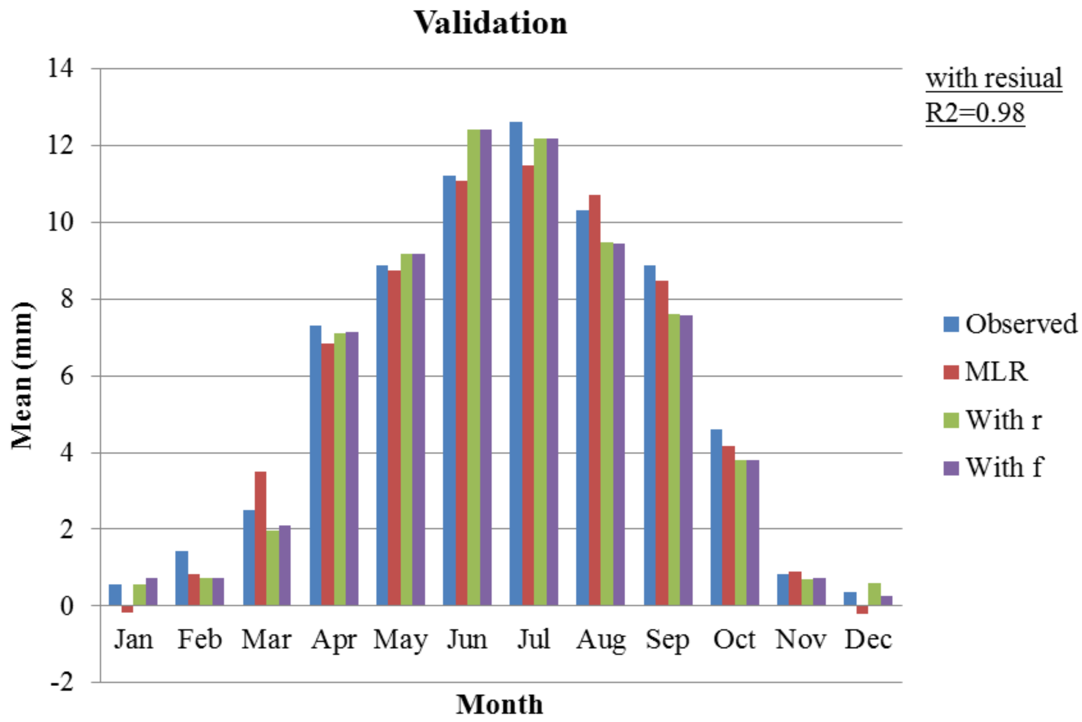

Fig 5.22 Validation for Bokakhat using HadCM3

The above results clearly show that CGCM3 is better than HadCM3 for Furkatting, Lengree, Rungagora, and Sockieting. NCEP model for Bokakhat is suitable for HadCM3. Therefore for future prediction CGCM3 Model has been used for first four stations and HadCM3 (IPCC_AR3) has been used for Bokakhat station.

5.4.2 MODEL FOR DRY DAYS

No. of dry days has been computed for Furkatting, Lengree, Rungagora and Sockieting. The time period is 2001 to 2010 for both observed and GCM data. Alternative years have been chosen for calibration and remaining years for validation. The results are presented below.

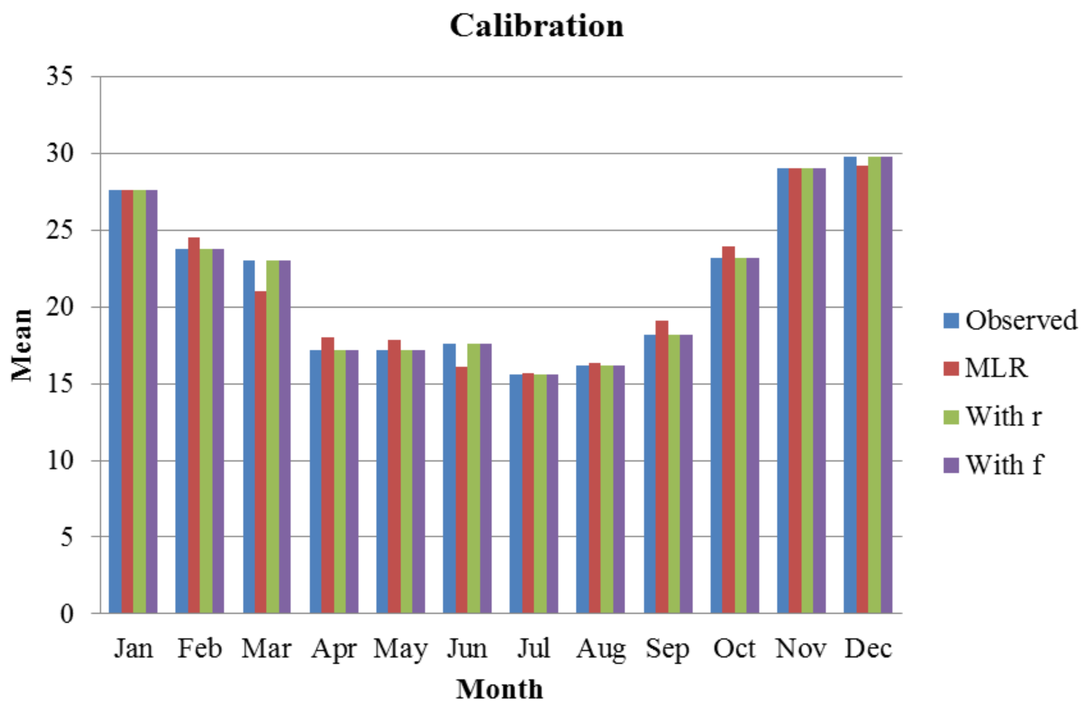

Fig. 5.23 Calibration for Furkatting Using CGCM3

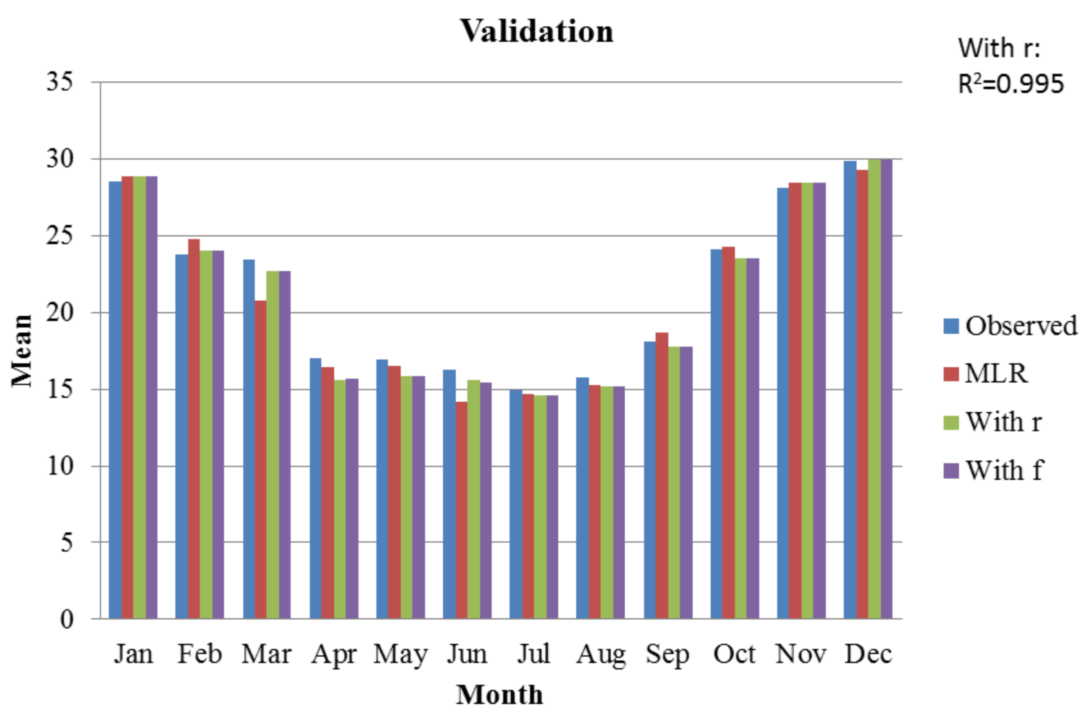

Fig. 5.24 Validation for Furkatting Using CGCM3

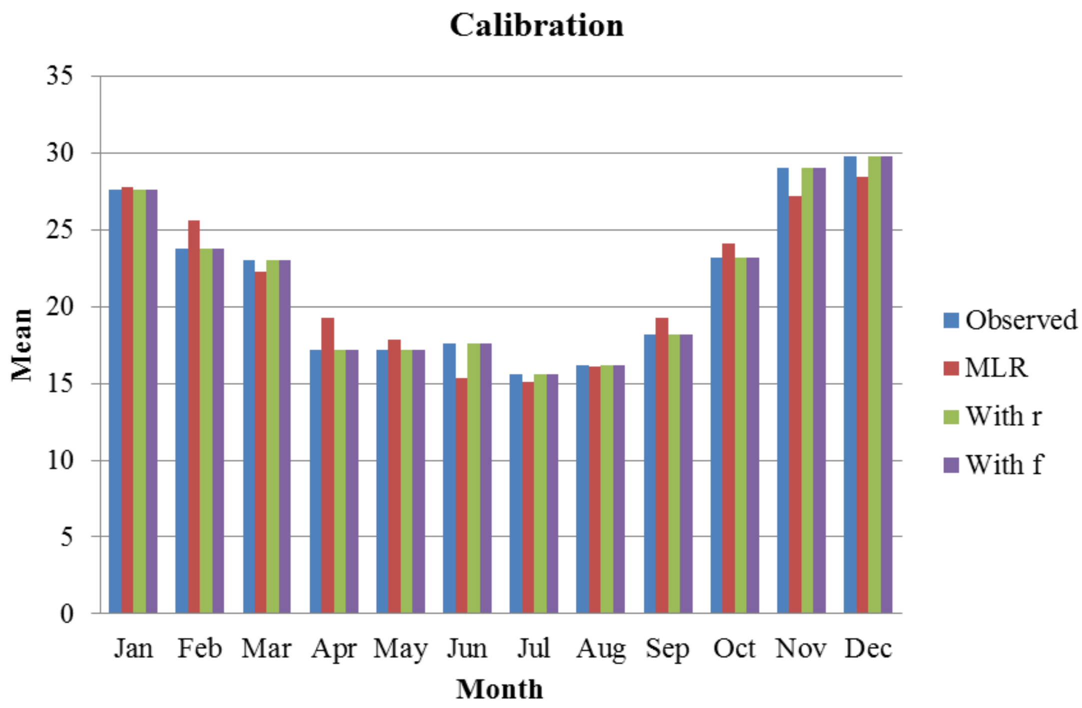

Fig. 5.25 Calibration for Furkatting using HadCM3

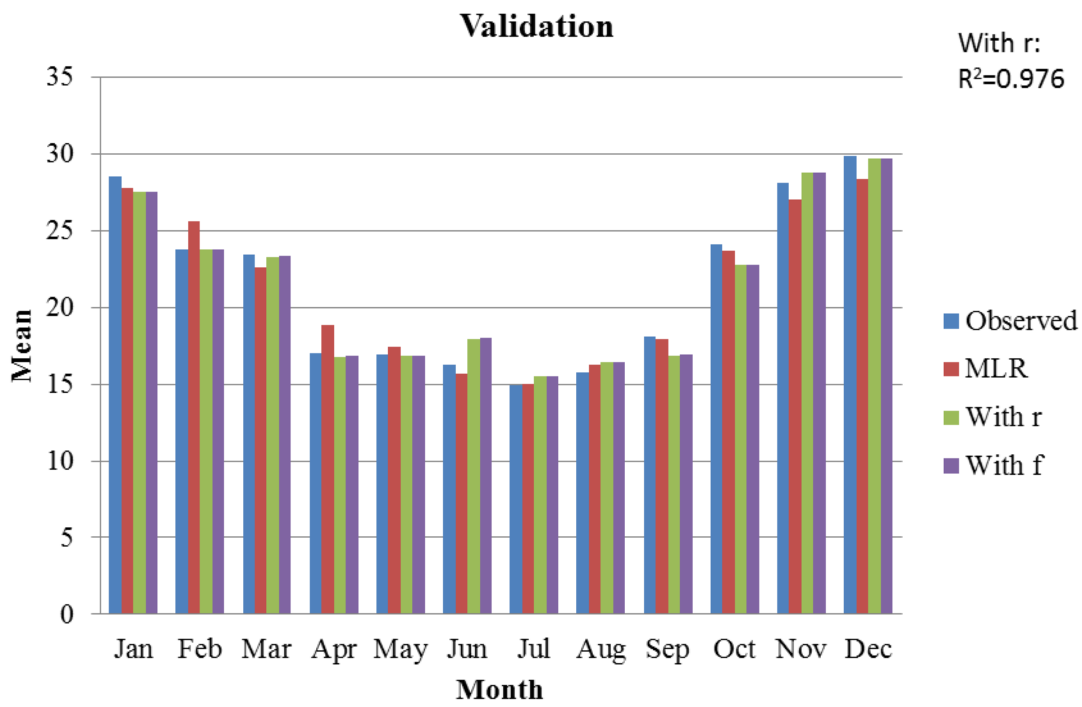

Fig. 5.26 Validation for Furkatting using HadCM3

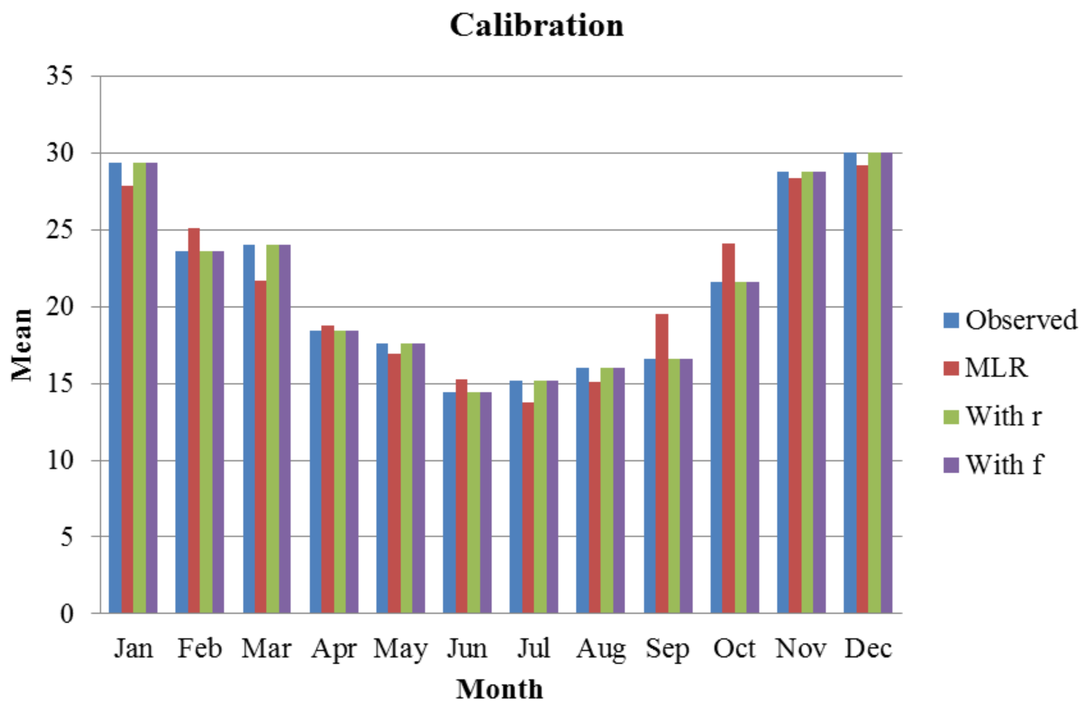

Fig. 5.27 Calibration for Lengree using CGCM3

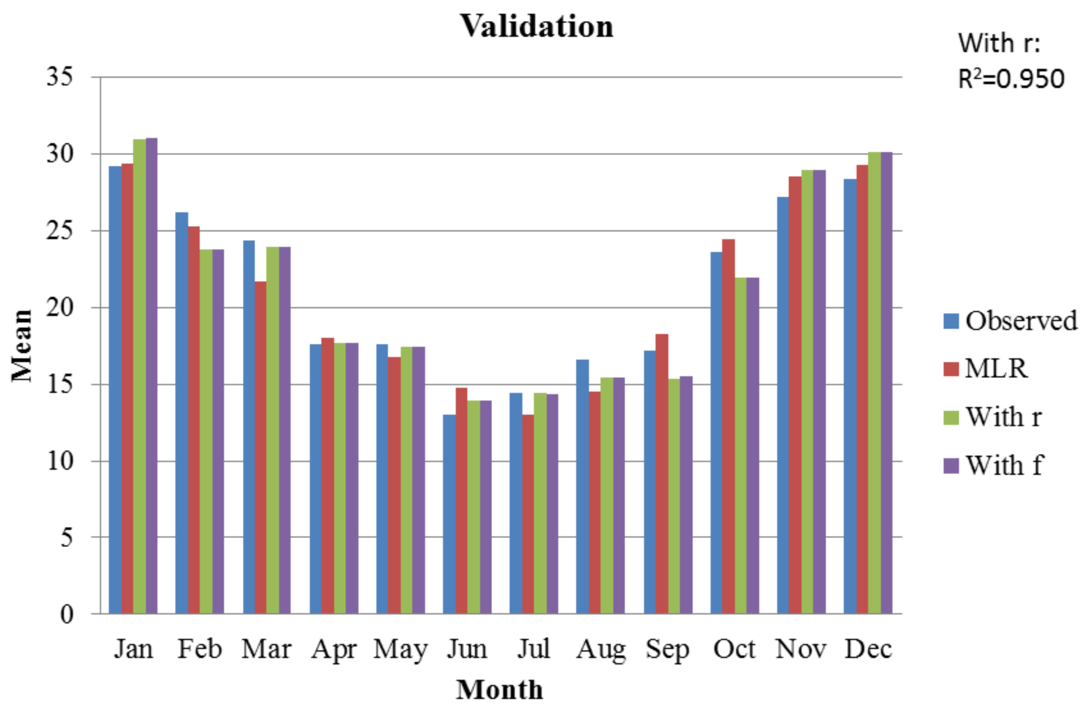

Fig. 5.28 Validation for Lengree using CGCM3

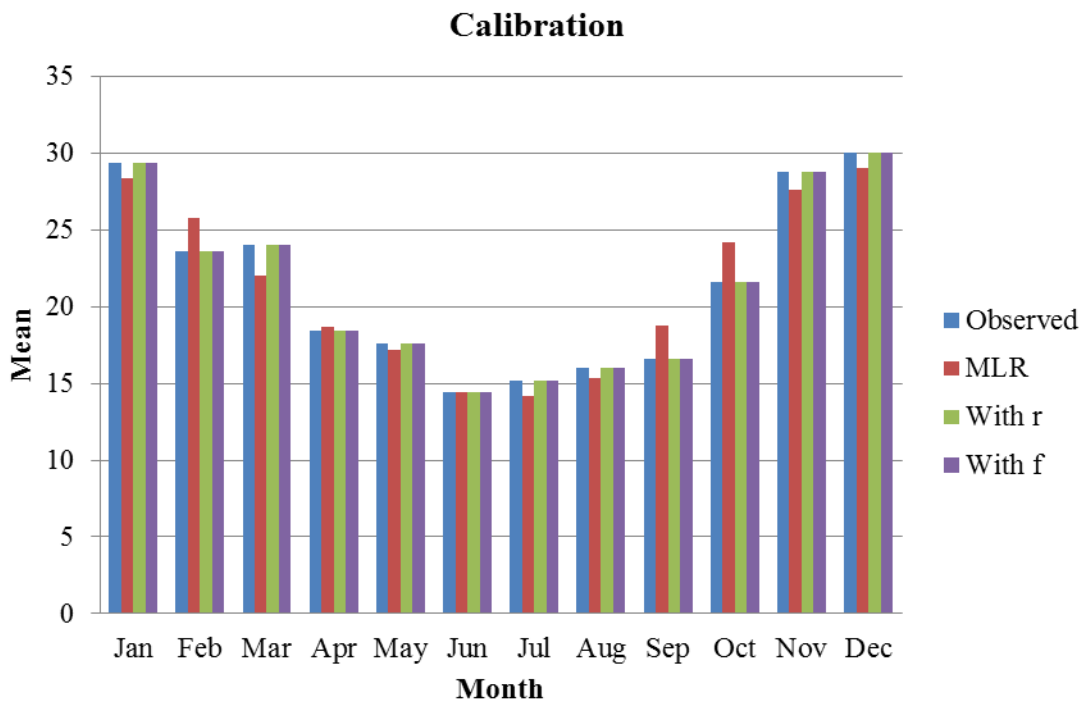

Fig. 5.29 Calibration for Lengree using HadCM3

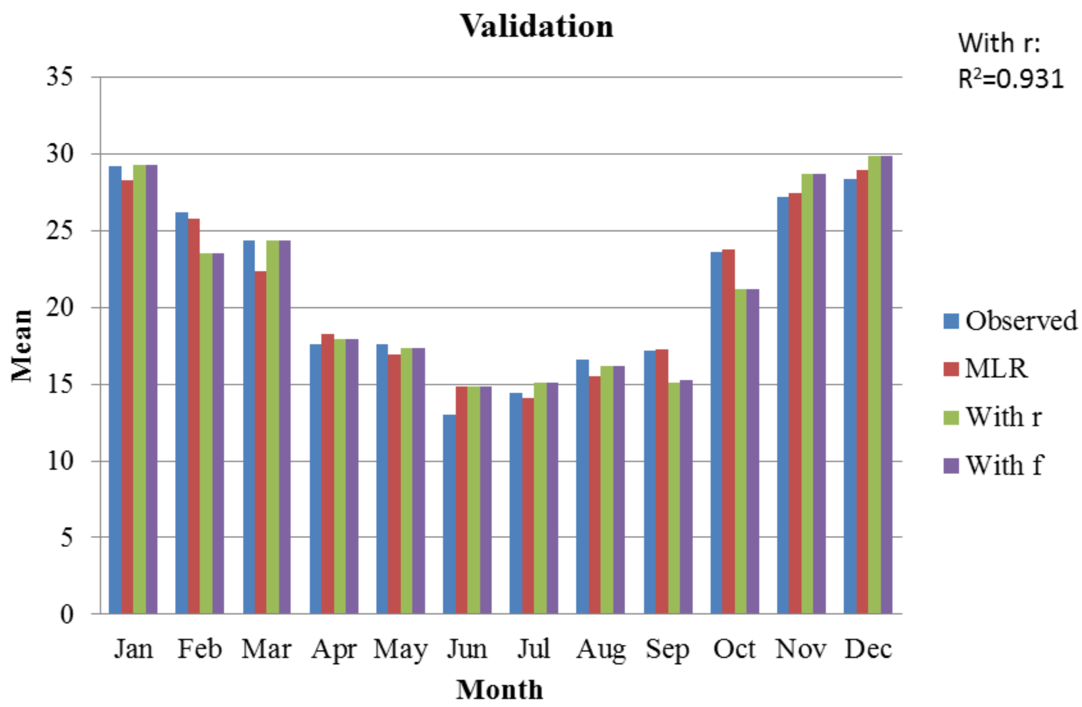

Fig. 5.30 Validation for Lengree using HadCM3

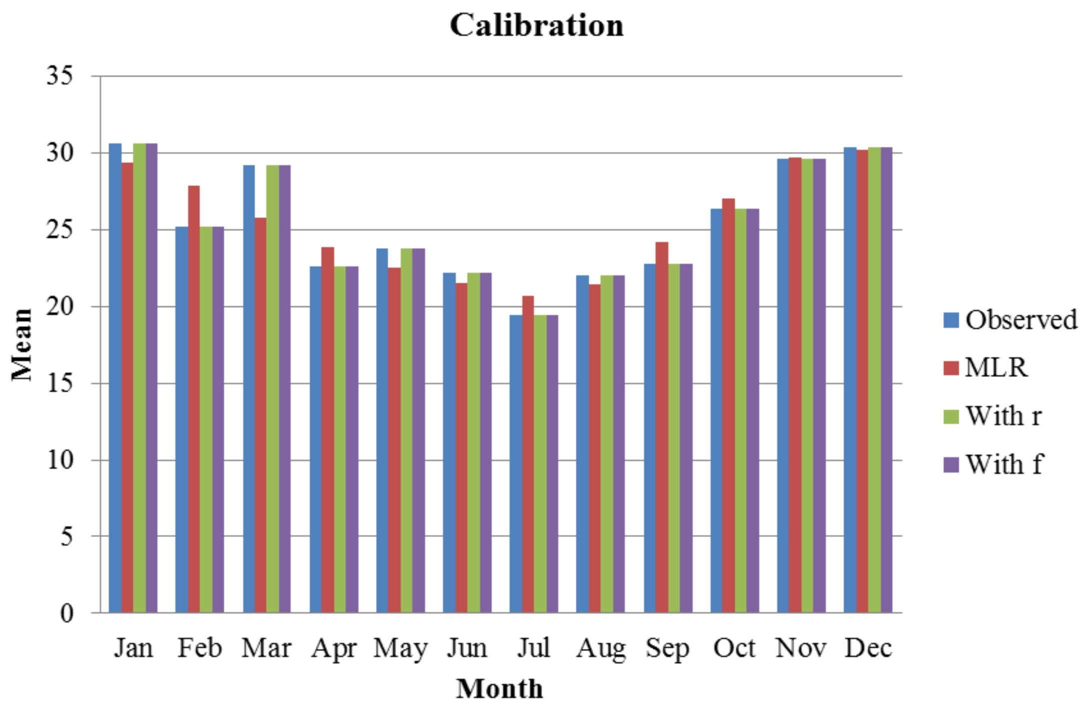

Fig 5.31 Calibration for Rungagora using CGCM3

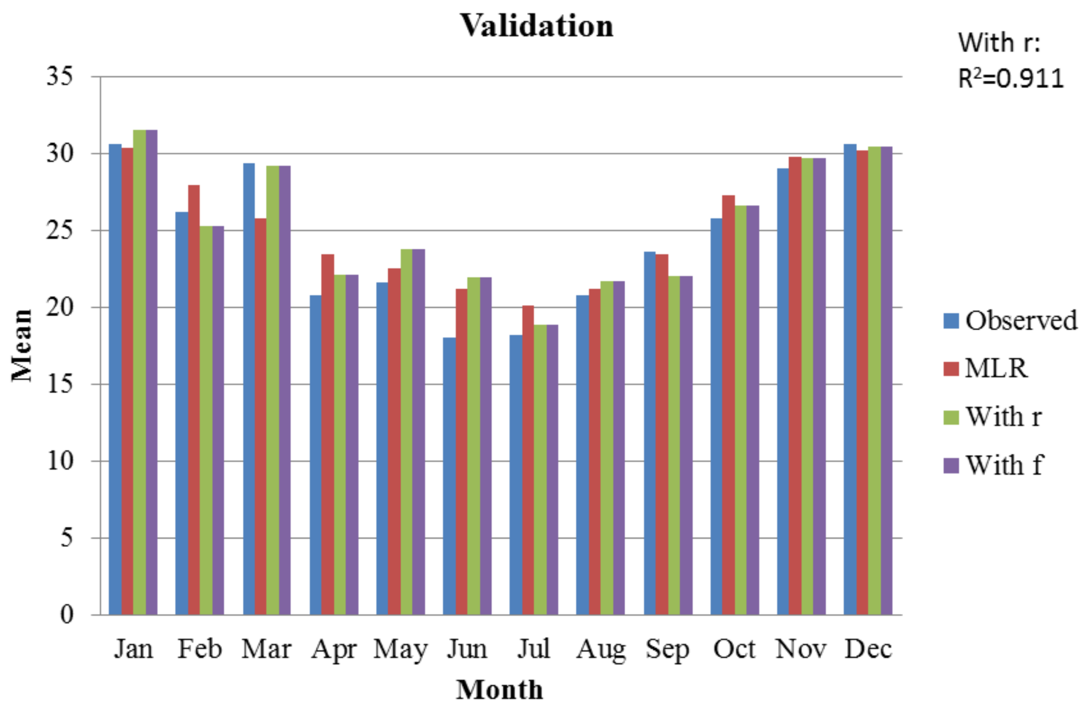

Fig 5.32 Validation for Rungagora using CGCM3

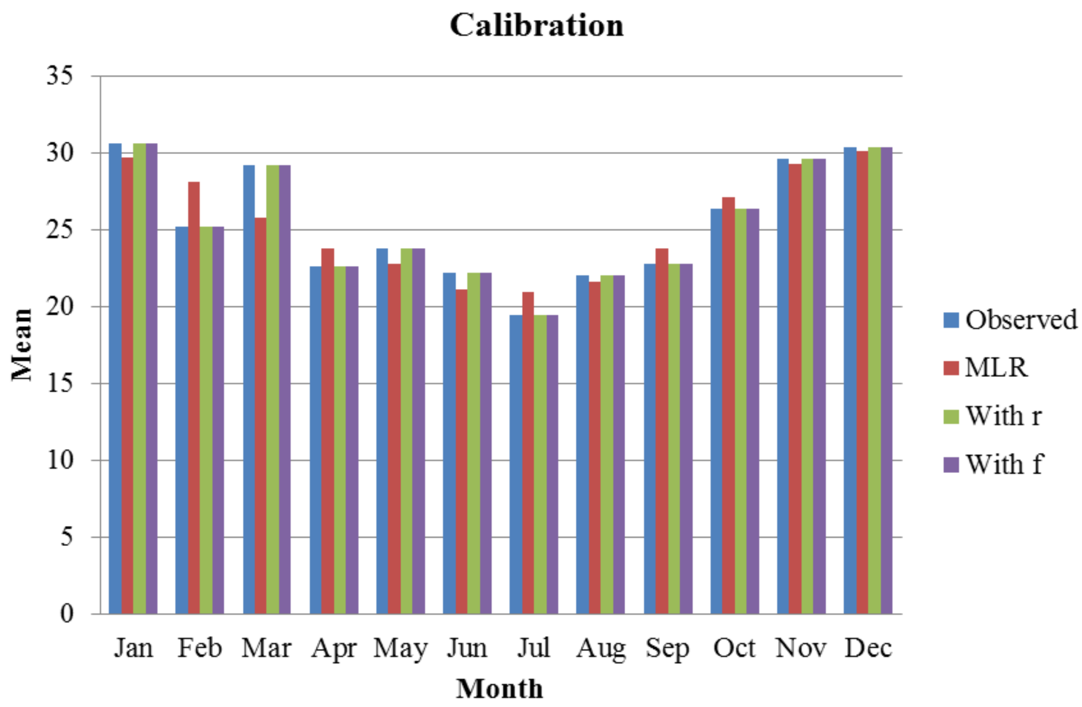

Fig 5.33 Calibration for Rungagora using HadCM3

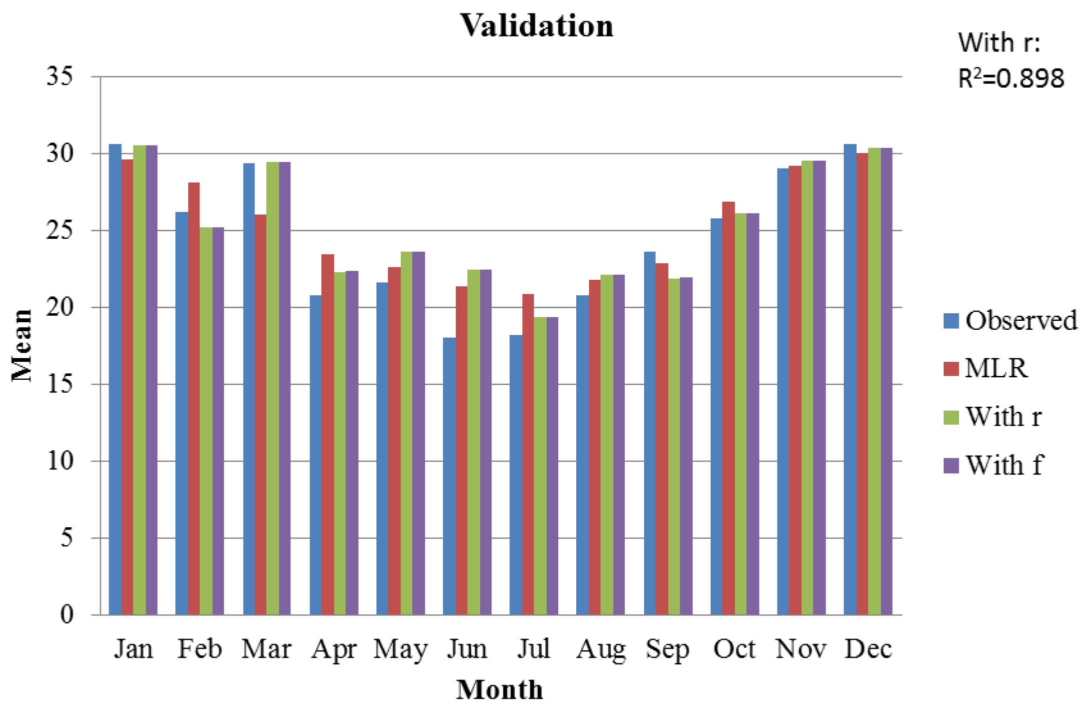

Fig 5.34 Validation for Rungagora using HadCM3

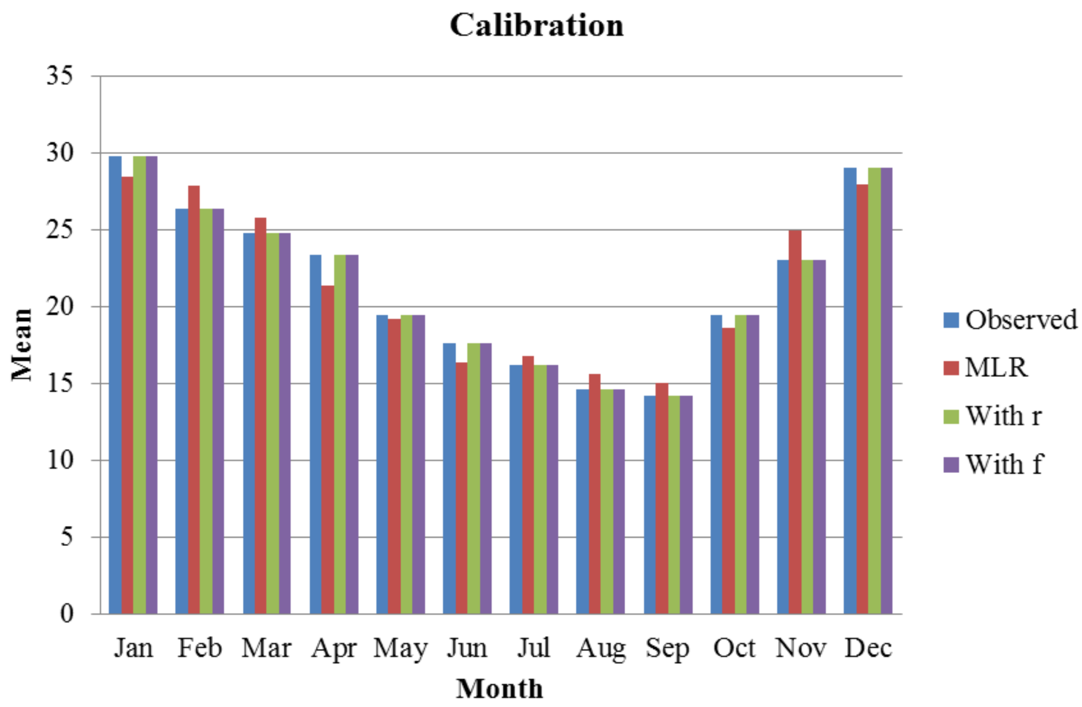

Fig. 5.35 Calibration for Sockieting using CGCM3

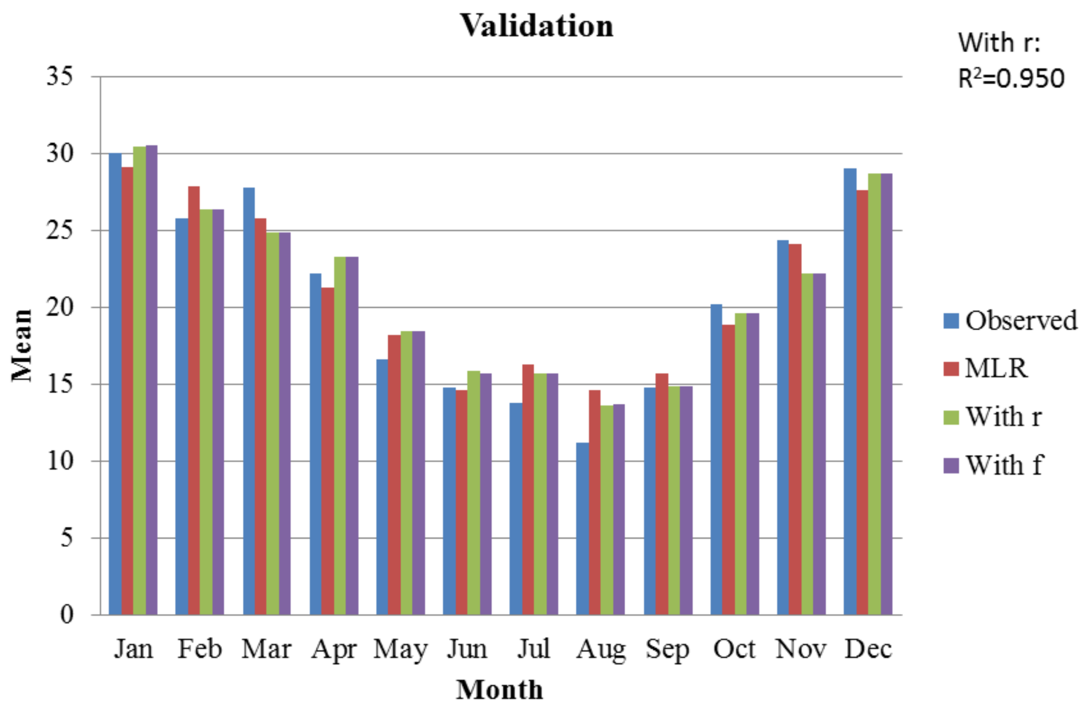

Fig. 5.36 Validation for Sockieting using CGCM3

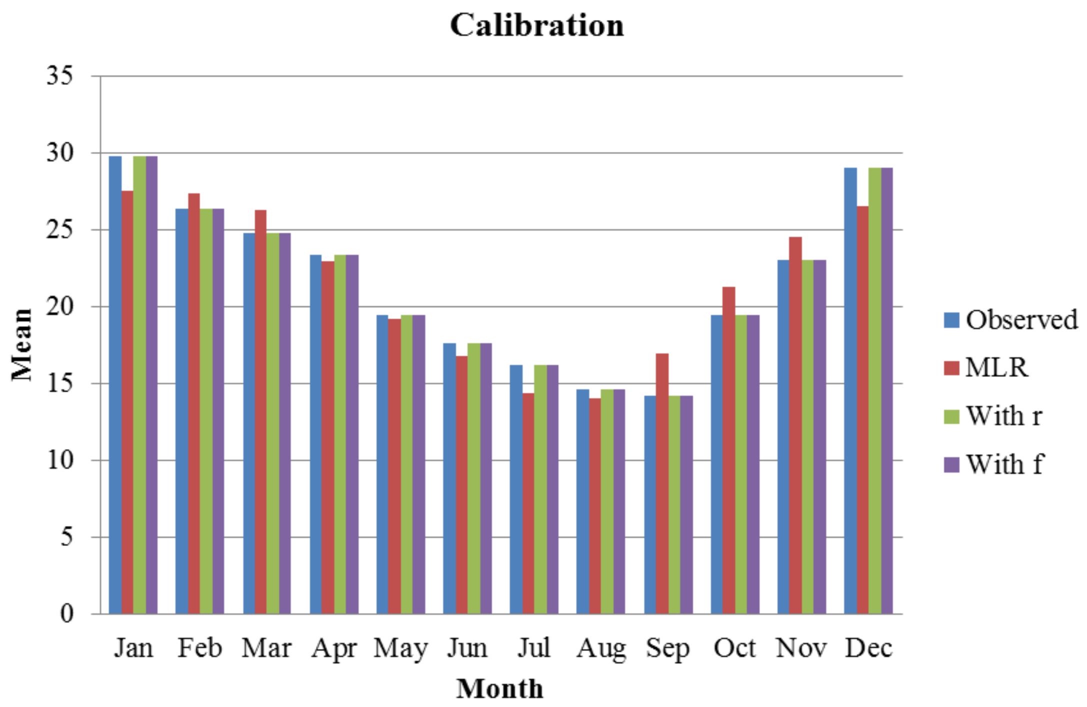

Fig. 5.37 Calibration for Sockieting using HadCM3

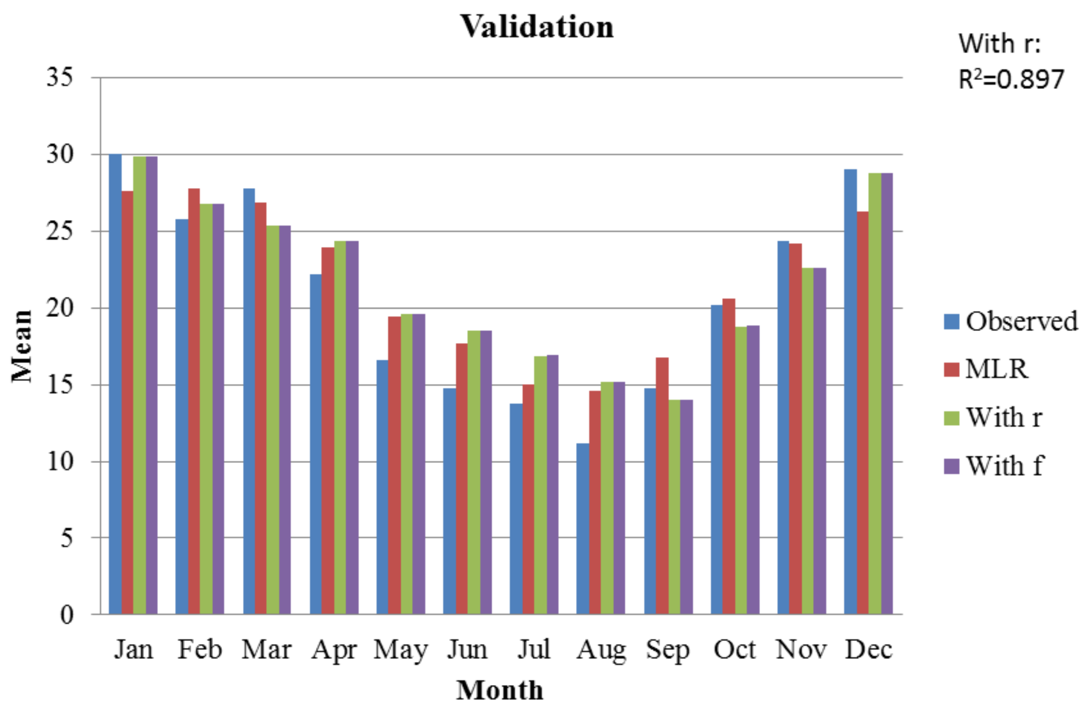

Fig. 5.38 Validation for Sockieting using HadCM3

The validation on the model for number of dry days with CGCM3 is better the HadCM3. Therefore CGCM3 model has been used for predicting future numbers of dry days.

5.5 FUTURE DATA GENERATION

The above models have been used to predict the future three set of data 2011 to 2040, 2041to 2070, 2071 to 2100. CGCM3 model with A2 Scenario has been used for the forecasting. The outputs are plotted below.

5.5.1 FORECASTING PRECIPITATION

The precipitation has been forecasted using the model and presented below.

In the below graphs, fig. 5.40 shows that the precipitation in the monsoon period for **Furkatting** station decreases but increases in the post-monsoon period. Past data shows that precipitation occurs more in July than in September and the predicted future data shows that the precipitation occurs more in September than in July but predicted highest precipitation occurs in August in both the cases and increases by 48% in the future.Fig. 5.41 shows that the peak flow for **Lengree** station occurs in June for the past data and in August for the predicted future data. The predicted data shows that the highest precipitation decreases by 9% in June but increases by 21% in August. This implies that the total shift in the rainfall season towards the post-monsoon period.

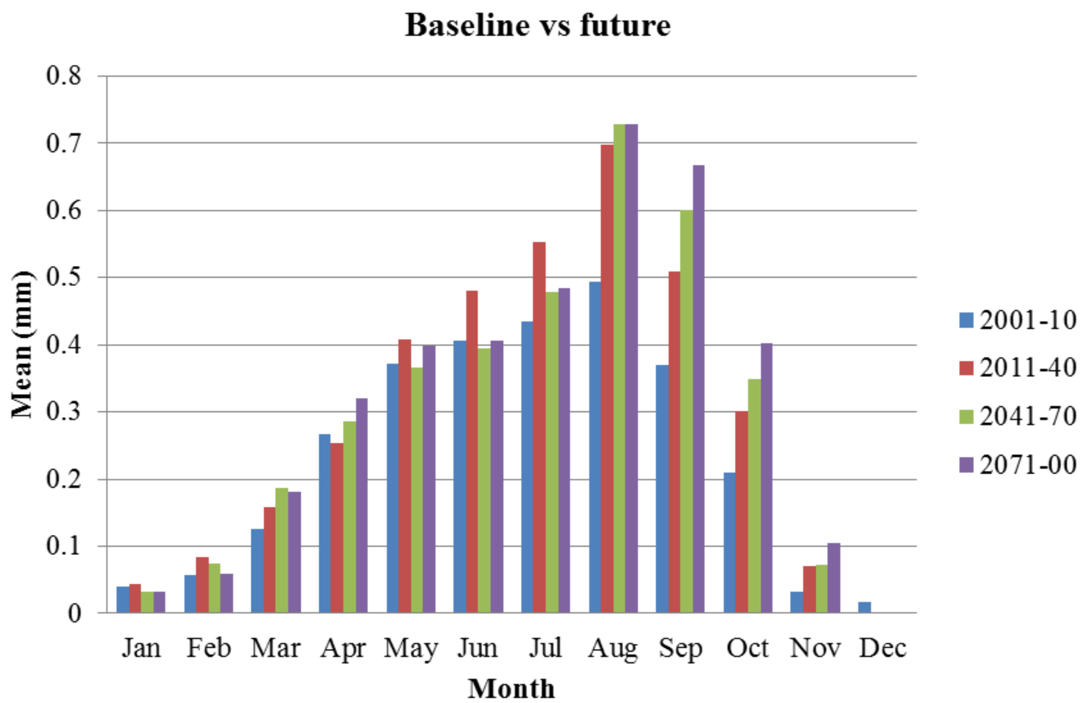

Fig. 5.39 Comparison of baseline and future precipitation in Furkatting Station

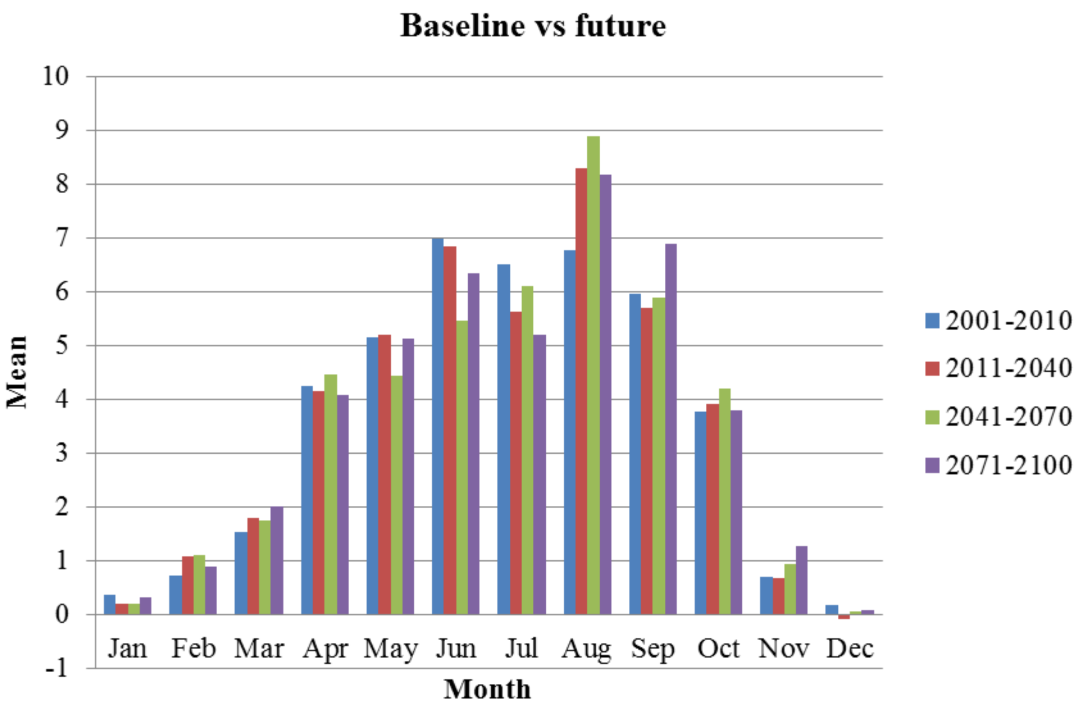

Fig. 5.40 Comparison of baseline and future precipitation in Lengree Station

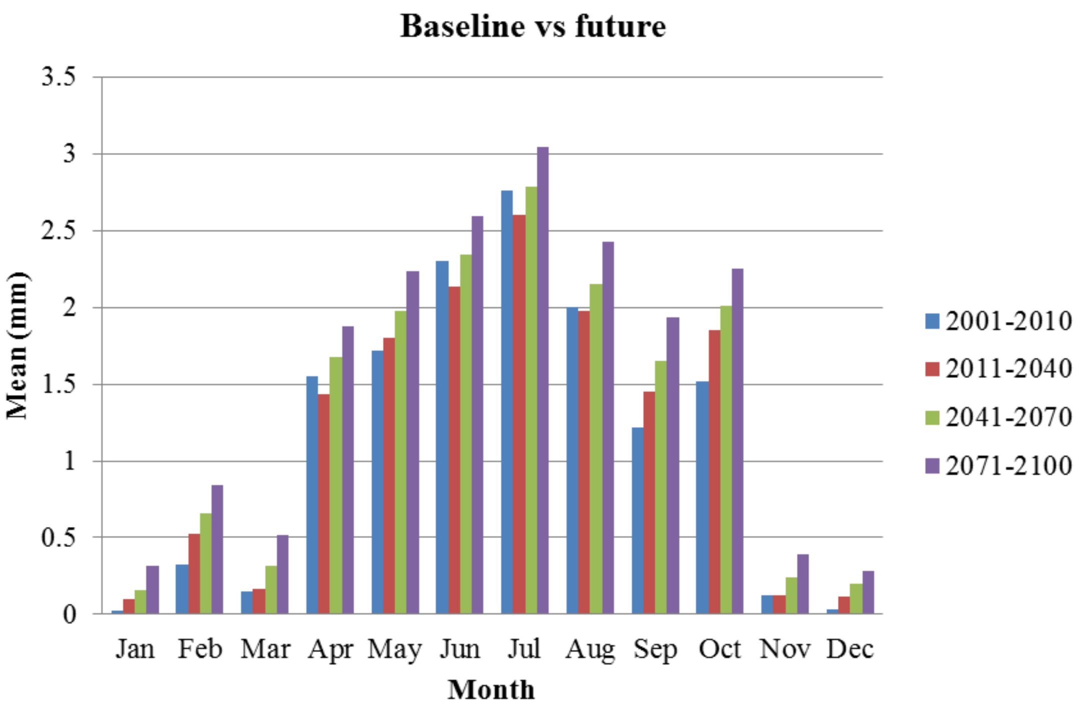

Fig 5.41 Comparison of baseline and future precipitation in Rungagora Station

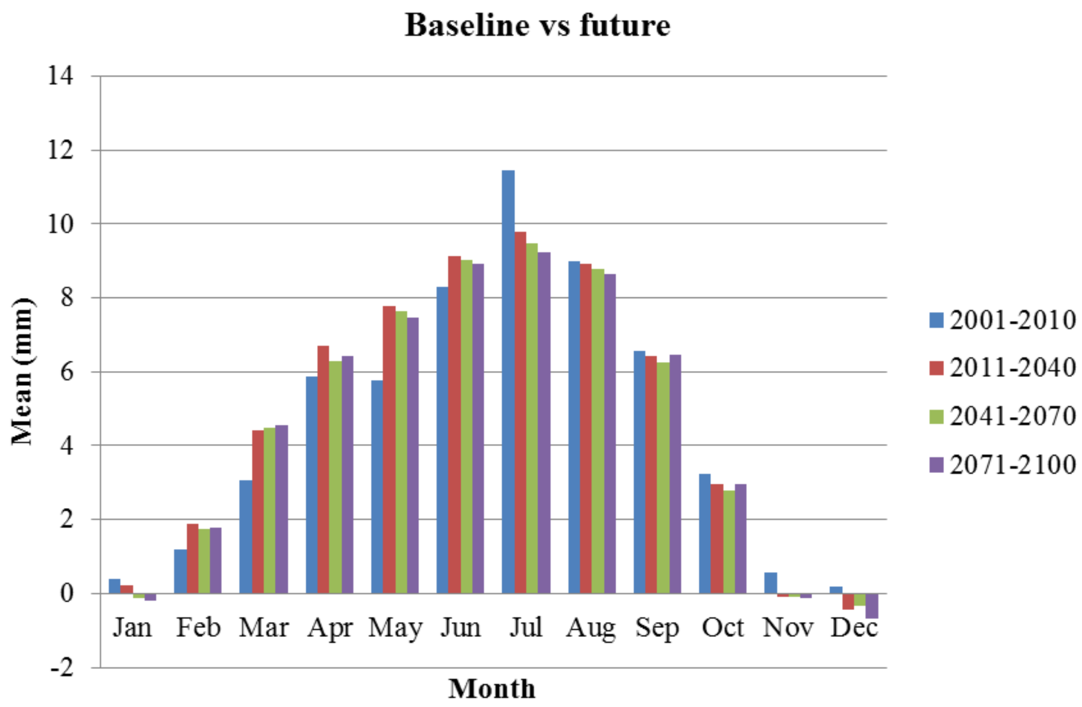

Fig. 5.42 Comparison of baseline and future precipitation in Sockieting Station

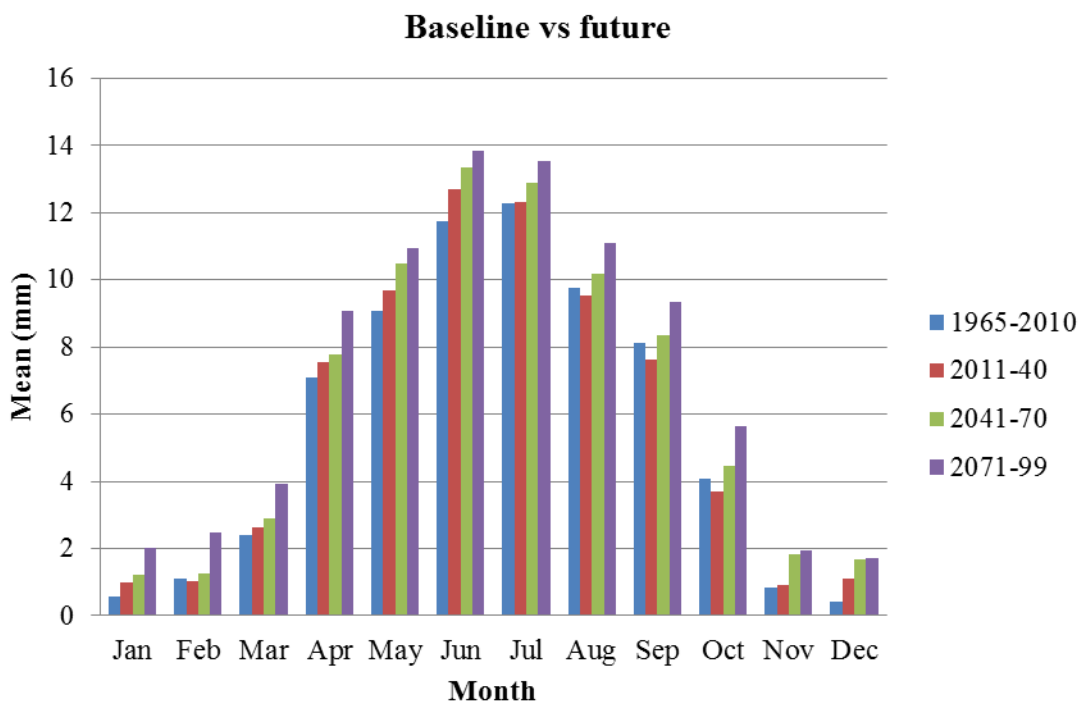

Fig. 5.43 Comparison of baseline and future precipitation in Bokakhat Station

Fig. 5.42 shows the variation of predicted and past precipitation. This graph shows that the precipitation for **Rungagora** decreases in the months January till August for the first three decades and increases in the months September till December for the same period. But the precipitation increases in all the months for the next six decades. The peak flow occurs in July for all the decades. The decrease in highest precipitation for the first three decades is 5.6% and the increase in the peak flow for the next last decades is 10%.

Fig 5.43 shows that the precipitation for **Sockieting** increases in the months January till June but decreases in the months July till December. Highest pericipitation occurs in July and decreases by 19%.

Fig 5.44 shows that the precipitation for **Bokakhat** increases for all the months. Highest precipitation occurs in the month of June with an increase of 18%.

5.5.2 FORECASTING DRY DAYS

The Number of dry days has been forecasted using the model and presented below.

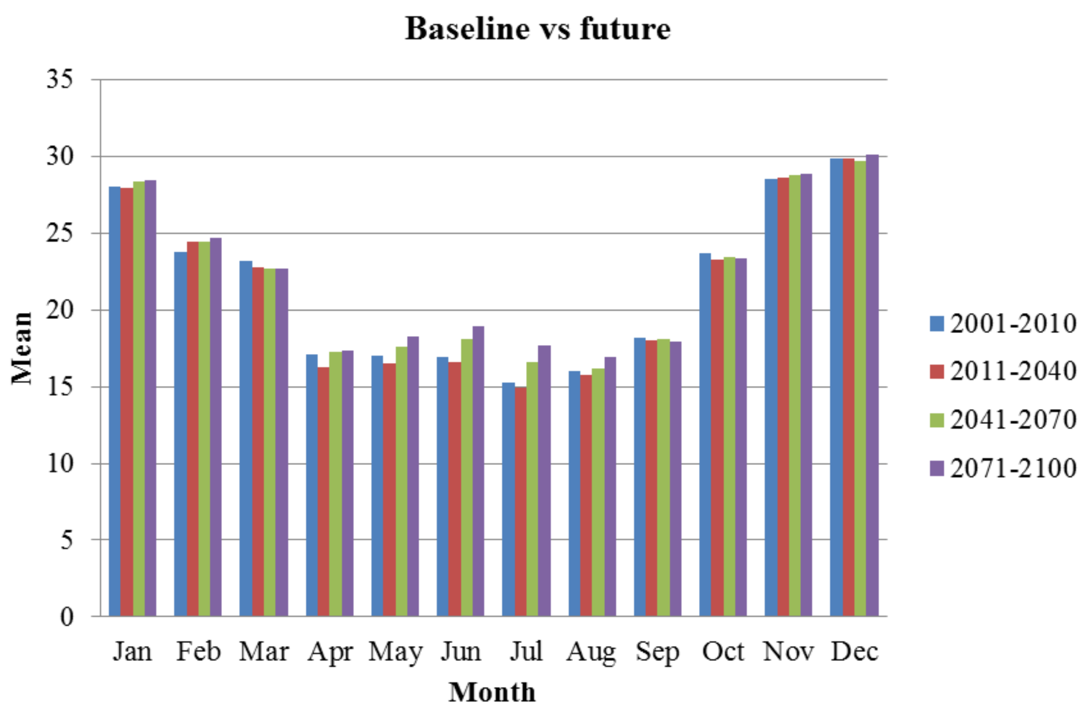

Fig. 5.44 Comparison of baseline and future number of dry days in Furkatting

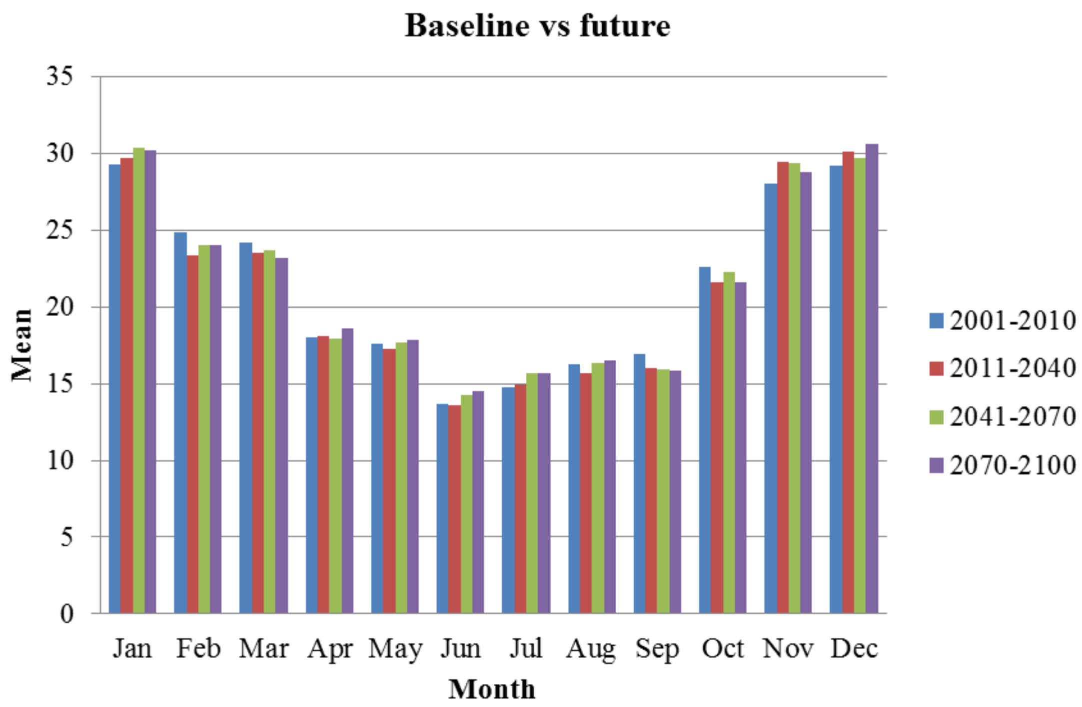

Fig. 5.45 Comparison of baseline and future number of dry days in Lengree

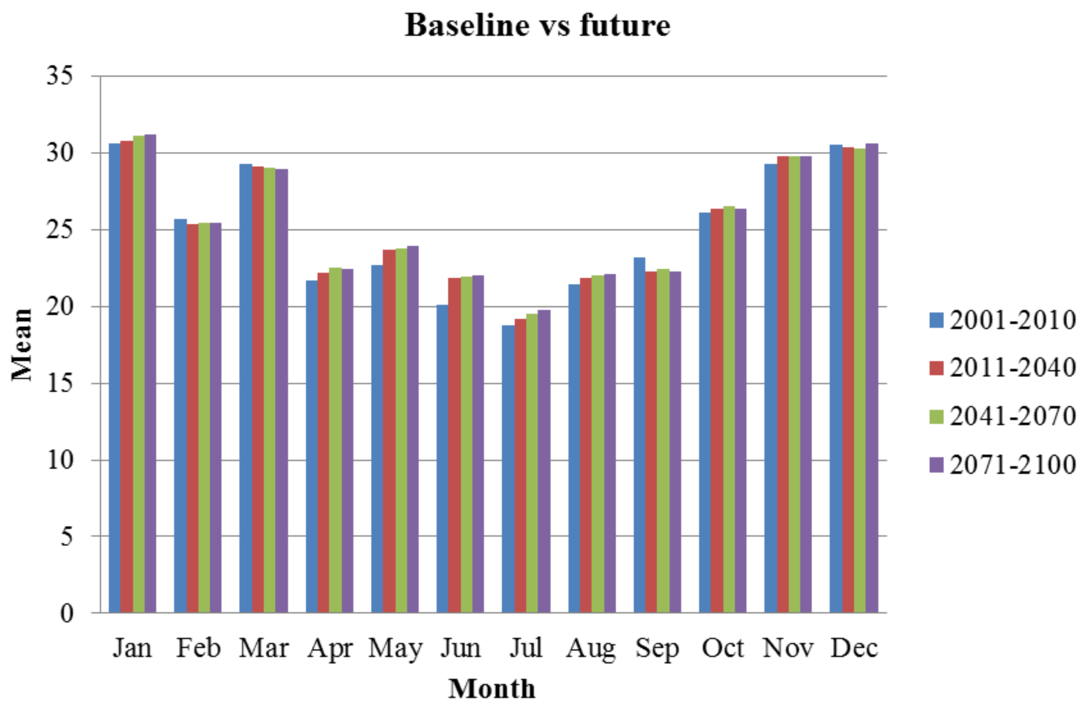

Fig 5.46 Comparison of baseline and future number of dry days in Rungagora

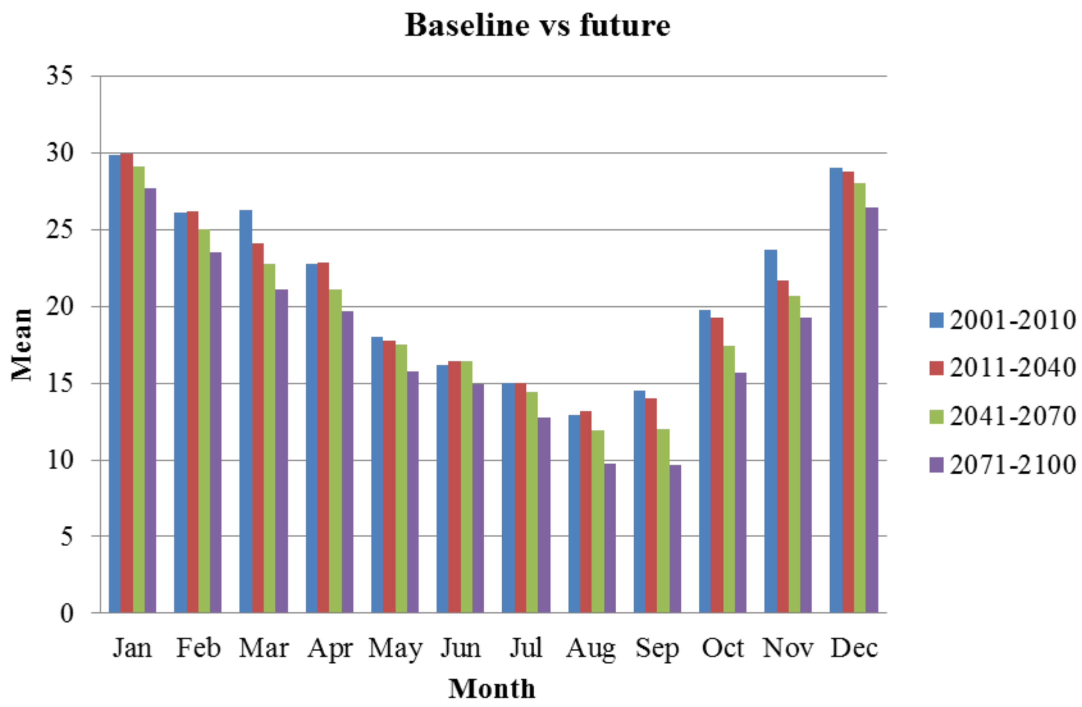

Fig. 5.47 Comparison of baseline and future number of dry days in Sockieting

The above figures show that the number of dry days increases in the future, as the highest precipitation increases, except in Sockieting where the number of dry days decreases in future with the decrease in the highest precipitation.

CHAPTER 6

DOWNSCALING USING ARTIFICIAL NEURAL NETWORK

6.1 NEURAL NETWORK

Neural Network is one of the tools used for methodological analyses of hydrological forecasting. It can be thought of as computational pattern that involves searching and matching procedures, which permit forecasting without an intimate knowledge of the physical or chemical processes, the statistical relationship between the sites on a map or any idea about what it is being modelled. The neural network only seeks the relationship between the input and output data and then creates its own equations to match the patterns in an iterative manner.

Neural networks are mathematical representations of a process that operates like nerve cells. Each network is made up of nodes and links like nerve cells. Forecasting has been followed in three clearly separate stages they are training mode, validation, testing phase. In 'training mode', the output is linked to as many of the input nodes as desired and pattern has been defined. The network is adjusted according to his error. In 'Validation', datasets are used at the stage to ensure the model is not over trained. In 'testing phase', the model is tested using data sets that were not used in training. If the forecasts are satisfactory then the model may be used in 'operational' or 'real time mode' to generate live forecasts. The accuracy of model has been decided through the performance in the real-time mode or independent validation mode.

The most useful neural networks in function approximation are Multi-Layer Perceptron (MLP). It consists of an input layer, several hidden layers and an output layer. The most popular algorithm is 'Back Propagation Neural Network' (BPNN) has been used in this study.

6.2 BACK PROPAGATION NEURAL NETWORK

Back Propagation Neural Network (BPNN) has been used to execute non-linear regression operations. This mechanism develops a function that concerns a set of input to a output in a data-driven environment. BPNN includes two mechanism, they are backward and feed forward.

6.2.1 BPNN OPERATION

In this Neural Network operation has been explained through the flowchart. The flowchart has given below.

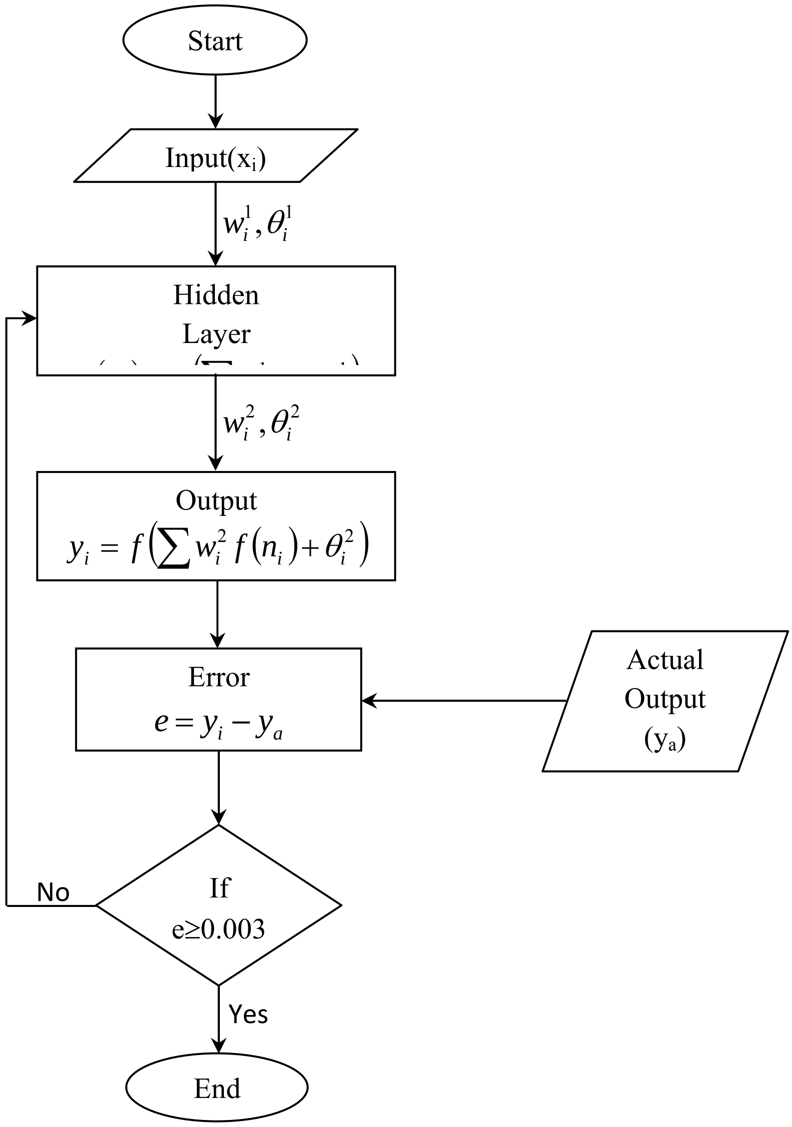

Fig 6.1 Flowchart for calculating the weightage

6.3 DATA USED

The data used for two stations (Bokakhat and Lengree) includes

- Precipitation Data: Observed monthly average precipitation time period for the Bokakhat site is from 1965 to 2010.

- Dry Days Data: Time period for this data set in Bokakhat site is from 1965 to 2010.
- NCEP_1965-2010: These are monthly average data, derived from NCEP reanalysis. These were interpolated respectively to each station.
- HadCM3A2_1965-2099: These data have been downloaded from IPCC-AR3 and have been interpolated for each station.

6.4 SELECTION OF PREDICTORS

The predictor selection has done by Pearson Correlation. Pearson Correlation is a simple correlation between the predictor and predictant. In the correlation test '0' represent weak correlation, whereas '1' represents strong correlation. The data have been normalised before entering into the Neural Network.

NCEP Predictors	Correlation of NCEP with observed precipitation in Bokakhat
Surface Air Temperature	0.776
Pressure	-0.777
Relative Humidity	0.541
Sea Level Pressure	-0.813
Zonal Wind Speed	0.523
Meriodinal Wind Speed	0.791
Air Tempareture @ 850hpa	0.796
Air Tempareture @ 500hpa	0.765
Air Tempareture @ 200hpa	0.762
Geo-Potential Height @ 850hpa	-0.769
Geo-Potential Height @ 500hpa	0.657
Geo-Potential Height @ 200hpa	0.755
Zonal Wind Speed @ 850hpa	0.532
Zonal Wind Speed @ 500hpa	-0.737
Zonal Wind Speed @ 200hpa	-0.768
Meriodinal Wind Speed @ 850hpa	0.844
Meriodinal Wind Speed @ 500hpa	0.262
Meriodinal Wind Speed @ 200hpa	-0.456
Relative Humidity @ 500hpa	0.592
Relative Humidity @ 200hpa	0.690

Table 6.1 Correlation between NCEP & Precipitation Data

HadCM3 Predictors	Correlation of HadCM3 with observed precipitation in Bokakhat
Sea Level Pressure	-0.82956
Relative Humidity	0.36039
Air Temperature @ 200hpa	0.61213
Air Temperature @ 500hpa	0.77276
Air Temperature @ 850hpa	0.79088
Surface Air Temperature	0.80450
Wind Speed	-0.69488

Table 6.2 Correlation between GCM & Precipitation Data

The common, strongly correlated predictors from NCEP model and GCM model has been chosen based on the above test. Those predictors are tabulated below.

Station	Predictands	Predictors
Bokakhat(1965-2010)	Precipitation	Mean sea level pressure Surface air temperature Air temperature @ 500hpa Air temperature @ 850hpa

Table 6.3 List of selected predictors

6.5 Application of Neural Network

The selected predicted has allowed entering into the network. The neural network consists of three layers: input layer, hidden layer, output layer. The block diagram of the network is given below

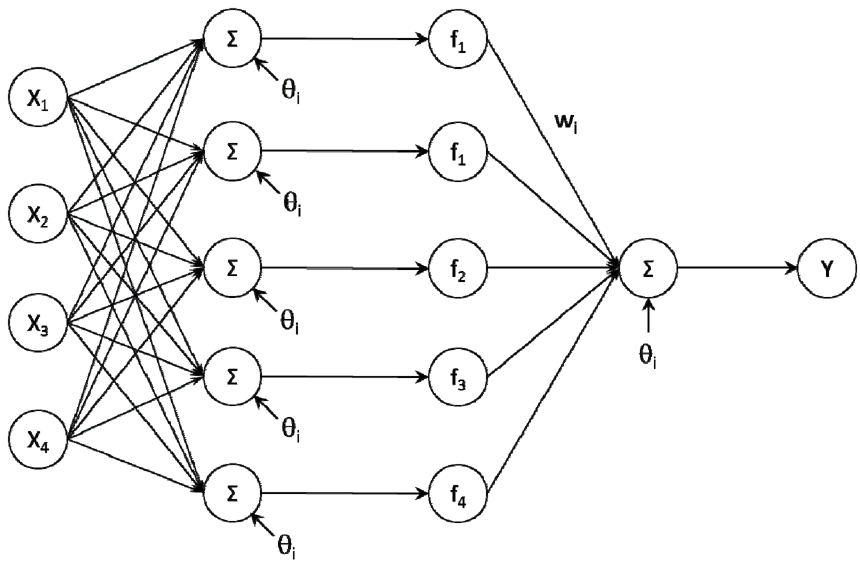

Fig. 6.2 Systematic diagram for Neural Network

6.6 MODEL TRAINING, VALIDATION AND TESTING

The network has been trained by using MATLAB. The outputs of performance, training, validation and testing are explained below with the graph.

6.6.1 PRECIPITATION MODEL FOR BOKAKHAT

The precipitation model uses the large scale variables from NCEP data - an observed data from 1965 to 2010. The data has been taken randomly for training (70%), validation (15%) and testing (15%).

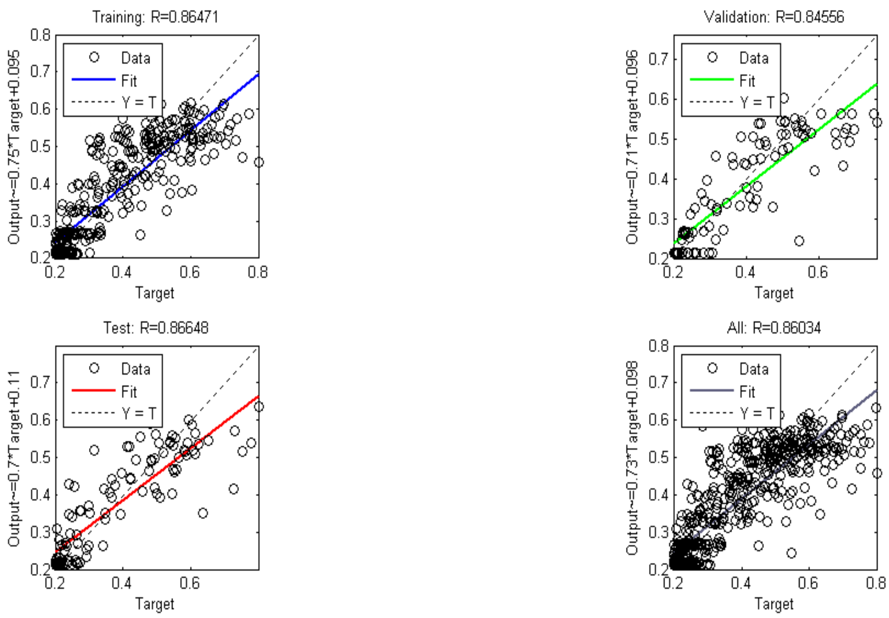

Fig. 6.3 Regression Curve for training, validation, testing using NCEP data

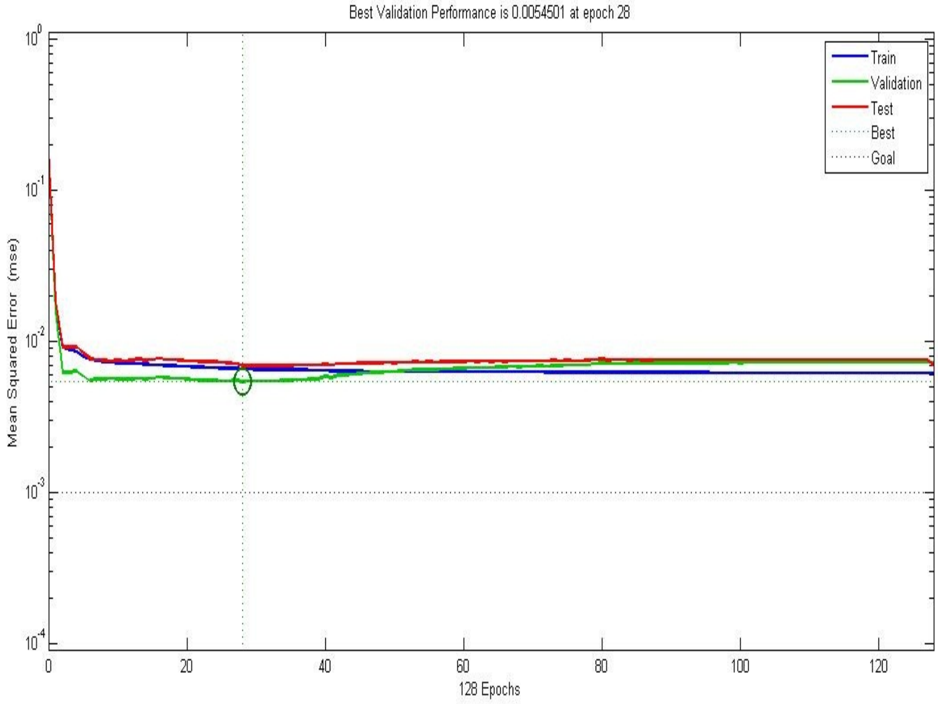

Fig. 6.4 Performance Curve Using NCEP data

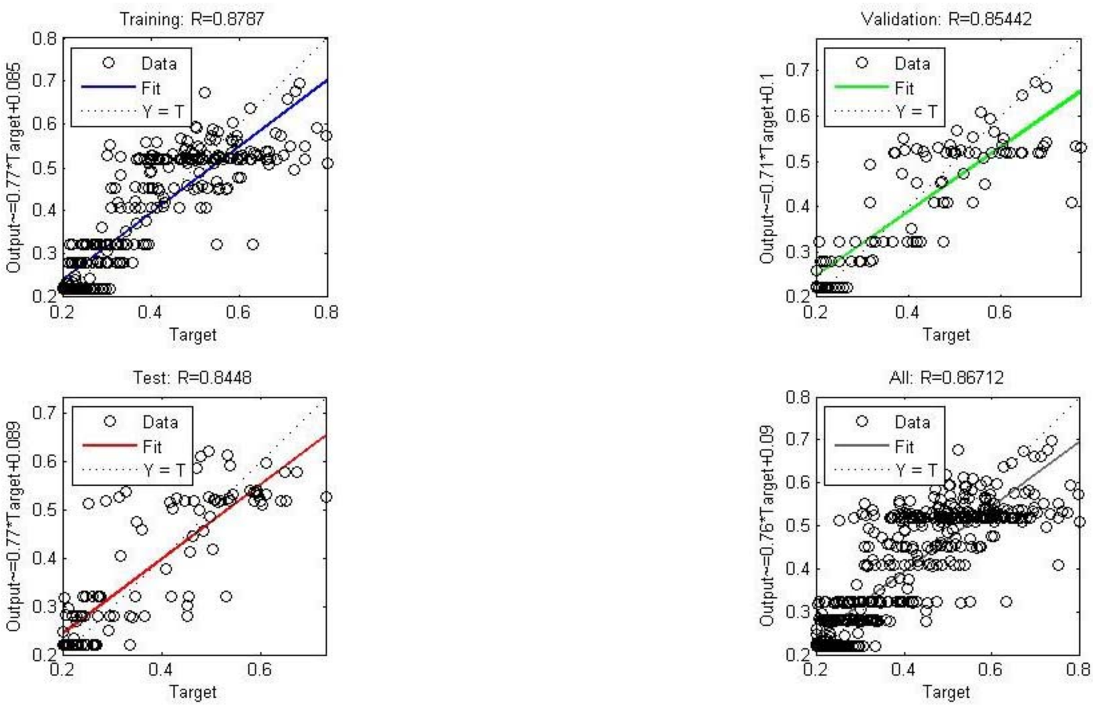

Fig. 6.5 Regression Curve for training, validation, testing using HadCM3 data

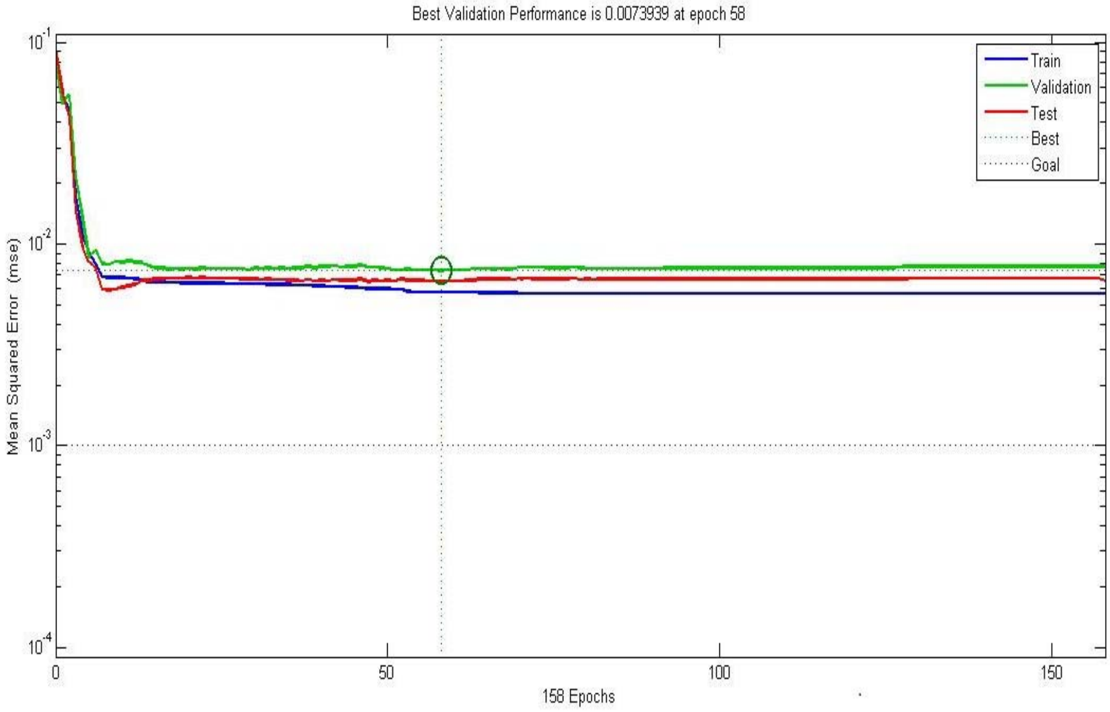

Fig. 6.6 Performance Curve Using HadCM3 data

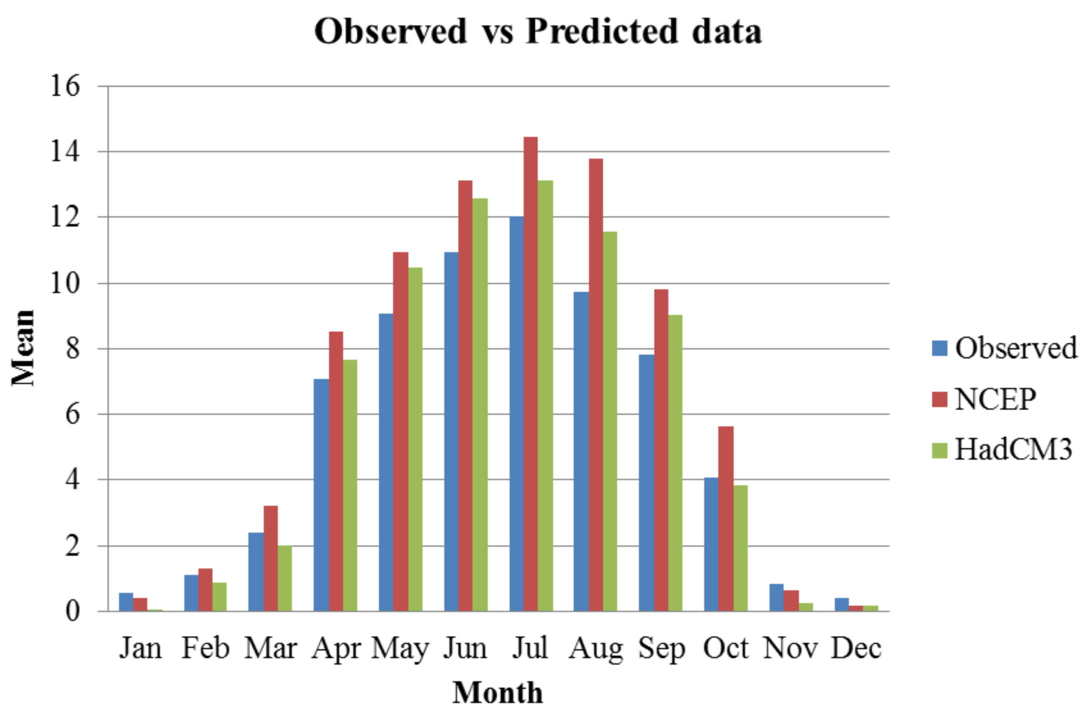

Fig. 6.7 Plot between Observed and predicted precipitation data

The above plots clearly show that the correlation between actual and predicted precipitation is 0.86 in both NCEP and HadCM3 data. The performance also better, mean square is approximately 0.006.

6.7 FUTURE DATA GENERATION

The future precipitation has been predicted using the above precipitation model. The time period has been grouped into 2011 to 2040, 2041 to 2070 and 2071 to 2099. Comparison of baseline and future has been given in a fig 6.8. It shows, in future, the precipitation is increases

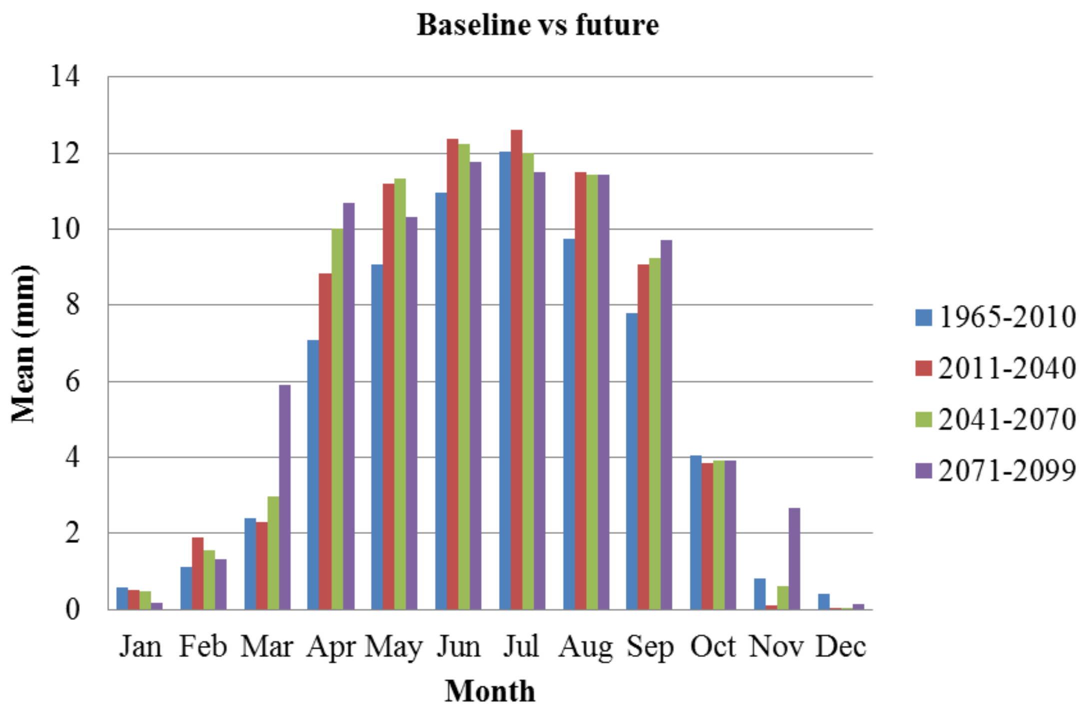

Fig 6.8 Base line vs. Future precipitation

6.8 SUMMARY

In this chapter, Artificial Neural Network has been used to downscale the precipitation in Bokakhat station. The total annual rainfall increases by 20% in future. In the previous chapter, regression analysis has been used. Both models show that the precipitation increases in the future.

CHAPTER 7

ANALYSIS OF RESULTS

This chapter describes the analysis of results obtained in the previous chapters. Chapter 5 shows clearly that in the future, the total precipitation increases and at the same time number of dry days also increases. Due to this phenomenon, the variation of average rainfall intensity in future rainfall in the future has been computed for each station.

The average intensity of rainfall (i_{avg}) is calculated by dividing the monthly average precipitation to the number of rainy days. Number of rainy days has been computed through the subtraction of number of dry days from the total number of days in a month.

$$i_{avg} = \frac{monthly\ average\ precipitation\ depth \times 30}{(total\ no.of\ days\ in\ a\ month - no.of\ dry\ days\ in\ a\ month)}$$

The average rainfall intensity for each station has been given below.

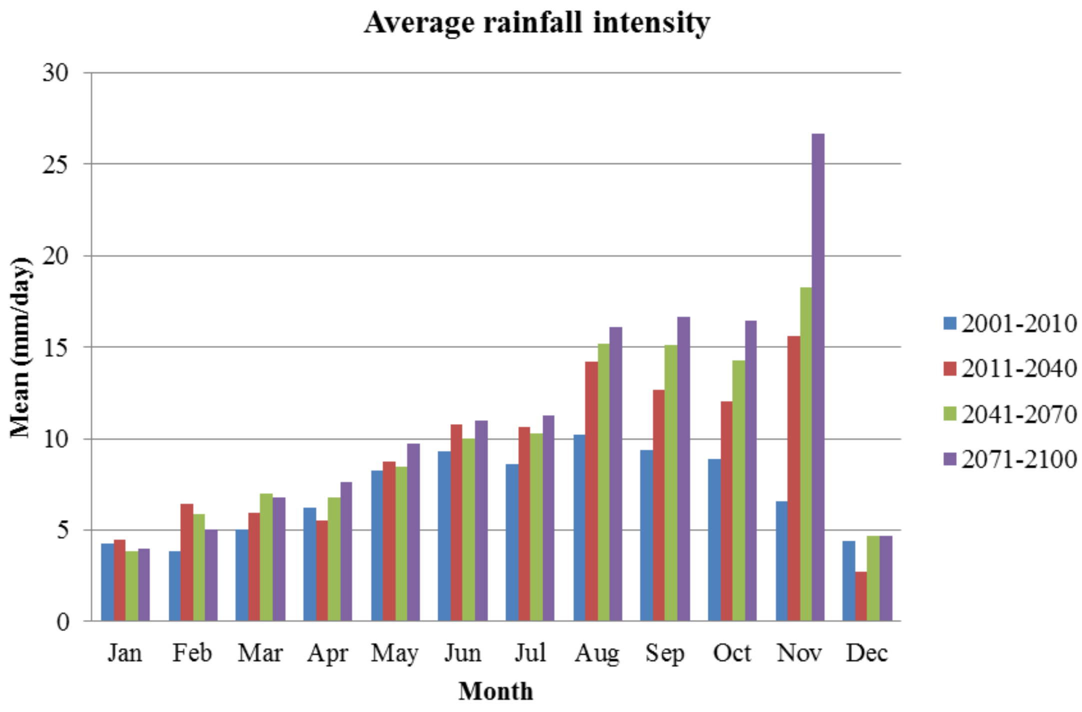

Fig. 7.1 Comparison of present and future i_{avg} for Furkatting station

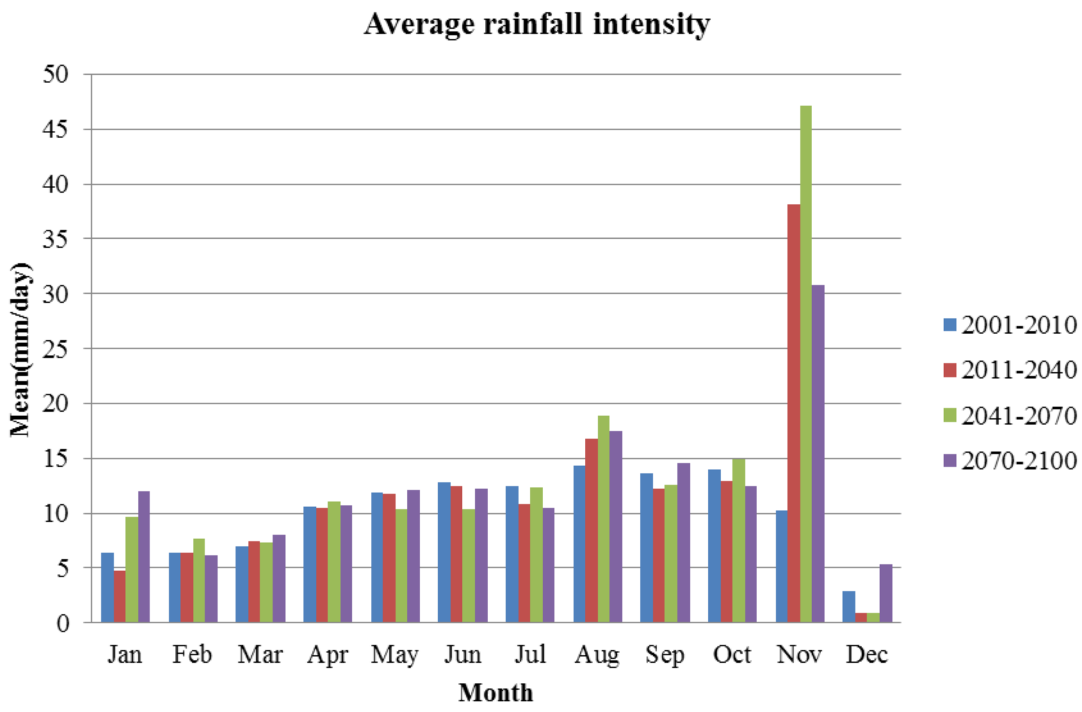

Fig. 7.2 Comparison of present and future i_{avg} for Lengree station

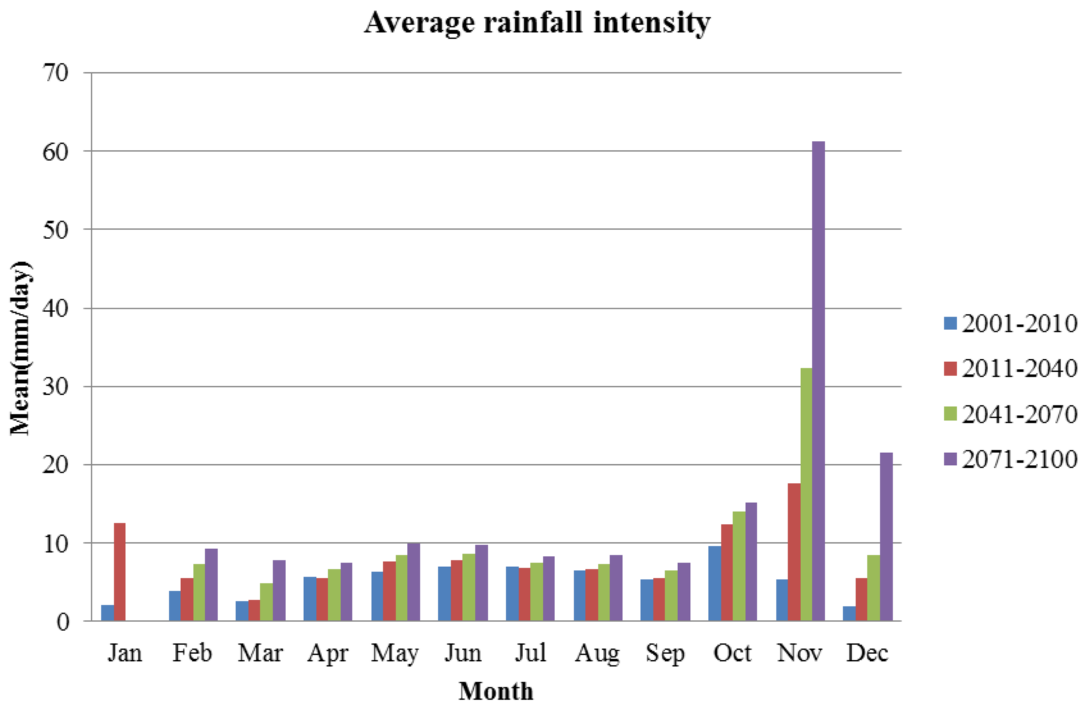

Fig. 7.3 Comparison of present and future i_{avg} for Rungagora station

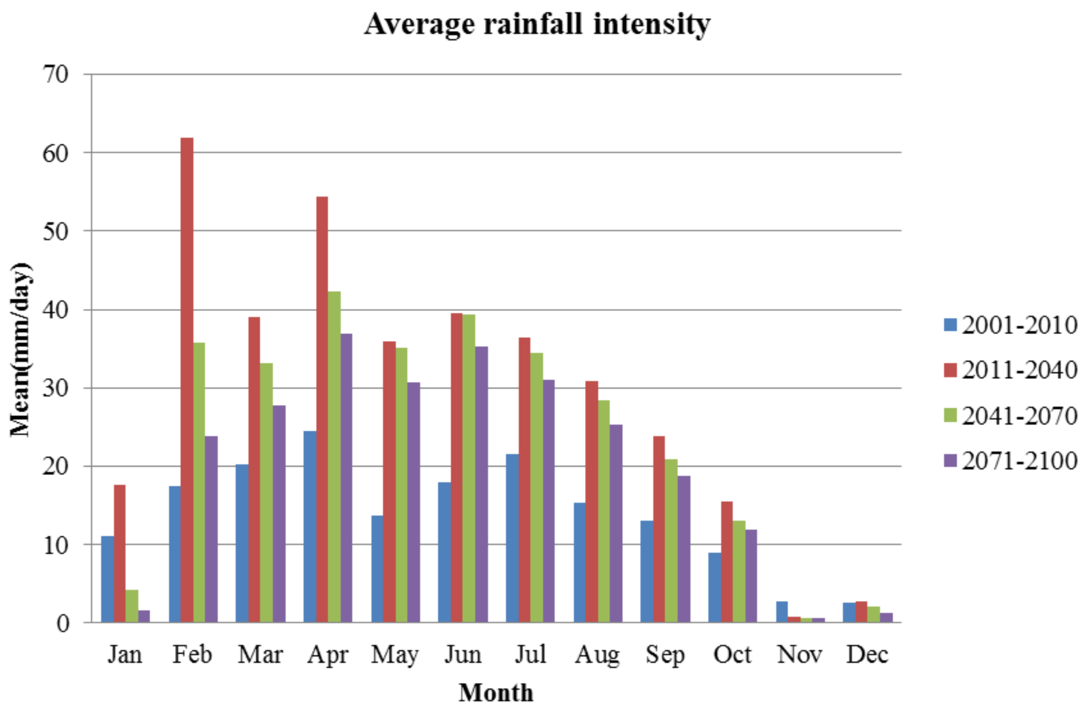

Fig. 7.4 Comparison of present and future i_{avg} for Sockieting station

In Furkatting station, the average intensity of rainfall slightly decreases in January and February but increases in rest of the months, in the future. In August, September, October and November, the rainfall intensity is too high, which may lead to flood. In Lengree the intensity of rainfall slightly decreases in monsoon period but increases in non-monsoon period. In Rungagora, the rainfall intensity is increases throughout the year and in Sockieting the rainfall intensity increases in the first 30 years and decreases in the later years. But, in all the stations, the future rainfall intensity increases due to the climate change. Therefore, the increasing trend of rainfall intensity increases the runoff, which increases the flow in the river that affects the river morphology.

CHAPTER 8

CONCLUSION, DISCUSSION AND FUTURE STUDY

In this study, the future precipitation and rainfall intensity has been predicted considering climate change impacts. Two methods have been used for downscaling the large climatic variables to local hydrological variables for impact studies. They are statistical downscaling and downscaling using ANN. These methods have been applied for five stations in the catchment of Dhansiri river basin. From this study, it can be concluded that in future, the precipitation as well as rainfall intensity will increase. It shows that low rainfall stations will receive relatively higher amount of precipitation but in high rainfall station, the precipitation will decrease in the future.

The increase in rainfall intensity is too high in November. Sockieting receives heavy rainfall compared to other places. In this place, the rainfall intensity decreases but in other places rainfall intensity increases. In future, this will lead to severe flood at some period and severe drought at other periods. It is obvious that this will affect the morphology of Dhansiri River.

To predict the change in morphology in river, stream flow variation is very important. Therefore, the further study will be in predicting the stream flow and study about the morphological change of the Dhansiri River.

REFERENCES

Alex Serrat-Capdevila, Juan B. Valdes, Javier Gonzalez Perez, Kate Baird, Luis J. Mata, Thomas Maddock III, August 2007, “Modeling climate change impacts – and uncertainty – on the hydrology of a riparian system: The San Pedro Basin (Arizona/Sonora)”, *Journal of Hydrology*, 347, pp. 48-96.

Athanasios N. Papanicolaou, Mohamed Elhakeem, Robert Hilldale, December 2007, “Secondary current effects on cohesive river bank erosion”, *Water Resources Research*, Vol 43.

Chu-Agor, M.L., Fox, G.A., Wilson, G.V., August 2009, “Empirical sediment transport function predicting seepage erosion undercutting for cohesive bank failure prediction”, *Journal of hydrology,* 377, pp. 155-164.

Clement Tisseuil, Mathieu Vrac, Sovan Lek, Andrew J. Wade, February 2010, “Statistical downscaling of river flows”, *Journal of Hydrology*, Vol. 385, pp. 279-291.

Craoll, R.W.H., Warwick, J.J., James, A.I., Miller, J.R., “Modelling erosion and overbank deposition during extreme flood conditions on the Carson River, Nevada”, *Journal of Hydrology*, 297, pp. 1-21.

Divya, Mehrotra. R., April 1995, “Climate change and hydrology with emphasis on the Indian subcontinent”, Hydrological Sciences *Journal- des Sciences Hydrologiques*,Vol. 40.

Dongdong Jia, Xuejum Shao, Hong Wang, Gang Zhou, January 2010, “ Three-dimensional modeling oh bank erosion and morphological changes in the Shishou bend of the middle Yangtze River”, *Advances of Water Resources*, 33, pp. 348-360.

Eduardo Zorita, Hans Van Storch, July 1998, “The Analog Method as a Simple Statistical Downscaling Technique: Comparison with More Complicated Methods”, *Journal of Climate*, Vol 12, pp. 2474-2489.

Gosain, A.K., Sandhya Rao and Debajit Basuray, Febrauary 2006, “Climate change impact assessment on hydrology of Indian river basins”, *Current science*, Vol. 90, No. 3, pp. 346-353.

Hauke Heyen, Eduardo Zorita, Hans Von Storch, june 1995, “Statistical downscaling of monthly mean North Atlantic air-pressure to sea level anomalies in the Baltic Sea”, *Tellus*, Vol. 48 A, pp. 312-323.

Hongwen Kang, Kyong-Hee An, Chung-Kyu Park, Ana Liza S. Solis, and Kornrawee Stitthichivapak, August 2007, “Multimodel output Statistical downscaling prediction of precipitation in tha Philippines and Thailand", *geophysical research letters*, Vol. 34,

Ichoro Kimura , Shinichiro Onda , Takashi Hosoda, Yasuyuki Shimizu. April 2010, "Computations of suspended sediment transport in a shallow side-cavity using depth-averaged 2D models with effects of secondary currents", *Journals of Hydro-environment Research*, pp. 153-161.

Jennifer G. Duan, November 2005, "Analytical Approach to Calculate Rate of Bank Erosion", *Journal of Hydraulic Engineering*, pp. 980-990.

Jinwon Kim, Norman L.Miller, March 2000, "A Seasonal Precipitation and Stream Flow Hindcast and Prediction Study in the Western United States during the 1997/98 Winter Season Using a Dynamic Downscaling System", American Meteorological Society.

Masoud Hessami, Philippe Gachon, Taha B.M.J. Ouarda, Andre St-Hilaire, October 2007,"Automated regression-based statistical downscaling tool", *Environmental modelling & software*, Vol. 23, pp. 813-834.

Masum Ur Rahman, Sarwat Jahan, Mir Mostafa Kamal., "Response of Climate Change on the Morphological Behaviour of the Major River System of Bangladesh"

Mohammad K aramouz, A na Hosseinpour, Sara Nazif, May 2011, "Improvement of Urban Drainage System Performance under Climate Change Impact: Case Study", *Journal of Hydrologic Engineering*, pp. 395-412.

Mujumdar, P.P., February 2008, "Implications of climate change for sustainable water resources management in India", *Physics and Chemistry of the Earth*, 33, pp. 354-358.

Nikolas E. Kotsovinos, April 1987, "Secondary currents in straight wide channels", *Appl. Math. Modelling*, Vol. 12, pp. 22-24.

R. L. Wilby, T. M. L. Wigley, D. Conway, P. D. Jones, B. C. Hewitson, J. Main, and D. S. Wilks , November 1998, "Statistical downscaling of general circulation model output: A comparison of methods", *Water Resources Research*, Vol. 34, No. 11, pp. 2995-3008.

Raj Hari Sharma, Narendra Man Shakya, November 2005, "Hydrological changes and its impact on water resources of Bagmati watershed, Nepal", *Journal of Hydrology*, 327, pp. 315-322.

Robert L. Wilby, Hany Hassan, Keisuke Hanaki, September 1997, "Statistical downscaling of hydrometeorological variables using general circulation model output", *Journal of Hydrology*, Vol. 205, pp. 1 - 19.

Ronald C. De Rose, Les R. Basher, October 2010, "Measurement of river bank and cliff erosion from sequential LIDAR and historical aerial photography", Geomorphology, Vol. 126, pp. 132– 147.

Subimal Ghosh, Deepshree Raje and Mujumdar P.P., April 2010, "Mahanadi stream flow: climate change impact assessment and adaptive strategies", *Current Science*, Vol. 98, No. 8, pp.1084-1091.

Subimal Ghosh, P.P. Mujumdar, July 2007, "Statistical Downscaling of GCM simulations to streamflow using relevance vector machine", *Advances in Water Resources*, Vol 31, pp. 132-146.

Vasubandhu Misra, Paul A. Dirmeyer, Ben P. Kirtman, June 2002, "Dynamic Downscaling of Seasonal Simulations over South America", *American Meteorological Society*.

X.-C. Zhang, November 2005, "Spatial downscaling of global climate model output for site-specific assessment of crop production and soil erosion", *Agricultural and Forest Meteorology*, Vol. 135, pp. 215–229.

Yonas B. Dibike, Paulin Coulibaly, October 2004, "Hydrologic impact of climate change in the Saguenay watershed comparison of downscaling methods and hydrologic models", *Journal of Hydrology*, Vol. 307, pp. 145–163.

Zhengyi Yao, Wanquan Ta, Xiapeng Jia, Jianhua Xiao , December 2010, "Bank erosion and accretion along the Ningxia – Inner Mongolia reaches of the Yellow River from 1958 to 2008",*Geomorphology*, 127, pp. 99-106.